Universitat Autònoma de Barcelona

DEPARTMENT OF BIOCHEMISTRY AND MOLECULAR BIOLOGY

CENTER OF ANIMAL BIOTECHNOLOGY AND GENE THERAPY

STUDY OF THE ROLE OF THE OVEREXPRESSION OF HIGH MOBILITY GROUP-AT- HOOK-1 (HMGA1) PROTEIN IN ADIPOSE TISSUE AND ITS IMPLICATIONS IN THE DEVELOPMENT OF OBESITY AND INSULIN RESISTANCE

ALTAMIRA ARCE CEREZO

This PhD thesis has been carried out under the direction of Dr. Efrén Riu Pastor at the Biochemistry and Molecular Biology Department of the Veterinary School of Medicine and at the Centre of Animal Biotechnology and Gene Therapy (CBATEG).

ALTAMIRA ARCE CEREZO **EFRÉN RIU PASTOR**

June 2013

BELLATERRA

A mis padres,
porque sin su apoyo, no hubiera llegado hasta aquí.

El final del camino de la tesis se acerca y me gustaría aprovechar la ocasión para dar las gracias a todas las personas con las que he tenido la suerte de recorrer las etapas de este camino, dentro y fuera del laboratorio. Sois muchos los que con vuestro apoyo habéis contribuido de una manera u otra a que este trabajo llegara a su fin. Porque sois muchos espero no olvidarme de nadie, y si lo hago, pido disculpas de antemano.

En primer lugar, me gustaría agradecer sinceramente a mi director de tesis, el Dr. Riu por haberme dado la oportunidad de realizar esta tesis doctoral en su grupo de investigación. Gracias por haber confiado siempre en mí y gracias por haberme enseñado a trabajar de manera independiente.

En segundo lugar, muchísimas gracias a la Dra. Martín-Duque por acordarte de mí en el momento y lugar adecuados. Gracias por tu ayuda durante las diferentes etapas de mi vida y de mi formación.

Gracias a la Dra. Fàtima Bosch por haberme acogido y tratado como a una más de su grupo.

Gracias Sylvie, porque un día pusiste este proyecto en marcha. Gracias por responder a mis preguntas de "un momentito" y por la ayuda prestada en estos últimos tiempos.

Muchas gracias Miquel, por ser un referente a nivel científico y personal. No tengo palabras para agradecer tu inestimable ayuda.

Al principio éramos dos en el grupo, pero con el tiempo llegaron ellos: Albert, Aida y Mireia. Muchísimas gracias por haber sido mis segundo, tercero y cuarto par de manos. Por ser la alegría de la "huerta", por aguantar mis nervios y por cuidarme… Gracias por ser los mejores compañeros de poyata, pero sobre todo gracias porque con vosotros he aprendido un montón.

Gracias a todos mis compañeros de laboratorio de la 3ª: Vicky, Alba, Carles, Edu, Albert Ribera, Laia, Luca, Joan, Iris, Sandra, Claudia y David; porque una parte de esta tesis es también vuestra. Gracias por los grandes momentos en el laboratorio y por hacer esta experiencia única. Gracias también por enseñarme el catalán y las tradiciones catalanas.

Gracias a las "supernenas" Cristina, Meritxell y Sara, porque juntas empezamos esta andadura. Ánimo y suerte en lo que os queda!

Gracias a las “originales”, Pilar y Vero, por compartir ese “aquel de fuera” que nos hace entendernos y por tener una fuerza de voluntad de hierro y arrastrarme así al SAF.

Mil gracias al resto del “equipo adiposo”, Sergio, Estefanía e Ivet. Por vuestro apoyo y ayuda. Por compartir vuestro conocimiento y el saber hacer en este tejido tan especial y por el tráfico de artículos.

Un especial recuerdo para los que estuvieron y ya echaron a volar: Xavi, Callejas, Ricardo, Chris Mann, Albert Ruzo y Judith. Y a los que han vuelto, Joel y Mercè; gracias por su amistad y por los buenos ratos, dentro y fuera del laboratorio.

Muchísimas gracias a las chicas de la cocina Jenny y Lidia por tener una risa contagiosa, por pero sobre todo porque sin vuestro trabajo, el nuestro sería mucho más difícil. Al resto de habitantes de la cocina, gracias Xavi León por amenizarnos los desayunos con tus monólogos. María Molas, gracias por ayudarme con las “celulitas”, pero sobre todo gracias por tu amistad. Gracias también a Marta por los innumerables bloques y por los buenos ratos a la hora de comer.

Gracias a la UAM y a Tura, por las analíticas de última hora y por conseguir que llegara pronto a los journals.

Gracias al servicio del estabulario, especialmente al Dr. Otaegui por la ayuda y cuidado de todos los ratones. Gracias Mireia por cuidar especialmente de mis ratones, pero sobre todo por sus abrazos. A las chicas de la UAT, Anna Arbós, Sandra y Anna Pujol, gracias por generar mis ratones y por los buenos ratos a la hora de comer.

Gracias al resto de compañeros del la 5ª planta, por aguantar estoicamente y colaborar en mis experimentos de frío. Y a los compañeros del grupo del Dr. Ruberte por su ayuda con las inmunos y por las risas del pasillo de la 4ª. Ánimo David, que ya queda menos!

Gracias a todos los servicios del CBATEG por hacer posible nuestro trabajo cada día: Montse Bellido y Rosmi por su ayuda con los asuntos administrativos y gracias a Teresa y Jèssica por la ayuda con los pedidos. Gracias a Carles Ros y al personal de mantenimiento, seguridad y limpieza. Gracias Luisa, Montse e Isa por ser la alegría de la mañana.

I would like to specially thank Dr. Malcolm Watford for his helpful discussions and critical comments and for the correction of this thesis.

De la gente de fuera del laboratorio: gracias a mis compañeras de piso de Barcelona, Marité, Salo, Sonia y Marta, porque vosotras también habéis vivido en primera persona esta tesis de principio a fin. A Celia y Fabián, gracias por su amistad. Gracias a mis amigas de Madrid: Ali, Helena, María y Susana; Porque da igual cuanto tiempo pase, siempre están ahí.

Pero sobre todo un "mil gracias" a mi GRAN familia; De entre todos, en primer lugar me gustaría agradecer a mis padres su apoyo incondicional y esa habilidad que tienen de estar cerca aún estando lejos. Gracias al resto de tíos y primos, sois únicos! Gracias por entender mis ausencias a lo largo de todos estos años.

I finalment, gràcies Màxim, per estar sempre ahi. Moltisímes gràcies pel teu support i paciència en aquests últims mesos.

Esta tesis ha sido posible en primer lugar, gracias a una beca predoctoral PIF, de la Universitat Autònoma de Barcelona financiada por el Ministerio de Educación y Ciencia, de la que he sido beneficiaria durante cuatro años. Las investigaciones se han realizado gracias a la financiación recibida del Ministerio de Educación y Ciencia, Plan Nacional I+D+I (SAF2011-23649**;** SAF2008-03083 and RYC-2006-001955); de la Unión Europea (MIRG-CT-2007-207745); del Instituto Carlos III, CIBERDEM: Diabetes y Enfermedades Metabólicas (AE2009) y de la Universitat Autònoma de Barcelona (EME2007-17).

18S	Ribosomal subunit 18S
28S	Ribosomal subunit 28S
ADP	Adenosine diphosphate
AKT	Serine/threonine protein kinase
AMP	Adenosine monophosphate
AMPK	AMP-Activated Protein Kinase
aP2	Fatty acid-binding protein 2/Fatty acid-binding protein 4 (FABP4)
aP2-HMGA1	Transgenic mice overexpressing HMGA1 in adipose tissue
APC	Antigen-presenting cell
ASCs	Adipose-derived stem cells
ATM	Adipose tissue macrophages
ATP	Adenosine tri-phosphate
BAT	Brown adipose tissue
BHBA	Beta-Hydroxybutyrate
BMI	Body mass index
BMP2	Bone morphogenetic protein 2
BMP4	Bone morphogenetic protein 4
BMP7	Bone morphogenetic protein 7
bp	Base pairs
BSA	Bovine Serum Albumin
C/EBPs	CAAT/Enhancer Binding Proteins
C/EBPα	CCAAT/enhancer-binding protein alpha
C/EBPβ	CCAAT/enhancer-binding protein beta
C/EBPδ	CCAAT/enhancer-binding protein delta
cAMP	Cyclic Adenosine Monophosphate
CBATEG	Centre of Biotechnology and Gene Therapy
CCL2	Chemokine (C-C motif) ligand 2
CCR2	Chemokine receptor-2
CD11b	Integrin alpha M II
CD11c	Integrin alpha X chain protein
cDNA	Complementary Deoxyribonucleic Acid
Ci	Curie
Cidea	Cell-death-inducing DFF45-like-effector A
Cidea	Cell-death-induncing-DF45-like-effector A
CMV	Cytomegalovirus
COXII	Cytochrome C Oxidase subunit II
cpm	Counts Per Minute
CREB	Cyclic AMP response element-binding protein
CtBP1	C-terminal binding protein 1
CtBP2	C-terminal binding protein 2

Cts	Threshold Cycle
DAB	Diaminobenzidine
dATP	Deoxyadenosine triphosphate
dCTP	Deoxycytidine triphosphate
DEPC	Diethyl pyrocarbonate
dGTP	Deoxyguanosine triphosphate
DNA	Deoxyribonucleic Acid
DTT	Dithiothreitol
dTTP	Deoxythymidine triphosphate
ECM	Extracellular matrix
EDTA	Ethylenediaminetetraacetic Acid
EE	Energy expenditure
ELISA	Enzime-linked immunosorbent assay
Elovl3	Elongation of very long chain fatty acids-like 3
epWAT	epididymal white Adipose Tissue
ER	Endoplasmic Reticulum
$FADH_2$	Flavin adenine dinucleotide
FAS	Fatty acid synthase
FFAs	Free Fatty Acid
Fw	Forward
GTT	Glucose tolerance test
H^+	Protons
HFD	High Fat Diet
HMGA1	High mobility group –AT-hook-1
IL-6	Interleukin-6
iNOS	Cytokine-inducible nitric oxide synthases
ITT	Insulin tolerance test
iWAT	Inguinal white adipose tissue
JNK	c-Jun N-terminal kinase
kb	Kilobase
kDa	KiloDaltons
Kg	Kilograms
LB	Luria-Bertani medium
M	Molar
mA	Milliampere
MAC-2	Galactoside-binding soluble 3
MCE	Mitotic clonal expansion
MCP-1	Monocyte chemo attractant protein-1
mg	Milligram
MGL-1	Macrophage galactose type C lectin 1
MIM	Mitochondrial inner membrane

min	Minute
mL	Millilitre
mM	milliMolar
MMPs	Metalloproteinases
MOPS	3-(N-morpholino)propanesulfonic acid
mRNA	Messenger RNA
MSC	Mesenchymal stem cells
mt-DNA	Mitochondrial DNA
mWAT	Mesenteric white adipose tissue
Myf5	Myogenic factor 5
MyoD	Myogenic differentiation 1
NADH	Nicotinamide adenine dinucleotide phosphate
nDNA	Nuclear DNA
NF-κB	Nuclear factor kappa-light-chain-enhancer of activated B cells
ng	Nanograms
nm	Nanometers
o/n	Overnight
ºC	Degree centigrade
oligo-dT	Oligo deoxitimine
OXPHOS	Oxidative Phosphorylation System
PAI-1	Plasminogen Activator Inhibitor 1
PBS	Phosphate-Buffered Saline
PCR	Polymerase Chain Reaction
PET	Positron Emission Tomography
PGC-1α	Peroxisome proliferator-activated receptor gamma coactivator 1-alpha
PMSF	Phenylmethylsulfonyl fluoride
PPARs	Peroxisome Proliferator-activated Receptors
PPARα	Peroxisome proliferator-activated receptor alpha
PPARβ/δ	Peroxisome proliferator-activated receptor beta and delta
PPARγ	Peroxisome proliferator-activated receptor gamma
ppm	Parts Per Million
PPREs	PPARg responsive elements
PRDM16	PR-domain-containing-16
Pref-1	Preadipocyte factor 1/Delta-like homolog-1 (Dlk-1)
Rb	Retinoblastoma protein
RBC	Red blood cells
RBP4	Retinol-Binding protein 4
RIA	Radioimmunoassay

RIP140	Receptor-interacting protein 140/Nuclear receptor interacting protein 140 (NRIP1)
RNA	Ribonucleic Acid
rpm	Revolutions per minute
RQ	Respiratory quotient
RT	Room temperature
Rv	Reverse
rWAT	Retroperitoneal white adipose tissue
RXR	Retinoid X Receptor
SDS	Sodium dodecyl sulfate
SDS-PAGE	Sodium Dodecyl Sulfate Polyacrylamide Gel Electrophoresis
SEM	Standard Error of the mean
SNS	Sympathetic Nervous System
SREBP-1a	Sterol Regulatory Element-Binding Proteins-1 alpha
SREBP-1c	Sterol Regulatory Element-Binding Proteins-1c
SREBPs	Sterol Regulatory Element-Binding Proteins
ssDNA	Single stranded DNA
STD	Standard diet
SV40	Simian vacuolating virus 4
SVF	Stromal vascular fraction
T1D	Type 1 diabetes
T2D	Type 2 diabetes
TAE	Tris-acetate-EDTA
TBS	Tris-Buffered Saline
TBS-T	Tris-Buffered Saline and Tween 20
TG	Triglyceride
Tg	Transgenic mice
TM	Masson's trichrome
TNF-α	Tumor necrosis factor-alpha
UAB	Universitat Autònoma de Barcelona
UCP1	Uncoupling proteína 1
V	Volts
WHO	Word Health organization
WHR	Waist-Hip ratio
Wt	Wild type mice
µg	Microgram
µJ	Microjoules
µl	Microliter

INDEX

1. SUMMARY

Obesity is a complex metabolic disorder that has reached epidemic proportions in both developed and developing countries. Moreover, obesity is a major risk factor that enhances the risk of developing other diseases such as insulin resistance, type 2 diabetes and cardiovascular diseases. These pathologies represent a great threat to global human health. Knowledge of the causes and mechanisms that trigger the development of these diseases is of vital importance for its prevention and treatment. However, the mechanisms through which obesity originates, develops and predisposes to other metabolic complications are not fully understood.

Adipocyte and obesity development have been largely studied through many cellular models. In addition, several rodent and nonrodent models have been generated for the better understanding of obesity physiopathogenesis. As High Mobility –AT-hook- Group-1 (HMGA1) proteins have been implicated on adipogenesis *in vitro*, we sought to examine the metabolic effects of HMGA1 overexpression in adipose tissue *in vivo*. To this aim, we generated a line of transgenic mice specifically overexpressing HMGA1 in adipose tissue.

Overexpression of HMGA1 in adipose tissue resulted in smaller adipose mass in aP2-HMGA1 transgenic mice. In addition, these animals showed normoglycaemia and normoinsulinemia in a fed and starved states. Furthermore, transgenic mice presented a higher metabolic rate. Despite less adiposity and smaller adipocyte mean area, no major differences in the adipocytes from epididymal white adipose tissue (epWAT) were detected. However, an active remodelling process was detected in this depot. In contrast, aP2-HMGA1 transgenic animals showed less adipose tissue mass and serious morphological alterations in brown adipose tissue (BAT). These changes implicated downregulation of genes and proteins involved in the brown adipocyte differentiation

programme, mitochondrial biogenesis and function, and lipid metabolism, leading to impaired thermogenic capacity of BAT. Gene expression analysis of epWAT and BAT from transgenic mice showed dysregulation of gene pathways involved in cell cycle, fatty acid and insulin metabolism, and adipogenesis.

When fed a high fat diet (HFD), transgenic mice gained less weight and showed lower adiposity than wild type littermates. Moreover, transgenic mice showed lower epWAT weight and decreased mean adipocyte area. Consistent with the lack of fat accumulation, lipid related metabolites and adipokine secretion were lower in transgenic mice in comparison with wild type mice.

In contrast to wild type obese and insulin resistant mice, transgenic mice remained protected against diet-induced obesity, insulin resistance and glucose intolerance. However, transgenic mice presented high macrophage infiltration in epWAT. Transgenic mice showed an increase in the percentage of total macrophages, although no shift from M2 anti-inflammatory to M1 proinflammatory macrophage population was observed. This was parallel to a reduction in the levels of pro-inflammatory cytokines, such as IL-6, MCP-1 and TNF-a, which were elevated in epWAT of HFD-fed wild-type mice.

Taken together, these results indicate that specific HMGA1 overexpression in adipose tissue impaired terminal differentiation of adipocytes. These effects protected transgenic mice from high fat diet-induced obesity, insulin resistance and glucose intolerance. Thus, this study suggests that HMGA1 proteins may be active players in adipogenesis and adipose tissue development, although the exact mechanism of action still remains unclear.

2. INTRODUCTION

1. OBESITY

Obesity is a metabolic disorder that has reached epidemic proportions in both developed and developing countries. Obesity is caused by an energy imbalance, when energy intake exceeds energy expenditure. Thus, the development of obesity depends on the net outcome between food intake and energy expenditure as well as on the distribution between different fat stores (Frühbeck et al., 2009). Obesity and its associated body fat mass gain is the consequence of chronic, long-term positive energy balanced (Schenk et al., 2008). Excessive fat accumulation occurs not only in adipose tissue but also in other organs during obesity development (Shoelson et al., 2007).

1.1. Obesity epidemics

The World Health Organization (WHO) estimates that there are more than 1 billion overweight adults worldwide, 475 million of whom are clinically obese (Cao, 2010). This increasing tendency makes obesity a great health problem, affecting both developed and developing countries (Figure 1) (Spalding et al., 2008).

In The United States of America, the prevalence of obesity among the population is higher than 30 %. In most European countries, at least 20 % of all adults are already obese and unexpectedly, high obesity levels are reported in the Middle East (also noted as the region with the highest national prevalence of type 2 diabetes in the world). South American, Asian and African countries are also showing a rapid increase in obesity prevalence (Figure 1) (Stommel and Schoenborn, 2010).

There are a wide range of 'obesogenic' factors contributing to the increased energy consumption and decreased energy expenditure that are responsible for obesity, including higher sedentary lifestyle, increased food availability, genetic and

P. Gné. f P. Vd PœPTVgN Tb aPgn ééés Té. VP. Vél SVnVé. d GdSPNGnd n ePTVé. él

d uVbP éGPXd VnPuN8698:yPd f s Ld nuN8698: PugN8698Y

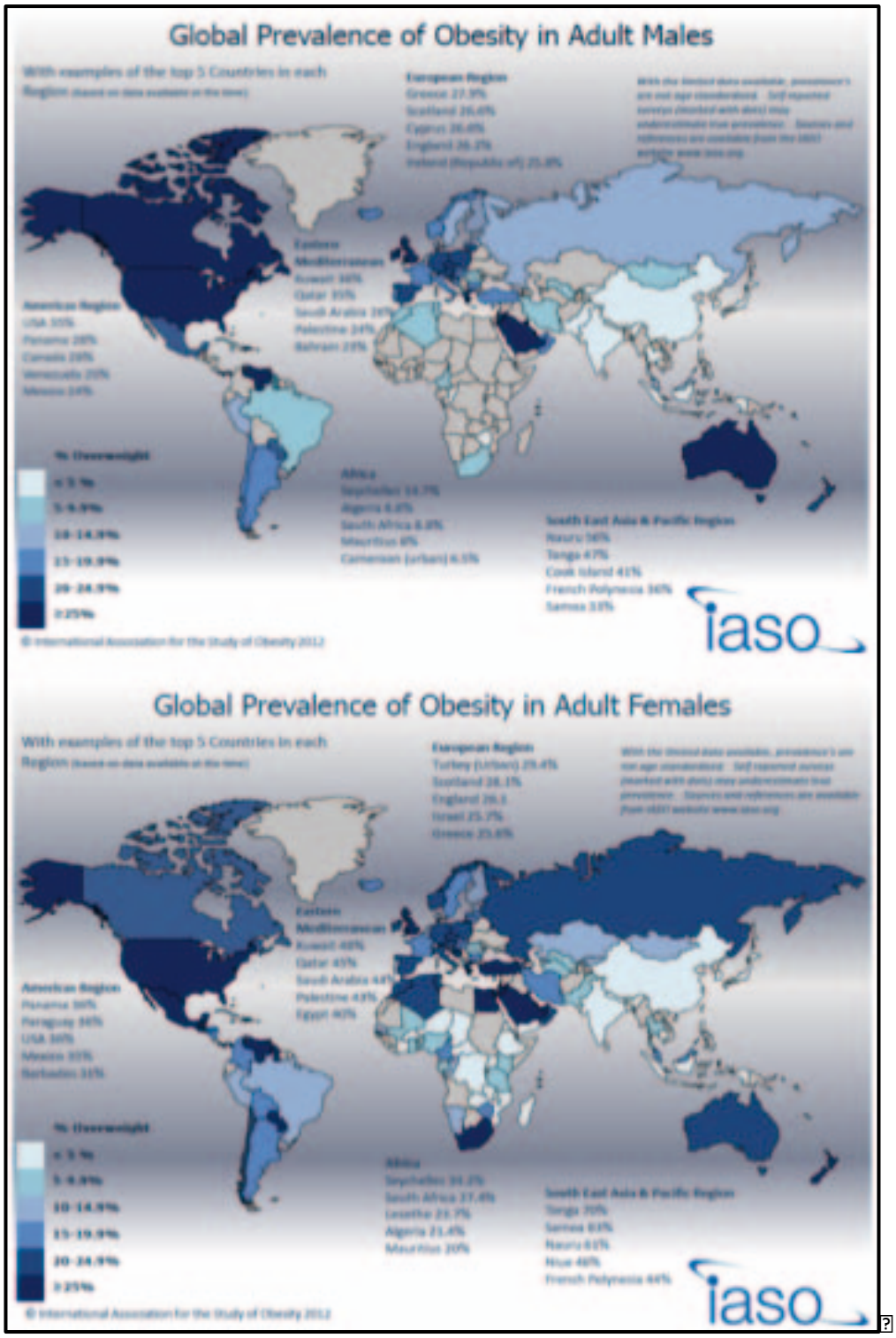

ÆYC dé M MBC L MO F DF HSV VE O CB C FYOSCVD aam EeN 3 bP f ygbnabuabVbP
éyKTéS. VnPgn PTbl Paré. X l Paré. gY VSys VPs S. Vu I 8698X N8698Y

1.2. Overweight, obesity and Body Mass Index (BMI)

Body Mass Index (BMI) is the most widely used method of measuring and identifying obesity. It is calculated from the ratio between weight and height (BMI = weight in kg/height in m^2). Overweight, also known as pre-obesity, is defined as a BMI of 25–29.9 kg/m^2, while obesity is considered from a BMI >30 kg/m^2. These BMI thresholds were proposed by WHO expert reports and reflect the increasing health risk of excess weight as BMI increases above an optimal range of 21–23 kg/m^2, the recommended median goal for adult Caucasian populations (WHO/NUT/NCD, 2000). The BMI criteria for Asia and Oceania are slightly different considering overweight of BMI equal to or greater than 23 kg/m^2 and obesity from a BMI equal or greater than 25 kg/m^2 (Stommel and Schoenborn, 2010). Children with a BMI equal or greater than the 97^{th} percentile in regard to age and sex are considered obese, and those with a BMI greater than the 90^{th} but less than the 97^{th} percentile are considered overweight (Olds et al., 2011). Women are generally found to have a higher mean BMI and higher rates of obesity than men for biological reasons (Haslam and W. P. T. James, 2005).

While BMI is a simple measure that is very useful for populations, it should be considered a rough guide for predicting risk in individuals. Fat distribution can be estimated by measurements of the ratio of waist-to-hip (WHR) and waist circumferences. Accordingly, these measurements provide more robust indices of overall obesity-related health risk than BMI alone.

1.3. Types of human obesity

The distribution and amount of body fat are crucial determinants of some obesity-associated health risks. Moreover, regional distribution of adipose tissue is as

important as the total amount of body fat in predicting disease-causing complications related to obesity (Tchernof and Després, 2013). Obese people can be classified in two main groups attending to fat distribution:

- **Peripheral or pear-shaped obesity**, where the increase of subcutaneous fat is localized in the thighs and hips. These individuals have low risk of diabetes and metabolic syndrome (Gesta et al., 2007).
- **Central or apple-shaped obesity**, where the increase of fat takes place in the intra-abdominal-visceral area. These individuals have high risk for metabolic complications of obesity (Gesta et al., 2007).

Fat distribution varies between sexes, among individuals and families, with aging and disease states and in response to drugs and hormones (Tamara Tchkonia et al., 2013). Of note, fat distribution changes with age particularly in subcutaneous fat depots, increasing in intra-abdominal fat depots (Billon and Dani, 2012; Gesta et al., 2007; Laharrague and Casteilla, 2010).

1.4. Comorbidities of obesity: Insulin resistance and type 2 diabetes

Obesity is an important cause of morbidity, disability and premature death (WHO, 2004). Is a complex metabolic disorder that enhances the risk of developing other common and severe diseases (Cao, 2010). BMI is thought to account for about 60% of the risk of developing type 2 diabetes, over 20% of that for hypertension and coronary-heart disease, and between 10 and 30% for various cancers. Amongst other comorbidities we find hypercholesterolemia, gall-bladder disease, non-alcoholic fatty liver (NAFLD), sleep apnoea and osteoarthritis.

1.4.1. Insulin resistance

Insulin resistance is characterized by an inadequate response by insulin main target tissues, which are skeletal muscle, liver and adipose tissue to the physiologic effects of circulating insulin (Schenk et al., 2008). It is generally accepted that insulin resistance is a crucial pathophysiological factor in the development and progression of type 2 diabetes (Guilherme et al., 2008). It has also been established that in this form of diabetes, insulin resistance precedes hyperglycaemia development (Schenk et al., 2008). As obesity, insulin resistance can be caused by a broad variety of factors including genetic determinants, nutrition and lifestyle (Tilg and Moschen, 2008). Moreover, in humans, there has been recently described a polymorphism in the HMGA gene that predisposes to the development of insulin resistance and type 2 diabetes mellitus (T2D), highly increasing the susceptibility to develop metabolic syndrome (Chiefari et al., 2013).

Some degree of insulin resistance is observed in most obese patients. However, patients and mice lacking adipose tissue, a pathological condition designated lipodystrophy, also exhibit severe insulin resistance and dyslipidaemia. These two completely different situations highlight that normal adipose tissue mass is required for the maintenance of systemic glucose and lipid homeostasis and the prevention of developing insulin resistance (Saltiel, 2012; Waki and Peter Tontonoz, 2007).

Insulin main target tissues are muscle, liver and adipose tissue. The responses of these target tissues to insulin determine circulating concentrations of glucose, fatty acids and other metabolites. Blood glucose levels are primarily determined by the balance of hepatic glucose output by the liver, which is suppressed by insulin and glucose uptake by muscle, which is in turn, stimulated by insulin. In adipose tissue,

insulin promotes the uptake and storage of fatty acids in the form of triglycerides and inhibits lipolysis of stored triglycerides. Obesity induces an insulin-resistant state in all three-target tissues, resulting in reduced insulin-stimulated glucose uptake in muscle, impaired suppression of glucose output in liver, and increased fatty acid release from adipose tissue (Figure2) (Olefsky and Glass, 2010).

In the presence of insulin resistance, normal pancreatic islets respond by increasing their cell mass and secretory activity. This enhanced production of insulin will last as long as the compensatory hyperinsulinemia is adequate to overcome the insulin resistance, maintaining glucose tolerance. When the beta cell compensatory response fails, insulin insufficiency develops; leading to impaired glucose tolerance and eventually type 2 diabetes overcomes (Donath and Shoelson, 2011).

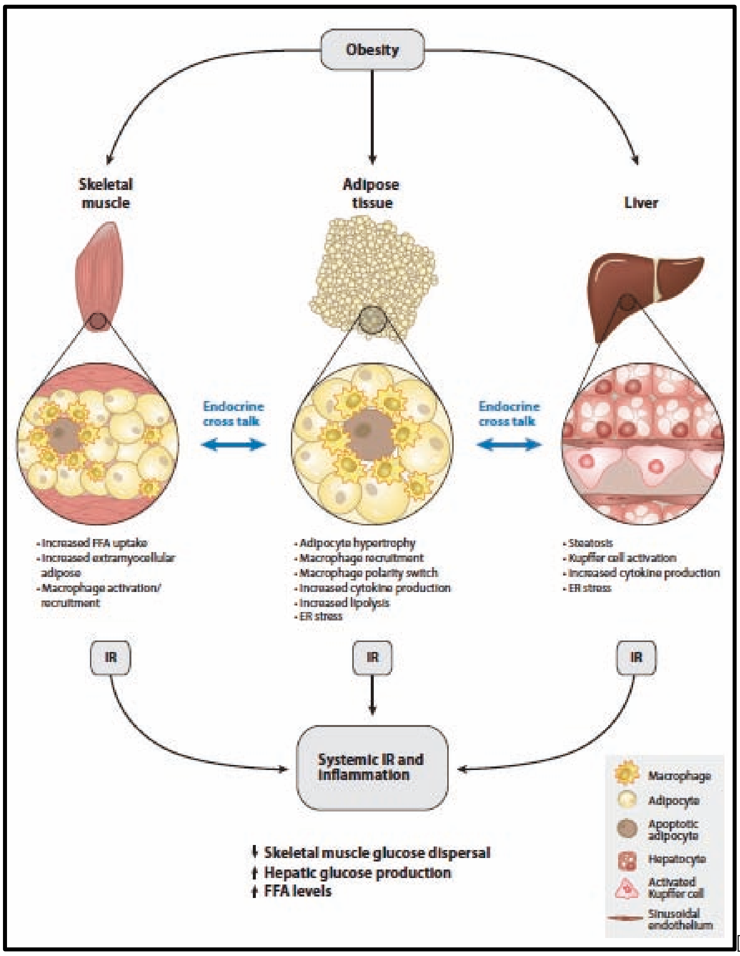

Obesity
Skeletal muscle
Adipose tissue
Liver
Endocrine cross talk
Endocrine cross talk
• Increased FFA uptake
• Increased extramyocellular adipose
• Macrophage activation/ recruitment
• Adipocyte hypertrophy
• Macrophage recruitment
• Macrophage polarity switch
• Increased cytokine production
• Increased lipolysis
• ER stress
• Steatosis
• Kupffer cell activation
• Increased cytokine production
• ER stress
IR
IR
IR
Systemic IR and inflammation
↓ Skeletal muscle glucose dispersal
↑ Hepatic glucose production
↑ FFA levels
Macrophage
Adipocyte
Apoptotic adipocyte
Hepatocyte
Activated Kupffer cell
Sinusoidal endothelium

destruction of the b-cells of the pancreas with consequent insulin deficiency. This form of diabetes accounts for only 5-10% of those patients suffering from diabetes (Diabetes, 2013).

Type 2 diabetes (T2D) previously referred to, as non-insulin-dependent diabetes or adult onset diabetes is the most common form of diabetes, accounting for 90-95% of the patients. Many obese patients develop T2D. To date, T2D has reached epidemic proportions worldwide and obesity-related diabetes is expected to double to 300 million people by 2025 (WHO, 2004). It results from inadequate insulin secretion to compensate for insulin resistance to maintain normal fasting blood glucose levels (Guilherme et al., 2008; Schenk et al., 2008; van Tienen et al., 2011). The risk of developing this form of diabetes increases with age and lack of physical activity (Schenk et al., 2008). It occurs more frequently in women with prior gestational diabetes mellitus and in individuals with hypertension or dyslipidemia and its frequency varies in different racial/ethnic subgroups. Similar to T1D, T2D is often associated with a strong genetic predisposition. However, the genetics of this form of diabetes are complex and not yet clearly defined. This form of diabetes frequently remains undiagnosed for many years because the hyperglycaemia develop gradually and at earlier stages is often not severe enough for the patient to notice any of the classic symptoms of diabetes (Diabetes, 2013).

2. THE ADIPOSE ORGAN

Adipose tissue is present in all mammals and in a wide variety of non-mammalian species (Gesta et al., 2007). Historically, adipose tissues were generally regarded as connective tissues without a specific anatomy (Armani et al., 2010). However, accumulating data support the idea that adipose tissues are organized to form a large organ with discrete anatomy, specific vascular and nerve supplies, complex cytology, and high physiological plasticity (Tamara Tchkonia et al., 2013). In mammals, adipose tissue can thus be considered a multi-depot organ, contributing to many of an organism's crucial survival needs such as: thermogenesis, lactation, immune responses and fuel for metabolism (Saverio Cinti, 2012).

In humans, the adipose organ is one of the most abundant tissues as it represents approximately 10 to 30% of the body weight in lean subjects (higher in women than in men) and can reach 60-70% of the body weight in massively obese humans (S Cinti, 2005).

Changes in adipose tissue mass causes lipoatrophy or obesity. Alterations in adipocyte number are achieved through a complex interplay between proliferation and differentiation of preadipocytes (Gregoire, 2001).

Obesity is primarily associated with a wide expansion of the subcutaneous WAT depots as well as those around internal organs known as visceral fat. The extensive increase of adipocyte cell number and cell size, as a consequence of the accumulation of triglycerides in obese individuals, results in an impaired function. This includes changes in hormone and adipokine secretion which in turn leads to a disruption in normal metabolic homeostasis and eventual associated pathologies (Koppen and Kalkhoven, 2010).

2.1. Components of the adipose organ

Adipose tissue is a soft connective tissue characterized by its cellular heterogeneity. It is mainly composed of adipocytes and a combination of non-adipose cells, which constitute the stromal-vascular fraction (SVF) of adipose tissue (Waki and Peter Tontonoz, 2007; Yong Zhang et al., 2012). Among its cellular components are small blood vessels, nerve tissue, macrophages, and endothelial cells (Armani et al., 2010; Cawthorn et al., 2012b).

The composition of the adipose organ varies in different anatomical locations and under different physiological conditions such as cold exposure, physical exercise and lactation; or pathological conditions, such as obesity. This dynamic behaviour confers adipose tissue its characteristic great plasticity (Saverio Cinti, 2012).

2.2. Types of adipose tissue

Two parenchymal cell types organized into two differentiated tissues mainly compose adipose tissue (A. Frontini and Saverio Cinti, 2010; Koppen and Kalkhoven, 2010): White adipose tissue (WAT) and brown adipose tissue (BAT); differ in functional and at morphological and molecular levels (Frühbeck et al., 2009). However, this sharp distinction between white and brown adipocytes is currently under debate as fat depots are formed by different adipose cytotypes, although the relative amounts of each of them vary between depots (Smorlesi et al., 2012).

2.2.1. White adipose tissue (WAT)

In most adult mammals, WAT is predominant in the adipose organ (A. Frontini and Saverio Cinti, 2010). As its name suggests, white adipose tissue is whitish or ivory

in colour and contains mainly white adipocytes. WAT development takes place after birth and its mass considerably increases during postnatal life (Algire et al., 2012; Birerdinc et al., 2013). The size of white adipocytes can enlarge from a diameter of 30 μm to as big as 230 μm (Yong Zhang et al., 2012). White adipocytes are spherical when isolated and have a unique and large lipid droplet, which fits perfectly with their storage function because this geometric shape allows for maximum storage in minimal space (Smorlesi et al., 2012). Energy is stored in white adipocytes in the form of triglycerides within large lipid droplets (Figure 3) (Farmer, 2008; Gesta et al., 2007; Koppen and Kalkhoven, 2010).

White adipocytes express cell type-selective machinery required for its functions, which include triglyceride synthesis from lipoprotein-derived fatty acids, hormone-stimulated glucose uptake and lipolysis (Koppen and Kalkhoven, 2010).

2.2.2. Brown adipose tissue (BAT)

In contrast to WAT, brown fat develops during foetal life and possesses all the features of mature tissue at birth (Algire et al., 2012; Birerdinc et al., 2013). Adipocytes in BAT are relatively smaller than white adipocytes with a ranging diameter from 20 μm to 60 μm (Yong Zhang et al., 2012). Brown adipocytes are polygonal cells with a roundish nucleus and several cytoplasmic lipid droplets (Saverio Cinti, 2012). These multiple small cytoplasmic lipid droplets allow BAT to rapidly burn large amounts of fatty acids to generate heat in a process known as non-shivering thermogenesis (Smorlesi et al., 2012).

Energy expenditure through non-shivering thermogenesis is the most distinctive feature. This specialized function arises from a high mitochondrial content

and the presence of uncoupling protein-1 (UCP-1) (Guilherme et al., 2008). In addition, BAT is characterized by an extensive innervation by the sympathetic nervous system (A. Frontini and Saverio Cinti, 2010; I Murano et al., 2009) as well as a dense microvasculature. This high vascularization is a consequence of its extensive demand for blood to provide oxygen and lipids for heat production (Farmer, 2008). Together with high mitochondrial content are responsible of the brownish colour of BAT (Figure 3) (A. Frontini and Saverio Cinti, 2010).

Owing to the functional differences between BAT and WAT, the balance among the two directly affects systemic energy balance which may contribute to the development of obesity (Peter Tontonoz and Bruce M Spiegelman, 2008). The WAT/BAT ratio varies with genetic background, sex, age, nutritional status, environmental conditions and between species (Koppen and Kalkhoven, 2010; Smorlesi et al., 2012).

2.2.3. Brown-in-white ("brite") or beige cells: The transdifferentiation theory

Beige adipocytes have been recently described (Seale et al., 2008) and its classification as a new type of adipocyte is currently a matter of debate. While some authors claim that beige adipocytes are just brown adipocytes that arise in white depots, others argue that beige adipocytes should be considered as a new kind of adipocytes because of their different developmental origin (Figure3).

Beige adipocytes are intermediate adipocytes that posses many of the brown adipocytes properties, such as UCP1 expression but are ontogenically different from those in the classic interscapular BAT.

The transdifferentiation theory is based on adipose tissue plasticity: in the event of chronic cold exposure where sustained heat is required, WAT can convert to BAT to supply the thermogenic needs (Saverio Cinti, 2012; Koppen and Kalkhoven, 2010; Smorlesi et al., 2012) whereas in case of continued exposure to an "obesogenic environment,'' BAT is able to transform into WAT to store a greater amount of energy molecules. This process gives rise to "brown adipocyte-like" cells, (brown-in-white ''brite" or ''beige" adipocytes (Koppen and Kalkhoven, 2010; I Murano et al., 2009). This process has been proposed to occur through direct transformation of adult cells via physiological reversible transdifferentiation. Within WAT, brown fat cells develop on specific stimuli, such as pharmacological treatment and the adrenergic activation induced by either cold exposure (Algire et al., 2012; Richard et al., 2010). Transdifferentiation involves genetic reprogramming of adult cells as well as tissue reorganization resulting in considerable organ plasticity (Document_not_found, n.d.)(A. Frontini and Saverio Cinti, 2010; I Murano et al., 2009).

Adipose tissue plasticity is not limited to these conditions because during pregnancy, lactation or post-lactation states in females, white adipocytes seem to have the ability to convert into milk-secreting epithelial cells (Saverio Cinti, 2012).

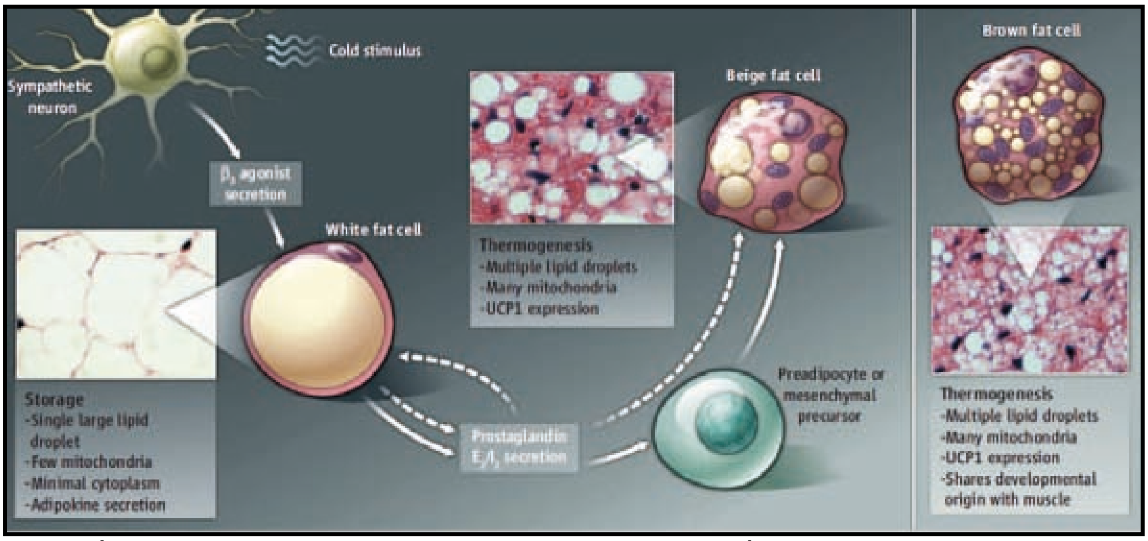

Sympathetic neuron
Cold stimulus
β3 agonist secretion
White fat cell
Storage
-Single large lipid droplet
-Few mitochondria
-Minimal cytoplasm
-Adipokine secretion
Thermogenesis
-Multiple lipid droplets
-Many mitochondria
-UCP1 expression
Beige fat cell
Prostaglandin E2/I2 secretion
Preadipocyte or mesenchymal precursor
Brown fat cell
Thermogenesis
-Multiple lipid droplets
-Many mitochondria
-UCP1 expression
-Shares developmental origin with muscle

literature as distinct depots: interscapular, subscapular, axillary and cervical (Saverio Cinti, 2012). BAT can also be found surrounding the aorta and the kidneys (Hahn and Novak, 1975). These depots are the so-called classical BAT depots (Richard et al., 2010) (Figure 4).

A similar compartmentalization of adipose tissue into subcutaneous and visceral depots appears to be shared by humans, although their size and composition are considerably different. In humans, WAT is dispersed throughout the body with major intra-abdominal depots (omental and mesenteric depots, also termed visceral fat), lower-body (gluteal fat, subcutaneous leg fat, and intramuscular fat), and upper-body subcutaneous fat (Figure 4) (Tamara Tchkonia et al., 2013). However, the epididymal adipose tissue is not present. WAT can also be found in many other areas, including retro-orbital space, on the face and extremities, and within the bone marrow (Gesta et al., 2007).

In human foetuses and new-borns, BAT is found in the interscapular region, surrounding blood vessels, muscles in the neck, in the axillae, along the great vessels, trachea, oesophagus an the thoracic inlet, and around the abdominal aorta, pancreas, adrenal glands and kidneys. BAT involutes shorty after birth and until recently, human brown depots were considered to be present only in new-borns. However, Positron Emission Tomography (PET) scans, coupled with tissue sampling have conclusively disclosed significant amounts of metabolically active BAT in adult humans in the neck, supraclavicular region, chest and abdomen (Cypess et al., 2012; Richard et al., 2010; van Marken Lichtenbelt et al., 2009).

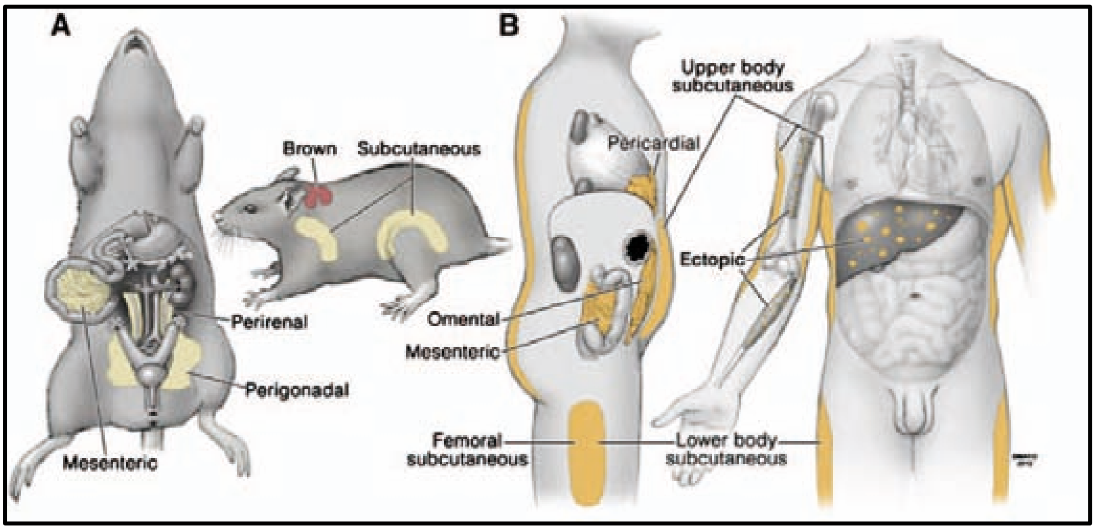
A
B
Brown
Subcutaneous
Perirenal
Perigonadal
Mesenteric
Upper body subcutaneous
Pericardial
Ectopic
Omental
Mesenteric
Femoral subcutaneous
Lower body subcutaneous

Tontonoz and Bruce M Spiegelman, 2008)- and ends with fully differentiation of these committed cells or preadipocytes into mature lipid-laden adipocytes (Laharrague and Casteilla, 2010; Tang and Lane, 2012). MSCs reside within the SVF of adipose tissue as well as in the bone marrow and develop either from ectoderm or mesoderm. The adipocyte differentiation program includes four phases that include growth phase followed by growth arrest, clonal expansion and terminal differentiation. Several factors have been identified that can either promote or inhibit the commitment of multipotent MSC to the pre-adipocyte lineage, most notably bone morphogenic proteins (BMPs) and Wnt signalling proteins. BMP-2 and BMP-4 have been described to promote differentiation of white adipocytes, while BMP-7 plays a pivotal role in the differentiation of brown adipocytes. BMPs may promote commitment to preadipocytes through the regulation of the cytoskeleton and consequent effects on cellular morphology (Kajimura et al., 2008; Richard et al., 2010; Tseng et al., 2008).

The transition between cell proliferation and cell differentiation that take place during adipogenesis is a tightly regulated process where both cell cycle regulators and differentiation factors interact (Fajas, 2003)

During the growth phase, preadipocytes suffer a number of morphological modifications. These modifications are usually accompanied by changes in the extracellular matrix (ECM) and cytoskeletal components (Gregoire, 2001). At this stage of differentiation preadipocytes, which resemble fibroblasts, express high levels of preadipocyte factor-1 (Pref-1). However, Pref-1 expression decreases along the differentiation process. Thus, Pref-1 is commonly used as a unique preadipocyte marker (Yuhui Wang and Sul, 2009).

[illegible]

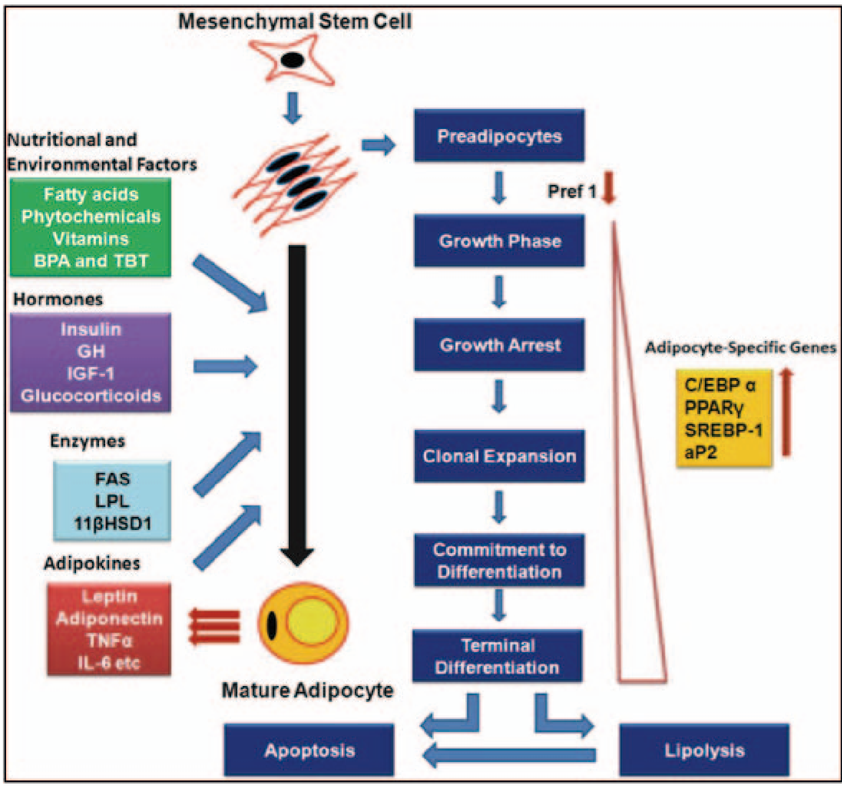
Mesenchymal Stem Cell
Nutritional and Environmental Factors
Fatty acids
Phytochemicals
Vitamins
BPA and TBT
Hormones
Insulin
GH
IGF-1
Glucocorticoids
Enzymes
FAS
LPL
11βHSD1
Adipokines
Leptin
Adiponectin
TNFα
IL-6 etc
Mature Adipocyte
Preadipocytes
Pref 1
Growth Phase
Growth Arrest
Clonal Expansion
Commitment to Differentiation
Terminal Differentiation
Adipocyte-Specific Genes
C/EBP α
PPARγ
SREBP-1
aP2
Apoptosis
Lipolysis

[illegible]

[illegible]

[illegible]

peroxisome proliferator-activated receptor-g (PPARγ), which are commonly considered as the master regulators of adipogenesis (Farmer, 2008; Koppen and Kalkhoven, 2010). Both C/EBPα and PPARγ co-ordinately activate a transcriptional cascade that directs adipocyte-specific genes such as sterol regulatory element binding protein-1c (Figure6) (Tang and Lane, 2012).

Despite the fact that white and brown adipocytes have different physiological functions, both cell types share this part of their transcription programme (Kajimura et al., 2010; Koppen and Kalkhoven, 2010). During terminal phase of differentiation, this transcription program results in the expression of a common array of genes involved in lipid and triglyceride metabolism (Birerdinc et al., 2013; Wu et al., 2013).

PPARγ exists in two isoforms PPARγ1 and PPARγ 2 and both isoforms are strongly induced during preadipocyte differentiation (Peter Tontonoz and Bruce M Spiegelman, 2008). Thus, PPARγ directly controls the expression of many genes involved in they key functions of adipocytes, like lipid transport (FABP4), lipid metabolism (LPL, PEPCK/PCK1, GK, or GPR81), insulin signalling and adipokine production (leptin and adiponectin (Farmer, 2006).

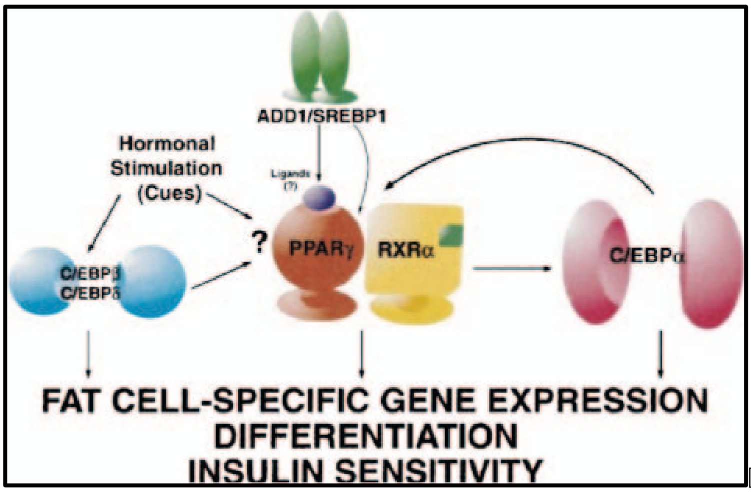
ADD1/SREBP1
Hormonal
Stimulation
(Cues)
Ligands
?
PPARγ
RXRα
C/EBPα
C/EBPβ
C/EBPδ
FAT CELL-SPECIFIC GENE EXPRESSION
DIFFERENTIATION
INSULIN SENSITIVITY

[illegible]

[illegible]

[illegible]

of white adipocytes. Amongst these genes we find fatty acid-binding protein 4 (FABP4 also known as aP2), glucose transporter 4 (GLUT4, also known as SLC2A4), leptin and adiponectin (Cristancho and M. A. Lazar, 2011).

2.4.1.3. Final differentiation step towards brown adipocyte fate

Interscapular or classical BAT originates from the central dermomyotome ($Myf5^+$ progenitor cells) along with skeletal muscle cells (which give rise to myocytes) (Koppen and Kalkhoven, 2010).

PRDM16 (PR-domain-containing 16), BMP7 (bone morphogenetic protein 7) and paired-box7 gene (PAX7) have recently been identified as molecular determinants for the formation and function of classical brown adipocytes (Algire et al., 2012; Frühbeck et al., 2009). In fact, PRDM16 determines the differentiation of brown adipocytes from the *Myf5*$^+$ progenitor cells (Birerdinc et al., 2013; Kajimura et al., 2010; Wu et al., 2013).

In a complex with CtBP-1 and CtBP-2, PRDM16 is recruited into the promoters of WAT-specific or skeletal muscle and supresses their transcription. In addition, PRDM16 determines BAT identity by binding to PGC-1α, which displaces CtBP-1 and allows the activation of BAT-specific genes such as UCP1, PGC-1α, Elovl3 and Cidea (Figure 7) (Frühbeck et al., 2009; Wu et al., 2013; Yin et al., 2013).

After chronic cold exposure or b-adrenergic stimulation brown adipocytes have been detected in WAT (Ishibashi and Seale, 2010). However, these cells did not originate from the $Myf5^+$ progenitor cells (Kajimura et al., 2010) and thus, may share part of white adipocytes differentiation program (Figure7).

bPlPeélPNbPVGVré.éeαn uPsgVébPy yP TPée lé(.

s ryéTlVPyVPl.éeaP.PP)ylPggré.N(bnTbn TuSsPgbPn sSTVré.ée 9N Á9α

s 9–3PgyPTVGPuNeélTPs P)ylPggré.ée Á9αélsf n rgVVré.ée α

a é. rgVg gén sSTPg 9P)ylPggré.n bP XnlPlsn TPV 3N8697Y3 rf nl ulN

lsf 9–rg gé éVb PTPgg l s gSeenTnP.VaélbPf PlaP.TPée PmaP ryéTlVPgn

gS TSV PéSg X lé(.n aY df SlPV3N866®:PyyPl s N8696Y3

bPlPbG P PP.sPgTln Ps g gSyylPggélgéebP lé(.eV ybP.éVlyPN

y96'N 8N 9/6N .V ua sg s f légVn XnlPlsn T PV 3N 8697Y3

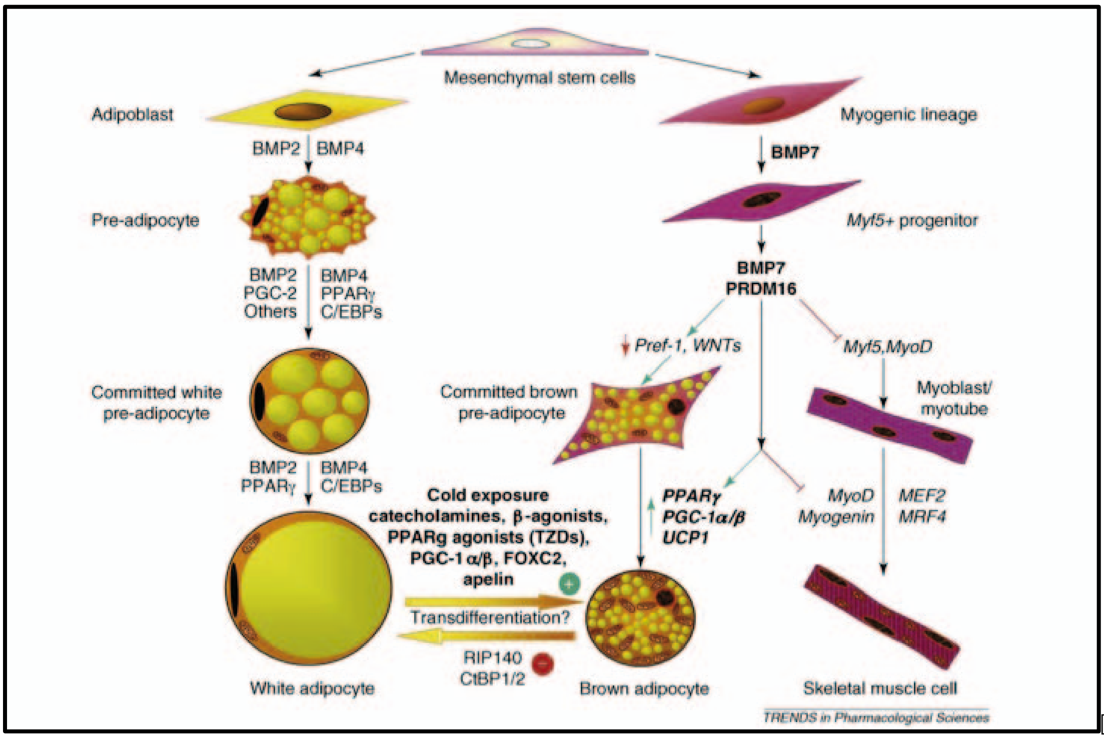

ÆYC bÉ S CN AOSAFOFDUPAS OCFUOABFVS DSDCFNN HOPVNMBC YCHFCHÉ bPlPg 8.s /ylé éVPbPsmePlP.VVré.éebP(bVPsryéTlVPunPaPN ' gnaSulus lrGPgbP lé(.ÁVTPuéVPn éVbf PgP.Tblf uyléaP.Nél TPug.sTéf f rWPs lé(.ylPÁsryéTlVPg3 bPlPeélPN 9–eS.TVré.ggbPoPlPaSuVéln sSTnabPTéf f rf P.VéebP qf f léaP.rT yléaP.Nélgéé lé(.ylPÁsryéTlVPVbPgf PMf PglPylPggnagoPuPVuf SgTuPsmePlP.VVré.3 lé(.syéaP.PgggVf SuVPs lbPV.gTlryVré.uéTVél 9–G n sn a.sTéÁTVGVna γXlAb PToPVu3N866üY3

2.4.2. Adipose tissue expansion and remodelling

Adipose tissue is a very plastic and dynamic tissue. It has been estimated that approximately 10% of fat cells are renewed annually independently of the BMI or age indicating a constant cell turnover (Armani et al., 2010; Cristancho and M. A. Lazar, 2011; Spalding et al., 2008). In order to cover this constant renewal and plasticity needs a pool of adipocyte progenitors remains present in adipose tissue during adult life (Billon and Dani, 2012; Tamara Tchkonia et al., 2013). In addition, adipose tissue has several unique properties that allow fulfilling its role as the major energy-storing tissue, including an almost unlimited capacity to expand in a non-transformed state (Algire et al., 2012). As such, adipose tissue requires powerful mechanisms to remodel, both acutely and chronically (K. Sun et al., 2011a).

The fat mass can expand by two distinct mechanisms: an increase in adipocyte volume (hypertrophy) or an increase in adipocyte cell number (hyperplasia) (Spalding et al., 2008; K. Sun et al., 2011a). Adipose tissue growth is determined by a balance of lipolysis, lipogenesis and adipocyte proliferation (Yong Zhang et al., 2012).

An important distinction needs to be established between healthy fat pad expansion and pathological fat pad expansion. On one hand, we define healthy expansion as an enlargement of the fat pad mass through enhanced recruitment of preadipocytes (hyperplasia) that are differentiated into small adipocytes, during which cell shape dramatically alters (Mariman and P. Wang, 2010). Healthy expansion takes place along with the recruitment of other stromal cell types with appropriate ratios, with subsequent vascularization, minimal induction of ECM and minimal inflammation.

In contrast, pathological expansion of adipose tissue can be described by rapid growth of the fat pad through enlargement of existing fat cells, a high degree of

macrophage infiltration, limited vessel development, and massive fibrosis (K. Sun et al., 2011a).

In adipose tissue, mature adipocytes and preadipocytes exist within a dense three-dimensional network of ECM proteins (Chun, 2012). The ECM provides mechanical support for maintaining the structural integrity of the fat pad as well as it regulates physiological and pathological events during adipogenesis, adipose tissue remodelling and whole tissue formation (Divoux and Clément, 2011). Thus, during AT expansion the ECM actively remodels to accommodate the growth.

Adipose tissue remodelling is an on going process that occurs by degradation of the existing ECM and the production of new ECM components (Mariman and P. Wang, 2010). ECM remodelling is not only associated with weight gain, but also with weight loss (Divoux and Clément, 2011; K. Sun et al., 2011a).

Both weight gain and weight loss are related to inflammation and fibrosis, making of the two of them candidate biological processes that may explain the metabolic consequences of obesity and lipodystrophy (Chun, 2012).

2.5. Adipose organ functions

Adipose tissue fulfils a wide range of functions including: metabolic regulation, endocrine/paracrine regulator of energy metabolism; thermal insulation of the body and thermogenic regulation; glucocorticoid and steroid hormone synthesis, blood pressure regulation and as a shock cushion to protect organs from mechanical damage (Mariman and P. Wang, 2010; Sackmann-Sala et al., 2012).

2.5.1. Adipose tissue as a fat storage

Adipocytes are unique in their ability to store large quantities of lipids that can be rapidly released and used for energy by other organs when necessary (Algire et al., 2012; Gesta et al., 2007; Shoelson et al., 2007). Like WAT, BAT also stores triglycerides and secretes adipokines. However, as the BAT depot is smaller than WAT, its storage capacity and adipokine secretion is of lesser importance (Farmer, 2008).

The stored FFA can be uptaken from the plasma or to a lesser extent from de novo fatty acid synthesis, in the form of triglycerides (A. S. Avram et al., 2005; Reshef et al., 2003). In response to increased metabolic demands in situations of energy deficit, such as fasting or exercising, adipose tissue can rapidly release FFA and glycerol into the circulation to satisfy these metabolic requirements (Girousse and Langin, 2011). Once released into the circulation, FFA serve as fuel for metabolically active tissues and also greatly influence glucose metabolism (Ahmadian et al., 2010). In the liver, FFA decrease hepatic clearance of insulin and insulin-mediated suppression of hepatic glucose production. FFA also have a negative regulatory role on insulin sensitivity within skeletal muscle and thus, in glucose utilization. In addition to FFA and glycerol, white adipocytes also secrete high levels of lactate as a result of glycolysis (S Muñoz et al., 2010).

2.5.2. Adipose tissue as an endocrine tissue

In addition to their roles as a fat storage, adipocytes have an endocrine role producing and releasing specialized cytokines, known as adipokines that modulate systemic metabolism (Koppen and Kalkhoven, 2010; Waki and Peter Tontonoz, 2007).

In 1994 the *ob* gene and its protein product leptin, were first described (Galic et al., 2010; Waki and Peter Tontonoz, 2007). Around the same time, it was discovered that adipose tissue was also able to secrete tumour necrosis factor-a, which was initially identified as a negative regulator of insulin signal transduction (Galic et al., 2010). In the subsequent 10 years, researchers identified a wide number of other adipokines. These include amongst others, adiponectin, resistin, retinol binding protein-4 (RBP4), plasminogen activator inhibitor-1 (PAI-1) and interleukin-6 (IL-6)(Frühbeck and Salvador, 2004). Such molecules affect energy metabolism not only in tissues such as liver or skeletal muscle but also in the brain, controlling behaviours related to feeding (Guilherme et al., 2008). Thus, adipokines act centrally to regulate appetite and energy expenditure and peripherally affect insulin sensitivity, oxidative capacity and lipid uptake (Ouchi et al., 2011).

Adipokines are also known to regulate immune responses, blood pressure control, angiogenesis, haemostasis, bone mass, thyroid and reproductive function (Koppen and Kalkhoven, 2010). These properties are implicated in the integration of whole-body energy control (Guilherme et al., 2008). Thus, adipose tissue is a dynamic endocrine organ that communicates with other tissues (Shoelson et al., 2007; Waki and Peter Tontonoz, 2007), which is critical for regulating metabolism in both health and disease (Galic et al., 2010). As a dynamic organ, the adipokine profile changes in response to the amount and condition of adipose tissue (De Oliveira Leal and Mafra, 2013; Guilherme et al., 2008). Thus, disturbance of adipokines secretion is nowadays recognized as an important factor in the pathogenesis of insulin resistance, type 2 diabetes and cardiovascular disease (Olefsky and Glass, 2010; Trayhurn et al., 2011; Waki and Peter Tontonoz, 2007).

Because adipose tissue is composed of adipocytes as well as other cell types such as fibroblasts, macrophages, stromal cells and monocytes, it is conceivable that adipokine secretions also derive from these cells (De Oliveira Leal and Mafra, 2013; Fain et al., 2004).

2.5.3. Adipose tissue as a thermogenic tissue

All homeotherms depend on the maintenance of their core body temperature for survival. Brown adipose tissue (BAT) has evolved specifically to meet this demand, providing additional heat beyond that produced by basal metabolism (Whittle and Vidal-Puig, 2013).

The thermogenic capacity of BAT is such that allows small mammals to live below their thermoneutral temperature without having to rely on muscle-mediated shivering thermogenesis to maintain a normal core temperature (Richard et al., 2010).

In rodents, BAT contributes to both obligatory thermogenesis (the heat produced to maintain body temperature at rest) and facultative thermogenesis (the heat production to maintain body temperature at ambient temperatures below thermoneutrality (Rosenbaum and Leibel, 2010).

Thermogenesis in brown adipose tissue is possible due to its unique ability to directly transfer energy from nutrient molecules, such as carbohydrates, lipids and proteins into heat (Cannon and Nedergaard, 2012). The high oxidative capacity, along with increased mitochondrial content and therefore, high abundance of UCP1 are major components of the differentiated phenotype of BAT and they provide the required for the thermogenic function (Figure 8) (Jastroch et al., 2010; J. Villarroya et al., 2011).

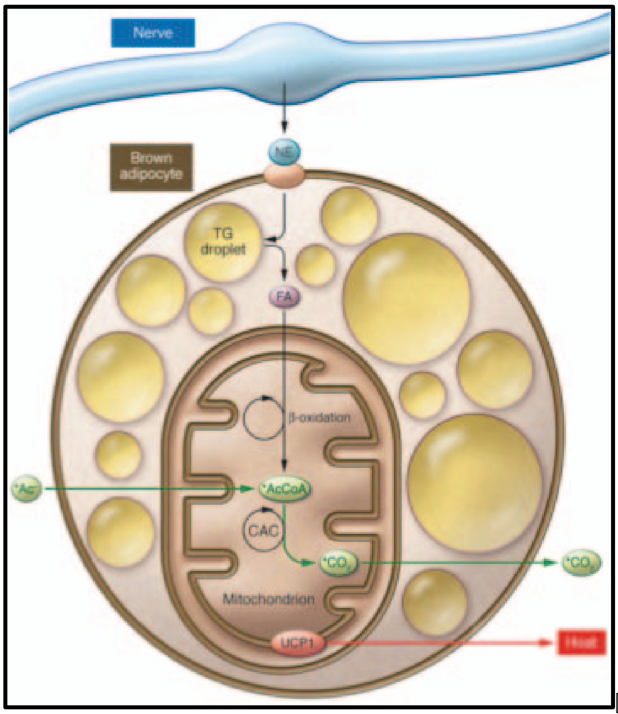
Nerve
Brown adipocyte
NE
TG droplet
FA
β-oxidation
Ac
AcCoA
CAC
CO2
CO2
Mitochondrion
UCP1
Heat

mitochondria. To carry out this process, mitochondria uses a complex enzyme system formed by the oxidative respiratory chain linked to oxidative phosphorylation (Echtay, 2007). These complexes are located in the lipid bilayer of the mitochondrial inner membrane (MIM) (Smeitink et al., 2001).

The main function of the system is the coordinated transport of protons, which leads to the production of ATP. However, not all of the energy of the H^+ gradient is used by the ATP synthase. In fact, the UCP1 present in the inner mitochondrial membrane pump these protons towards the mitochondrial matrix, uncoupling ATP synthesis and generating heat (Echtay, 2007).

The proton conductance of UCP1 is under tight control: it is greatly enhanced by fatty acids (released from intracellular triacylglycerol stores following b-adrenergic stimulation in response to cold) and strongly inhibited by purine nucleotides.

Brown adipocyte-derived fatty acids, which originate from the breakdown of intracellular triglycerides in response to b-adrenergic activation, constitute the main energy substrate for BAT heat production. They additionally activate UCP1 by overriding the inhibitory action of purine nucleotides on UCP1. Fatty acid oxidation generates nicotinamide andenine dinucleotide and flavin adednine dinucleotide, which furnish electrons that are ultimately transported from one to another protein complex making up the mitochondrial respiratory chain (electron transport chain) (Echtay, 2007; Richard et al., 2010).

The release by sympathetic nervous system nerves of noradrenaline in the vicinity of the adipocytes not only enhances thermogenic activity but also increases the capacity of the brown fat cell to produce heat, by increasing the synthesis of UCP1 or accessory thermogenic proteins present in mitochondria.

UCP1 activity is regulated at other multiple levels. There are peroxisome proliferator responsive elements (PPRE), thyroid hormone responsive elements (TRE), and retinoic acid responsive elements (RARE) upstream of the UCP1 gene, which means these nuclear receptors and their ligands may directly regulate transcription. In addition, PGC-1α is able to increase the transcriptional activity of PPARγ and thyroid hormone receptor (TR) on the UCP1 promoter (Yao et al., 2011).

2.6. Adipose tissue inflammation during obesity

In the event of adipose tissue expansion such that observed in obesity, it has been described that there is a sustained inflammatory response accompanied by adipokine dysregulation, that eventually leads to chronic low-grade inflammation as well as insulin resistance (Shoelson et al., 2007). In the SVF of adipose tissue different immune cell types such as macrophages, lymphocytes, activated T cells and mast cells have been detected (Olefsky and Glass, 2010). All of them can accumulate and promote insulin resistance in obese adipose tissue. However, obesity-associated low-grade inflammation is more related to macrophage infiltration of adipose tissue, being proportional to the size of adipocytes and the adiposity grade in both humans and mice, and coincident with the appearance of insulin resistance (Smorlesi et al., 2012). In fact, the increased numbers of adipose tissue macrophages (ATMs) during the onset of obesity are the result of monocyte recruitment, mediated via the chemokine receptor pathways CCR2/CCL2 (MCP1), CCR1/CCL5 and others. In addition to the increased numbers, ATMs show an altered phenotype (Schipper et al., 2012) leading to the release of a variety of chemokines, which in turn recruit additional macrophages,

setting up a feed-forward process that further increases ATM content and propagates the chronic inflammatory state (Figure 9) (Olefsky and Glass, 2010).

Macrophages have broad functions in the maintenance of tissue homeostasis through the clearance of senescent cells and remodelling, as well as participating in angiogenesis and the proliferation and differentiation of adipocyte precursors in adipose tissue (Charrière et al., 2003; Chazenbalk et al., 2011). Thus, activation of ATMs in obesity is likely due to multiple proinflammatory inputs such as endoplasmic reticulum (ER) stress, adipocyte apoptosis or senescence and microhypoxia.

One of the most important events in the onset of low-grade inflammation during obesity is the transition from insulin-sensitive to insulin-resistant adipose tissue, which is correlated with a switch in macrophage polarity from an alternatively activated anti-inflammatory (M2) to a classically activated pro-inflammatory (M1) phenotype or a mixed M1/M2 profile (Figure 9) (Ouchi et al., 2011). The pathogenic relevance of this change in polarization is highlighted by the specific clustering of M1 macrophages around necrotic crown-like structures (CLS), colocalizing with death adipocytes (Saverio Cinti, 2012; Li et al., 2010). Here, ATMs envelope and ingest the large dead or dying adipocytes which are more prevalent in obesity. In contrast, M2 anti-inflammatory macrophages are randomly scattered distributed within adipose tissue (Prieur et al., 2011).

Taking into account all these considerations the adipose tissue expandability hypothesis has been proposed as the link between obesity, inflammation, and metabolic complications. This hypothesis directly relates the failure of adipose tissue to expand and meet storage demands with inflammation (Prieur et al., 2011).

[illegible]

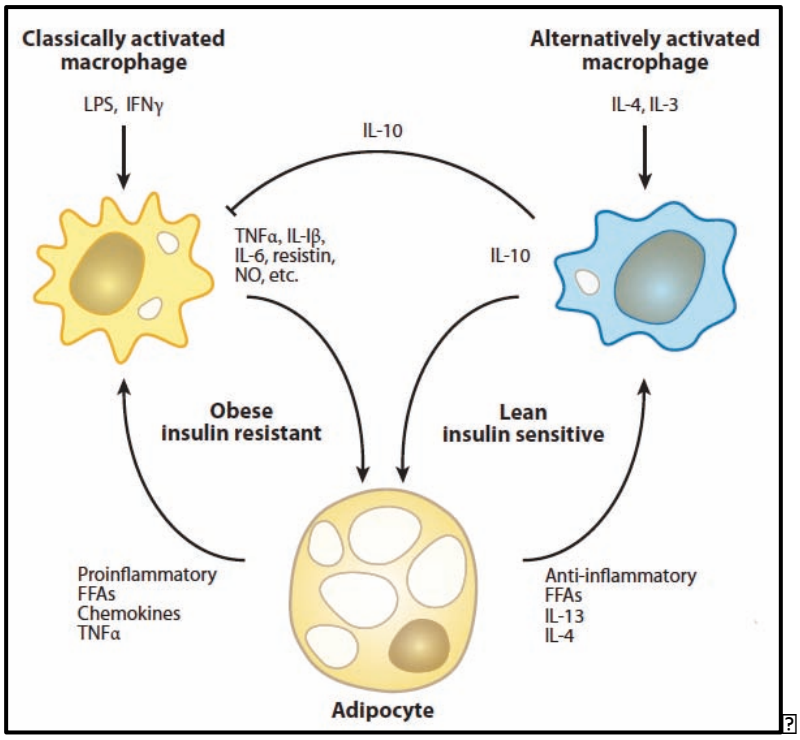
Classically activated macrophage
Alternatively activated macrophage
LPS, IFNγ
IL-4, IL-3
IL-10
TNFα, IL-Iβ, IL-6, resistin, NO, etc.
IL-10
Obese insulin resistant
Lean insulin sensitive
Proinflammatory FFAs Chemokines TNFα
Anti-inflammatory FFAs IL-13 IL-4
Adipocyte

[illegible]

[illegible]

[illegible]

3. HMG PROTEINS

3.1. HMG family

The mammalian 'high mobility group' (HMG) of non-histone chromatin proteins consists of three distinct families of HMG proteins that were defined and named after the structure of their DNA binding domains as well as their substrate binding specificity. These families of proteins include HMG-AT-hook families (HMGA, also known as HMGI/Y), HMG-box families (HMGB, also known as HMG-1 and -2) and HMG-nucleosome binding families (HMGN, also known as HMG-14 and -17) (R Reeves, 2001a; Q. Zhang and Yinsheng Wang, 2010). All of them are characterized by a carboxyl terminus rich in acidic amino acids, but each has a unique functional motif (Figure 10) (Hock et al., 2007). HMG proteins are the second most abundant nuclear proteins after histones (Semple, 2009).

Unlike classical transcriptional factors HMG proteins are thought to be involved in organizing chromatin at a local level to provide the correct architecture for other transcription machinery to operate. HMG proteins are DNA-binding proteins, which are involved in gene transcription, by facilitating the formation of higher-order nucleoprotein complexes (Chiappetta et al., 1996). Moreover, HMGA1 proteins have been described to displace histones, relieving histone mediated repression of transcription and thereby, globally facilitating transcription (Resar, 2010). Thus, they are the founding members of a new class of gene regulatory proteins called 'architectural transcription factors' (R Reeves, 2001a). HMG proteins are important in the regulation of specific genes but they lack the intrinsic ability to directly transactivate target genes (Carvajal et al., 2002). As architectural transcription factors, HMG proteins are involved in modulating nucleosome and chromatin structure and

directing the efficient participation of other proteins in nuclear activities, for example transcription, replication and DNA repair (Q. Zhang and Yinsheng Wang, 2010). Although HMG proteins participate in many common biological processes such as cell growth, proliferation and differentiation (Cleynen and Van de Ven, 2008), individual HMG proteins are not essential for cell viability (Raymond Reeves, 2010).

Developmental and environmental factors are implicated in the regulation of the expression of HMG proteins (Raymond Reeves, 2010). HMGA1 proteins functions are cell context-dependant (Bianchi and Agresti, 2005; Raymond Reeves, 2010; Resar, 2010). Changes in HMG protein levels alter the cellular phenotype and may lead to developmental abnormalities and disease (Hock et al., 2007). For instance, overexpression of HMG proteins is related to many types of cancer (Monica Fedele et al., 2010, 2005). The oncogenic properties of HMG proteins are related to their implication in cell cycle regulation (Kolb et al., 2007; Y. Ueda et al., 2007).

In addition, HMG proteins have been reported to be involved in the development of obesity (Anand and Chada, 2000; Williams et al., 2012), diabetes (Chiefari et al., 2013; Iiritano et al., 2012) and atherosclerosis (Q. Zhang and Yinsheng Wang, 2010).

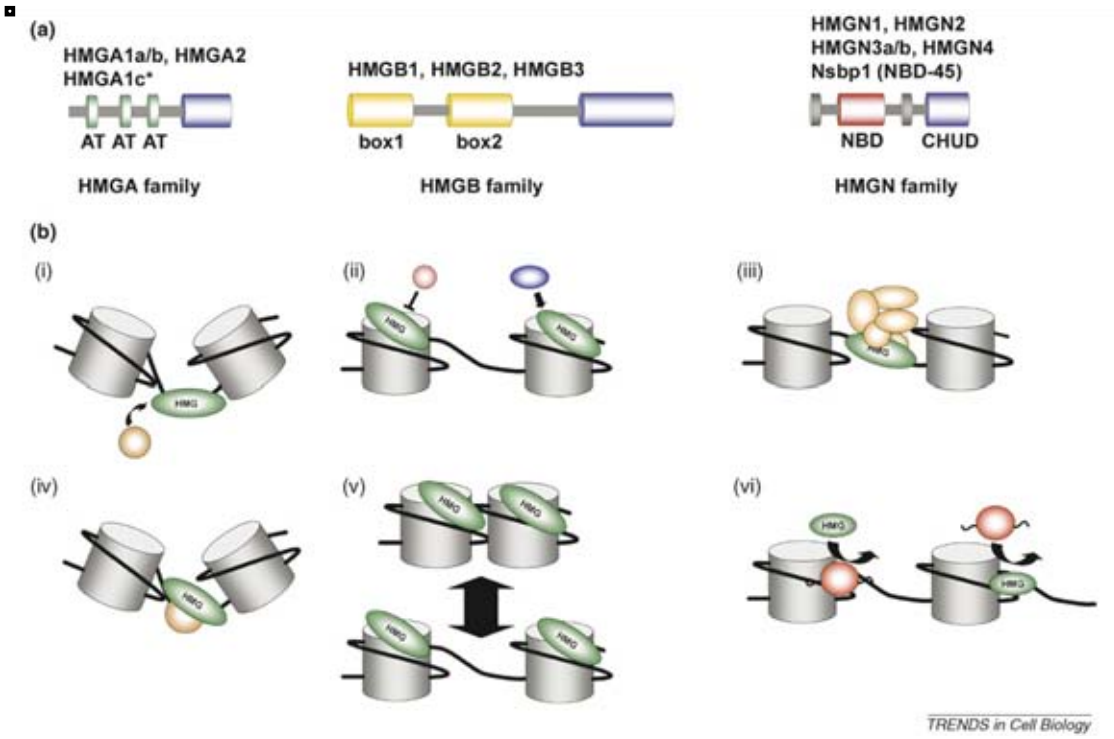

Figure 10. Architectural functions of HMG proteins. (a) The main structural features of the HMGs. **(b)** HMG proteins alter chromatin structure by a variety of mechanisms. (i,ii) HMG proteins alter the chromatin structure and facilitate the binding of additional factors. This can be mediated through (i) their DNA bending activity, or by (ii) either preventing or facilitating access of modulating factors to chromatin. HMGA proteins can also bind to nucleosomes (iii) HMGs are part of the chromatin binding module of regulatory multiprotein complexes. (iv) HMG proteins facilitate structural transitions at sites to which they are targeted by specific regulatory factors. After targeting, they can induce DNA bending and (v) chromatin unfolding or chromatin compaction. (vi) HMG proteins compete with other nuclear proteins for chromatin binding sites, altering the local or global structure of the chromatin fiber (Hock et al., 2007).

3.2. HMGA1

The HMGA1 group presents three copies of an “AT-hook” DNA-binding motif and an acidic carboxyl-terminal tail (Q. Zhang and Yinsheng Wang, 2010). The mammalian HMGA gene family is composed of two functional members HMGA1 (HMGI/Y) and HMGA2 (HMGI-C) (R Reeves, 2001a).

Alternative splicing of transcripts from HMGA1 genes gives rise to three protein products HMGA1a (HMG-I), HMGA1b (HMG-Y) and HMGA1c (HMG-I/R). The HMGA1a (HMG-I) and HMGA1b (HMG-Y) proteins are nearly identical in sequence and are the

most abundant of the three splice variants in mammalian cells, (R Reeves, 2001a; Raymond Reeves, 2010). HMGAs are abundantly expressed in early embryonic life but are hardly detectable in adulthood (Q. Zhang and Yinsheng Wang, 2010).

HMGA1 proteins lack significant secondary structure that provides them a high degree of intrinsic flexibility. This fact plays a critical role in enabling the HMGA proteins to participate in a wide variety of biological processes (R Reeves, 2001a; Raymond Reeves, 2010).

3.3. Mechanism of action and function

HMGA proteins participate in a wide variety of nuclear processes such as chromosome and chromatin dynamics. HMGA proteins exert their functions by binding to specific structures in DNA, chromatin or other proteins in a sequence-independent manner; since they recognize structure, rather than a particular nucleotide sequence (Cleynen and Van de Ven, 2008). By binding to DNA or proteins, HMGAs induce structural changes in the substrates with which they interact. Thus, they are directly involved in specific gene expression, which is crucial for their diverse roles in differentiation (Hock et al., 2007). Although directly implicated in gene regulation, HMGA1 action may depend on the cellular context (Martinez Hoyos et al., 2004; Masashi Narita et al., 2006; Resar, 2010).

HMGA proteins are key actors in the formation of the enhanceosome, complex assemblages of transcription factors and cofactors on nucleosome-free control regions of genes. Depending on the target gene, DNA conformational changes introduced by HMGA can either facilitate or prevent the assembly of enhanceosomes, hence

affecting gene transcription. Another function of HMGAs within enhanceosomes is to recruit transcription factors to DNA (Carvajal et al., 2002).

HMGAs also play an important role in chromatin dynamics during the cell cycle as well as on during chromatin condensation (Cleynen and Van de Ven, 2008; Y. Ueda et al., 2007). This occurs through recruitment of chromatin remodelling complexes to gene regulatory regions containing positioned nucleosomes during the transcriptional activation process (Raymond Reeves, 2010). High expression of both HMGA proteins in undifferentiated and proliferating mesenchymal cells of early embryos indicate an important role of HMGA proteins in the regulation of stem cell proliferation (Shah et al., 2012) and differentiation (Brocher et al., 2010). HMGA1 is mainly expressed during cell differentiation, whereas HMGA2 expression is mainly present during cell growth and proliferation (Ismail et al., 2012).

HMGA1 overexpression is implicated in tumourigenesis of both malignant and benign tumours, promoting aberrant expression of genes involved in tumour progression, cell proliferation and apoptosis (Arlotta et al., 2000; Hock et al., 2007; Giovanna Maria Pierantoni et al., 2003). However, recently HMGA proteins have also been directly involved in the process of senescence, interacting wit other senescence regulators to stabilize the senescent state. This way, HMGA proteins can have both oncogenic properties and antioncogenic properties (Kuilman et al., 2010; Masashi Narita et al., 2006).

3.4. Regulation of the expression of HMGA1

HMGA gene expression can be regulated in response to many different cellular stimuli (Cleynen and Van de Ven, 2008) and as mentioned before, are cellular context-

dependent (Bianchi and Agresti, 2005). HMGA1 proteins can be induced by many growth factors such as the tumorigenic agent 12-O-tetradecanoyl phorbol-13-acetate (TPA). In addition, HMGA expression can be repressed by activation of a differentiation program. Transcriptional deregulation is probably a major mechanism related to the aberrant expression of *HMGA1* in tumours. This could be due to the extreme complexity of *HMGA1* gene structure, as it comprises four different transcription start sites. However only a few *cis*-acting elements have been characterized on the *HMGA1* promoter (Cleynen and Van de Ven, 2008).

In addition, HMG proteins are subject to a wide range of post-translational modifications (PTMs) including lysine acetylation/ methylation/ formylation/ SUMOylation, arginine methylation and serine/threonine phosphorylation, which contribute to the regulation of their biological activities (Q. Zhang and Yinsheng Wang, 2010).

3.5. HMGA1 in adipogenesis

As stated above, HMG proteins are involved in common biological processes such as cell growth, proliferation and differentiation (Cleynen and Van de Ven, 2008). Recently, it has been described that HMGA1 proteins may participate in adipocyte differentiation (Esposito et al., 2009). In this differentiation process, specific transcription factors such as CCAAT/enhancer-binding proteins (C/EBPs) are required (R M Melillo et al., 2001). A key step in adipocytes differentiation is that growth-arrested preadipocytes re-enter the cell cycle before undergoing terminal differentiation (Esposito et al., 2009).

HMGA1 implication in adipogenesis may occur by a physical interaction of C/EBP proteins with HMGA1, hereby functionally cooperating in their transcriptional activity (Cleynen and Van de Ven, 2008). For instance, it has been recently shown that HMGA1 exert a negative effect on the proliferation of adipocytic 3T3-L1 cells. However, these proteins have a positive effect on differentiation of these cells (R M Melillo et al., 2001). Similarly, it has been demonstrated that HMGA1, by binding to RB and to C/EBP, may functionally cooperate with these proteins to activate and/or repress different promoters. In fact, HMGA1 may be involved in the assembly of highly regulated higher order complexes, which are essential both for growth arrest and for the expression of the differentiated phenotype of adipocyte precursors. In this way, HMGA1 proteins are required for the formation of the RB-C/EBPs protein complex that is essential for the expression of several adipocyte-specific genes (Esposito et al., 2009).

3. OBJECTIVES

During the onset of obesity adipocyte functionality is lost, which has been related to impaired transcriptional regulation of key factors controlling adipogenesis. HMGA1 proteins have been described as active players in adipogenesis, although their exact role remains elusive.

Therefore, in order to shed light on the role of HMGA1 during adipose tissue development and its metabolic implications in obesity and related diseases, the general objective of this work was **to examine the effects of HMGA1 overexpression in adipose tissue *in vivo***.

This general aim has been subdivided into two specific goals:

1. **To genetically modify adipose tissue of mice to increase HMGA1 expression.**
   1.1. To generate transgenic mice overexpressing HMGA1 specifically in adipose tissue.
2. **To determine the systemic and local effects of HMGA1 overexpression in adipose tissue.**
   2.1. To study the metabolic effects of a standard-chow feeding in transgenic mice overexpressing HMGA1.
   2.2. To study the metabolic effects of high fat diet feeding in transgenic mice overexpressing HMGA1.
      2.2.1. To study adipose tissue inflammation profile in transgenic mice.

4. RESULTS

1. STUDY OF LONG TERM HMGA1 EXPRESSION IN ADIPOSE TISSUE IN VIVO

Adipose tissue development and pattern of expression of mRNA of many genes involved in adipogenesis has been well documented. However, little is known about *Hmga1* endogenous expression over time in this tissue. In order to determine the role of HMGA1 in development and evolution of adipose tissue, we analysed its expression levels at distinct stages of development in epididymal white adipose tissue and brown adipose tissue from wild type mice (Figures 1 and 2).

HMGA1 expression pattern was then compared to that of a preadipocyte marker gene (preadipocyte factor-1, *Pref-1*; also known as delta-like homolog-1, *Dlk-1*), mature white adipose tissue marker (*aP2*) and a typical brown adipose tissue marker gene (*Ucp1*).

1.1. Study of *Hmga1* expression in white adipose tissue

As white adipose tissue develops mainly after birth, making it difficult to isolate it for its analysis (Charrière et al., 2003), we first determined *Hmga1* expression levels on 3-week-old mice.

The analysis of *Hmga1* mRNA levels by qPCR revealed that *Hmga1* was highly expressed in young adult mice and gradually decreased during adulthood. This was in accordance with what has been previously described (Monica Fedele et al., 2005). *Pref-1* is commonly used as a unique preadipocyte marker (Armengol et al., 2012; Yuhui Wang and Sul, 2009). Interestingly, *Hmga1* mRNA expression pattern was very similar to that of *Pref-1*, which progressively decreased in young adulthood (Figure 1).

The pattern of *Hmga1* mRNA expression in epWAT was then compared with that of *aP2*. Contrary to what happened with *Hmga1* expression, *aP2* expression

al sS uln TlPg PséGPlVf P3bPgPlPgSUgSaaPgV2VbV *H*P)ylPggré. yV VPl. TéS. VPlg *1*P)ylPggré. . s lPV2géf Pbé(gl PuV PsVéVbV éee *d* *H* gSaaPgVn a yéggn uPléuPéee 9n s nyéaP. Pgrgn (bnVPs nyégPVggSP *m*, *i* XnaSlP9Y3

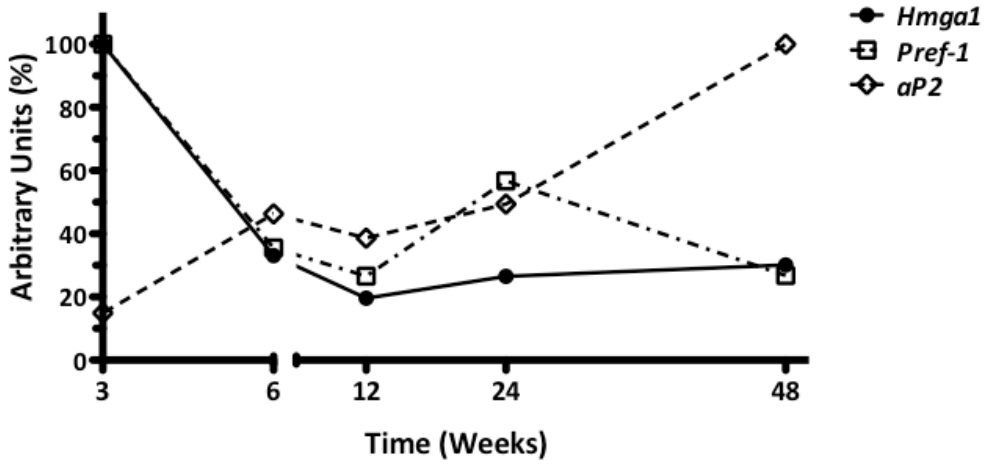

ÆYC dé MSA GBC HHAFO FD ABFE OARN CT CE O HEAO B FDUAVSVB NA FL CSAN É élf uné. (gyPleélf Ps Sgn aVbP yuy6bé SgPoPPyn aaP. P3 TbG uSP1PylPgP. Vg3VbPf P. éeeV uPgV2K. nf ugP)ylPggPs gyPlTP. V2aPéeeVbPf P. G uSP V2VbPVf Péeef)nf uP)ylPggré. éeeP Tb aP. PN(bnTb(ggPVé966 l nVlIS. nVgN Y3

dégÉSY VEFD GBC HHAFOAO CFUO ABFH SAHY

bP. (lgngéee *H*f uPGPug lMPlPGPl Ps VbV *H*(g3 bnabu P)ylPggPsn . P(Á él. g3 bP bnabPgV2uPGPugéTTSllPs lnabV2e VPl nVbo s al S uln sPTlPg Ps sSln a sPGPuéyf P. VN PTéf n a f égV S. sPVPTV uPn lé(. eV eléf /®Á (PPoÁéus f nTP X naSlP8Y3 nf nPl yV VPl. ée P)ylPggré. (g eéS. sn *d* *H*f N (bnTb yléalPggnGPu sPTlPg Ps e VPl nVbN lPT bn a nVgué(PgV2uPGPugéeP)ylPggré. n lé(. eV eléf /®Á(PPogÁéus f nTP3 bP yV VPl. ée *H*f P)ylPggré. n (g Téf yl Ps(nVbVbV éee *sH* VlynTl lé(. s nyégPVggSPf l oPlaP. P3 lé. Vl l Vé(bV by yP. Ps(nVbo *H*P)ylPggré. NVbP P)ylPggré. ée Vbng aP. P al S uln TlPg PséGPlVf P3 Slylngn auN(P éeS. s VbV VbP *sH*P)ylPggré. (g n nV Ps n

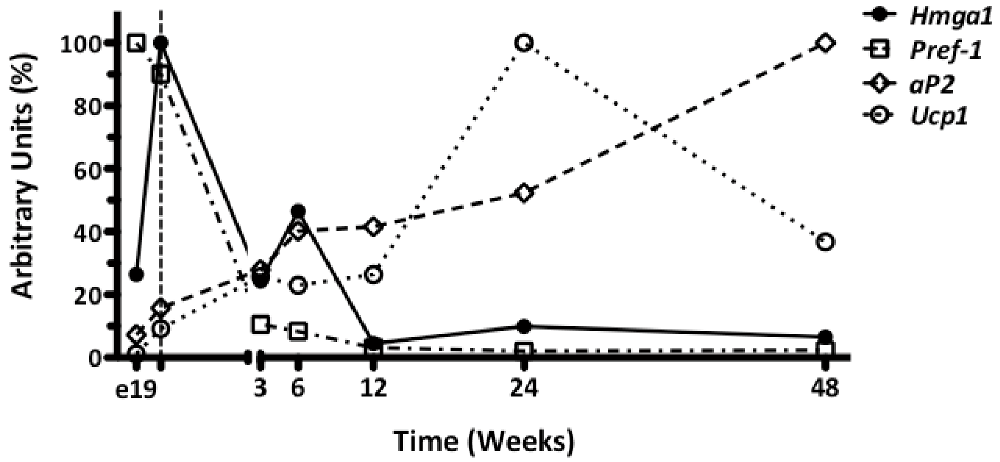

Hmga1
Pref-1
aP2
Ucp1
Arbitrary Units (%)
100
80
60
40
20
0
e19
3
6
12
24
48
Time (Weeks)

was generated in which *HMGA1* coding sequence was placed under the control of fat-specific adipocyte binding protein 2 promoter (aP2) – also known as fatty acid binding protein 4 (Fabp4). aP2 is a member of the intracellular lipid binding protein family, highly and constitutively expressed both in brown and white adipocytes. These features allow the aP2 promoter to be commonly used to direct the expression of a transgene to adipose tissue (Graves et al., 1992).

2.1. Construction of the aP2-HMGA1 chimeric gene

To obtain the aP2-HMGA1 chimeric gene, a 480 bp fragment *Hinc*II—*Pvu*II of the coding sequence of mouse HMGA1 was extracted from pCMV-SPORT6-HMGA1 plasmid and subcloned into the *Sma*I site of the paP2-SV40 plasmid containing the 5.5 kb of the fat-specific regulatory region of the *aP2* gene and the SV40 polyadenylation signal. The resulting plasmid was designated paP2-HMGA1-SV40 (Figure 3).

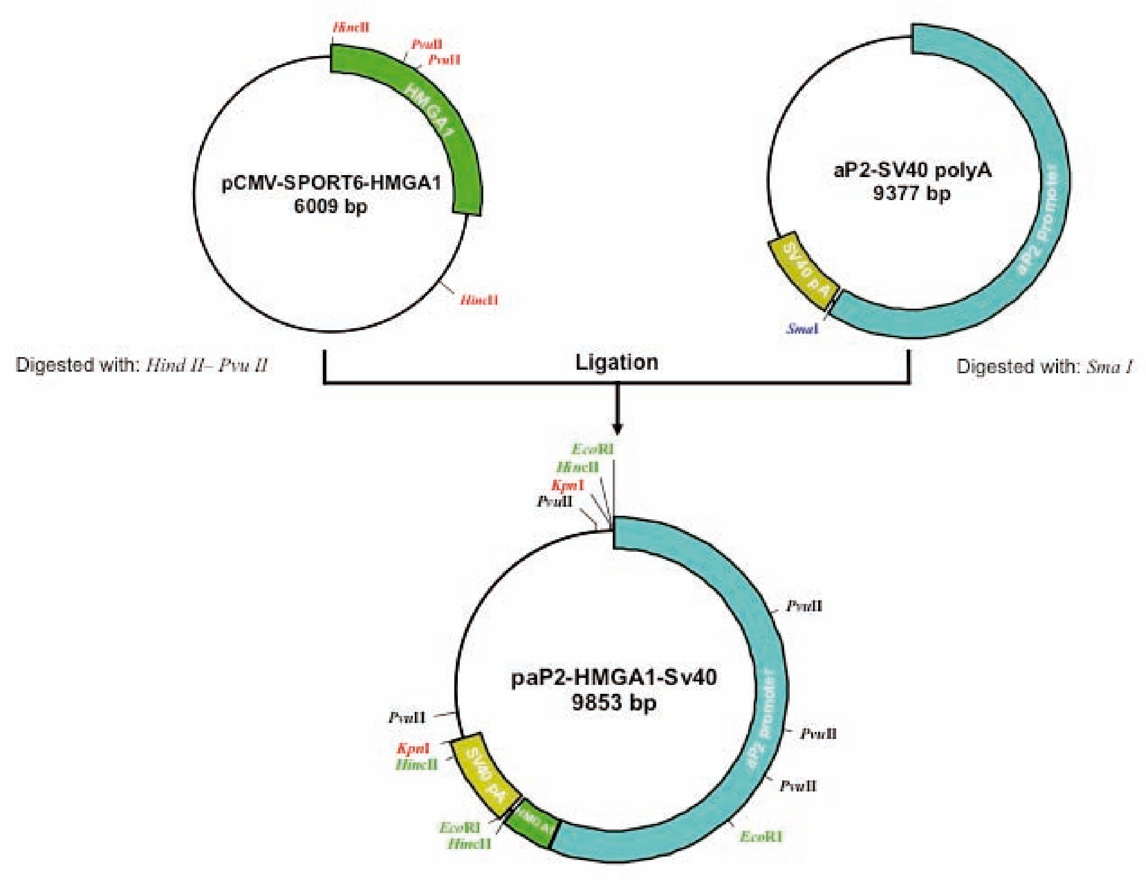

HincII
PvuII
PvuII
HMGA1
pCMV-SPORT6-HMGA1
6009 bp
HincII
aP2-SV40 polyA
9377 bp
SV40 pA
aP2 promoter
SmaI
Digested with: Hind II– Pvu II
Ligation
Digested with: Sma I
EcoRI
HincII
KpnI
PvuII
PvuII
paP2-HMGA1-Sv40
9853 bp
PvuII
KpnI
HincII
SV40 pA
PvuII
PvuII
EcoRI
HincII
HMGA1
EcoRI
aP2 promoter

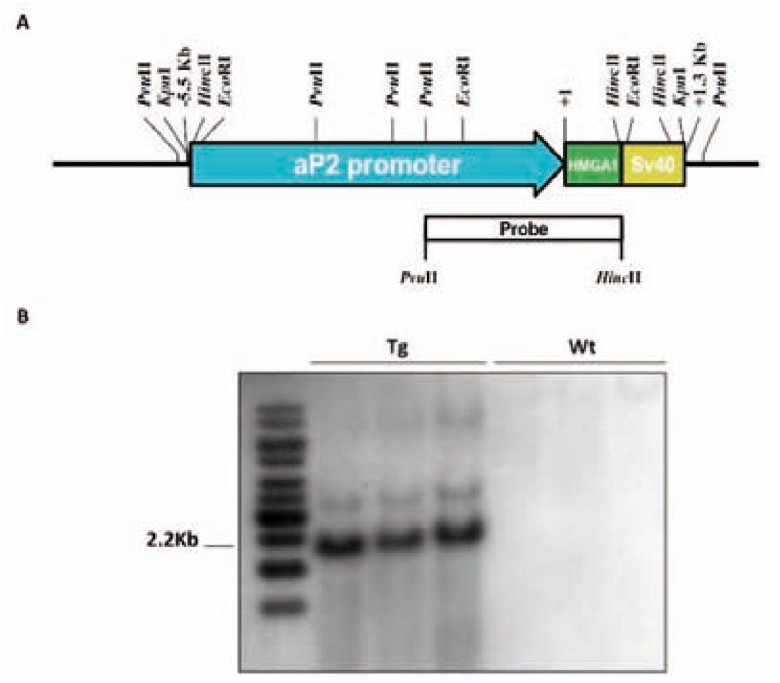
A
PvuII
KpnI
-5,5 Kb
HincII
EcoRI
PvuII
PvuII
PvuII
EcoRI
+1
HincII
EcoRI
HincII
KpnI
+1,3 Kb
PvuII
aP2 promoter
HMGA1
Sv40
Probe
PvuII
HincII
B
Tg
Wt
2.2Kb

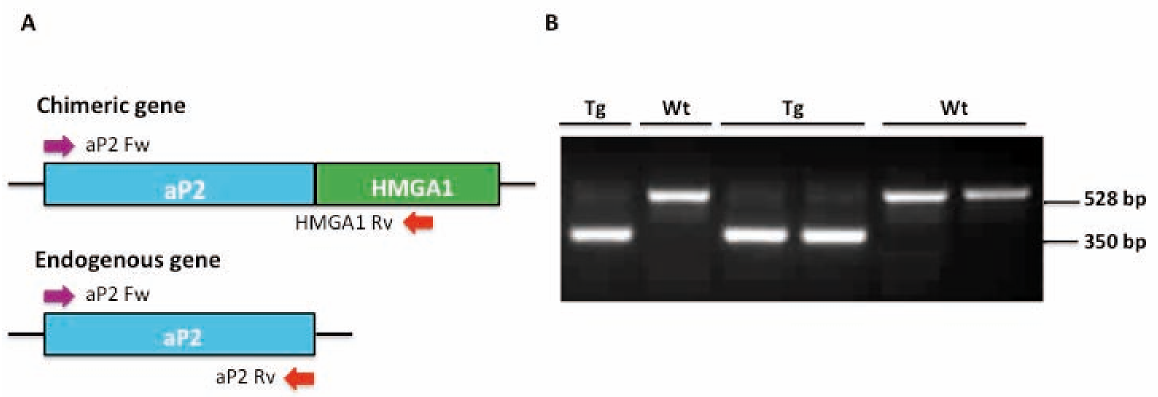
A
B
Chimeric gene
aP2 Fw
aP2
HMGA1
HMGA1 Rv
Endogenous gene
aP2 Fw
aP2
aP2 Rv
Tg
Wt
Tg
Wt
528 bp
350 bp

accordance with what was previously observed, *Hmga1* mRNA levels were significantly higher in all adipose fat depots analysed. While *Hmga1* expression was highly induced in BAT, only mild *Hmga1* mRNA levels were observed in mWAT (Figure 6B). Although epWAT, iWAT, rWAT and mWAT are all white adipose tissue depots, it has been described that different depots display different features in terms of proliferation, differentiation and gene expression profiles (Billon and Dani, 2012). This could explain the differences observed in the *Hmga1* mRNA expression levels of these fat depots.

The aP2 promoter is commonly used to drive specific expression of transgenes to the adipose tissue. However, it has been described that the aP2 protein is also expressed to a lesser extent in other tissues such as macrophages (Makowski et al., 2005; Urs et al., 2006). To check *Hmga1* expression in macrophages, we isolated macrophages from epWAT, spleen and blood (Figure 6C). Relative expression levels of *Hmga1* were analysed in tissue pools of 3 wild type or transgenic animals. *Hmga1* expression was highly induced in macrophages from epWAT of transgenic mice. In addition, a marked increase was also observed in macrophages from spleen and blood of transgenic mice compared to wild type mice.

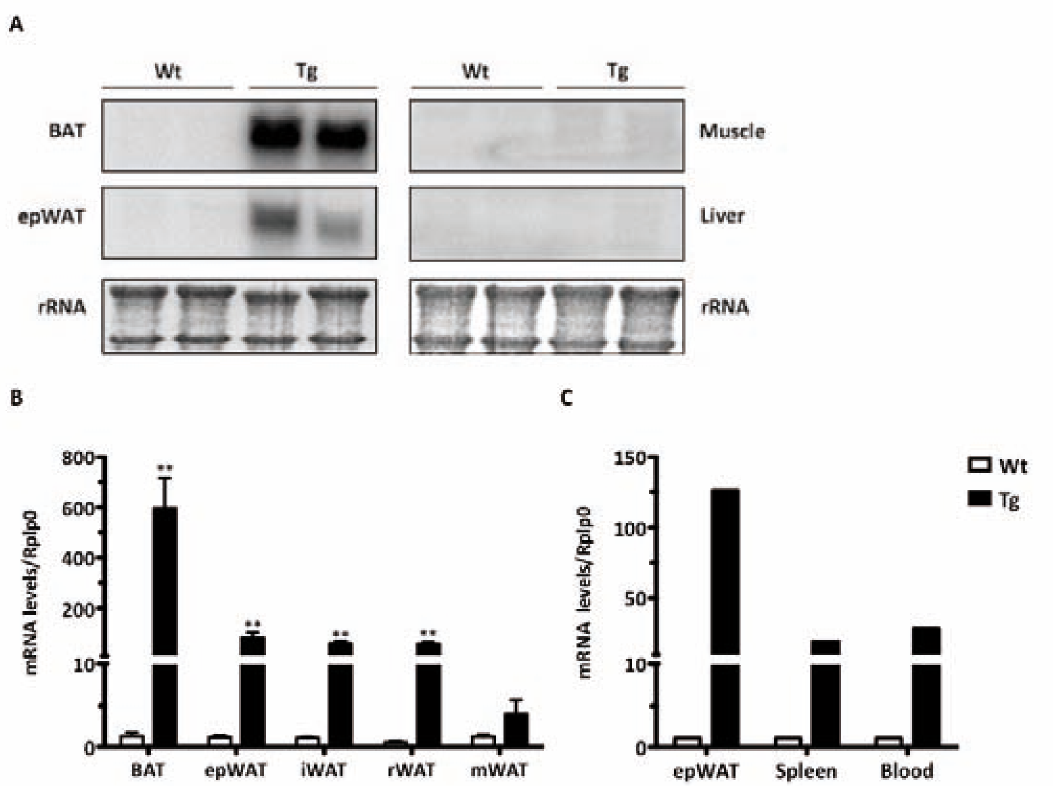

A
Wt
Tg
Wt
Tg
BAT
epWAT
rRNA
Muscle
Liver
rRNA
B
C
mRNA levels/Rplp0
800
600
400
200
10
0
BAT
epWAT
iWAT
rWAT
mWAT
**
150
100
50
10
0
epWAT
Spleen
Blood
Wt
Tg

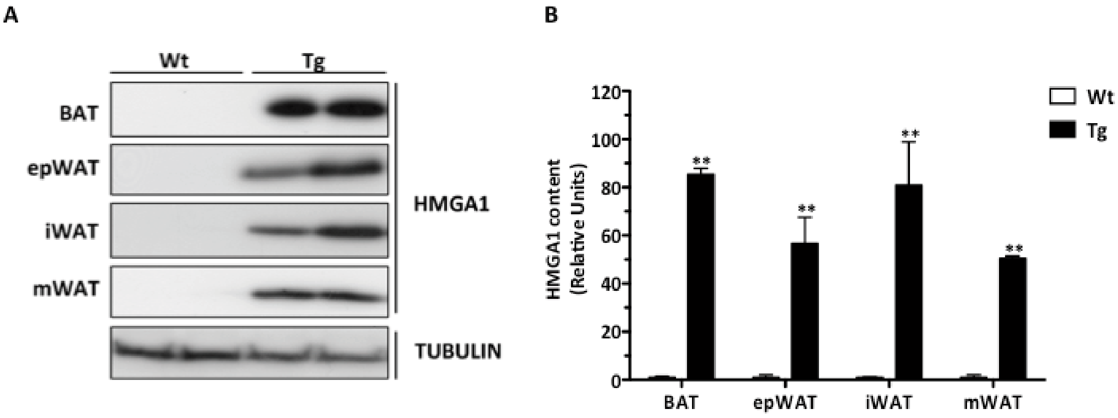

A
B
Wt
Tg
BAT
epWAT
iWAT
mWAT
HMGA1
TUBULIN
HMGA1 content
(Relative Units)
120
100
80
60
40
20
0
**
BAT
epWAT
iWAT
mWAT
Wt
Tg

[illegible]

[illegible]

[illegible]

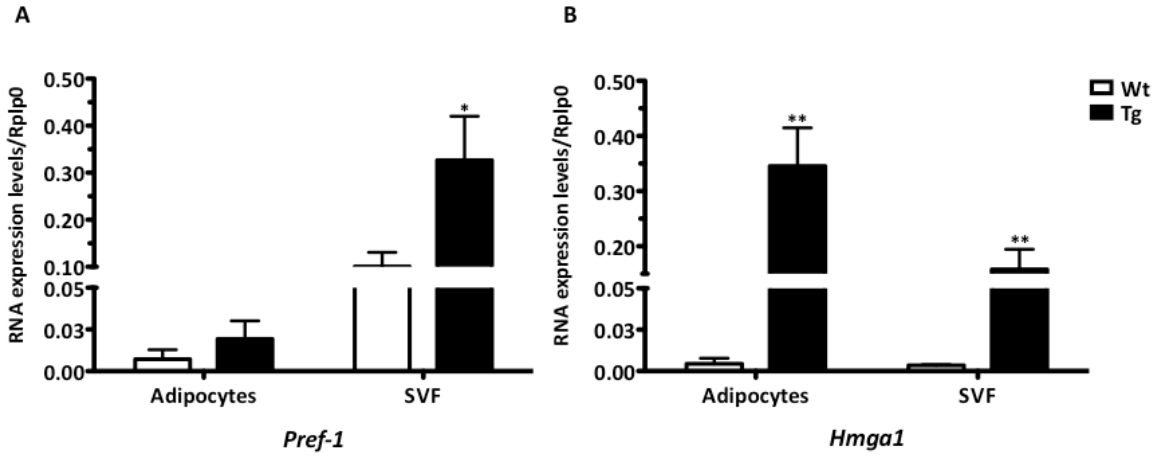
A
B
RNA expression levels/Rplp0
0.50
0.40
0.30
0.20
0.10
0.05
0.03
0.00
*
**
Adipocytes
SVF
Wt
Tg
Pref-1
Hmga1

[illegible]

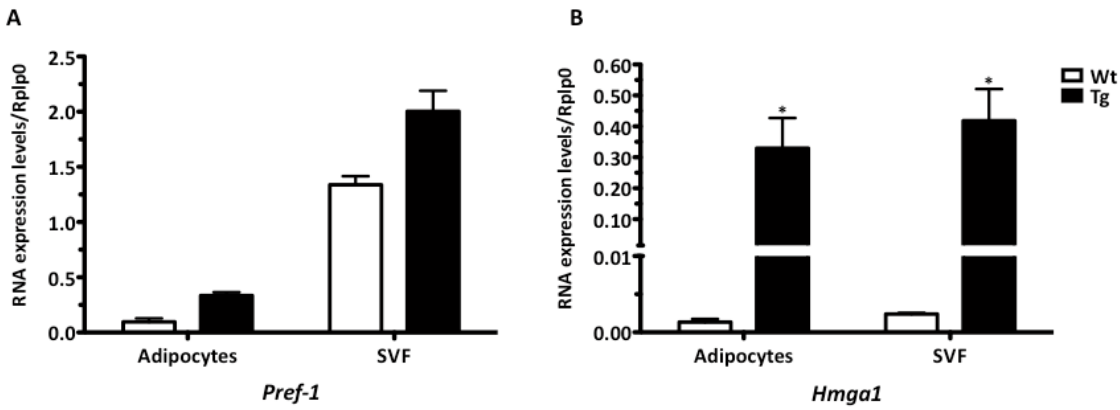

A
RNA expression levels/Rplp0
2.5
2.0
1.5
1.0
0.5
0.0
Adipocytes
SVF
Pref-1
B
RNA expression levels/Rplp0
0.60
0.50
0.40
0.30
0.20
0.10
0.01
0.00
Wt
Tg
Adipocytes
SVF
Hmga1

3. CHARACTERIZATION OF aP2-HMGA1 TRANSGENIC MICE

Whether HMGA1 is involved in adipogenesis, adipocyte functionality, insulin resistance or the development of obesity *in vivo* remains unclear. To this aim, in this part of the study we determined the metabolic effects of specific HMGA1 overexpression in adipose tissue.

3.1. Systemic effects of high levels of expression of HMGA1 in adipose tissue

3.1.1. Determination of body weight and food intake

First, body weight was measured weekly from weaning to the age of 6 months in wild type and transgenic male mice with the goal of making a comprehensive monitoring of its evolution over time (Figure 10A). A slight increase in body weight was observed in transgenic mice when compared to wild type mice throughout the experiment (Figure 10A).

Body weight regulation depends upon the balance between energy intake and expenditure. Because of the differences in body weight gain observed between wild type and aP2-HMGA1 transgenic mice, the amount of food intake was controlled. To this aim, animals were housed individually and food intake was measured weekly. Total food intake recorded as food consumption (g/day), was then normalized by body weight gain for each group. No differences in food intake were observed between wild type and transgenic mice, as food consumption was similar between genotypes (Figure 10B).

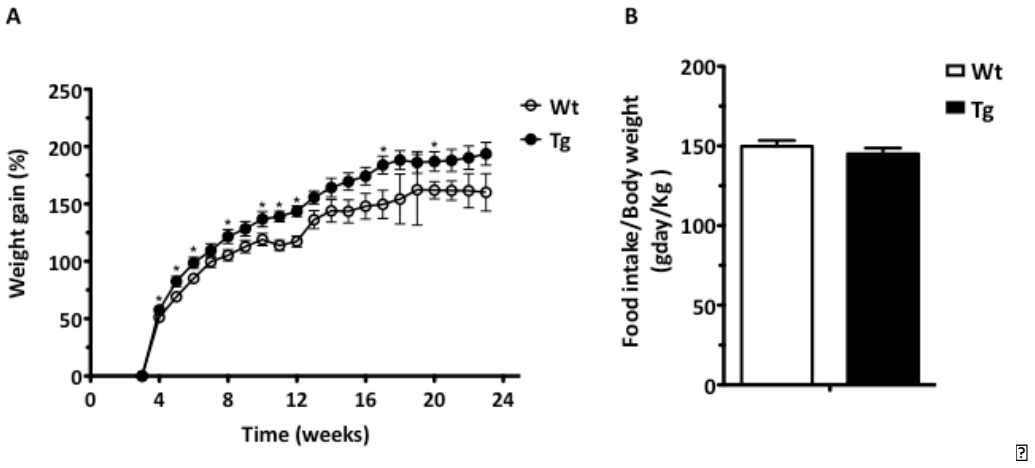

AEYC dl LFMSAFOFDFVU AEPSEAOOS SONAOSAFOFDDFFAOST 3 PrabVa X Y (g PPoF PgSlPs lf P. naX (PPogYvé-f évbgX8/ (PPogY3 éésh VoPXaxs lYef (ns VyPX Vm. saV. gaP. nTXaYf nTP (gP)ylPggPs g nu éésh VoPyPlf éSgP és I (PrabVX aY V lPf P. - ee VaPgV-f nTPelPTbaléSy3 f63 6K, dA (nsÁVyPf nTP3

méd g DD SHFDPAEPMVL MEFD GBC H-AFOFD dFO ABFHSVOFSP C FCEOEN H-

b aPgh és I (PrabV P elPMSP. Vu ggéTnY Ps (nbo VPlY né. gh nyégPVggSP f gg3n TP 8Á 9V gaP. nTf nTPgbé(Psn TlPgPs és I (PrabVTéf yl Ps vé (nsVyPf nTPN(P P)VsPVPlf n Ps VbP nyégnVsPalPPn VbPgPf nTP3 éVbng f N f nTP (PlP PSVb míPs s nee PlP. V nyégnV yl P PVPlg (PlP g gPggPs 3

nigVNf l légTéynTGP. V uGngné. ée VbP éyP. Ps sé f n TG nV ué(Ps VbP é gPlGY né. ée Pynsns I f N gS TSV PéSgÁn aSn u s GngTPl (bnVP nyégP VggSP el éf (nsVyP sV gaP. nTf nTP3 Vnon au NPynsns I f sh aSn e Y sPyéVge éf V. gaP. nTf nTP (PlP lPs STPs Téf yl Ps vé VbégP ée (nsVyPf nTPX naSlP99Y3

n TP és I e Y Té. VP. V ng (PuÁPgV ugbPsn s nTY él ée nyégnV N(P. P)V Y VPf yVPs vé sPVPlf n P(béuP és I Téf yégnVné. ée V gaP. nTf nTP3 éVbng P. s N (béuP és I VnauTPlns P Té. VP. V (g f P g SlPsn P)V T Vg eléf VbP T ébéuT sn aPgVné. ée és I T T ggPg3 lnauTPlns P Té. VP. V ée V gaP. nTf nTP gbé(Ps yl é. éS. TPs sPTlPg P (bP. Téf yl Ps vé Vb Y ée (ns VyPf nTPX naSlP99Y3

Moreover, weight of BAT as well as that of epWAT, iWAT and rWAT was significantly reduced in transgenic mice when compared to wild type mice. This decrease was even more pronounced in brown adipose tissue, which weighed significantly less in transgenic mice. However, no differences in mesenteric fat pad weight were observed between wild type and transgenic mice (Figure 11C). Reduction in the adipose depots mass in transgenic mice suggested a certain degree of lipodystrophy of these mice. As whole body weight increase in transgenic mice was not due to an increase in fad depots mass, we sought to determine the origin of such weight gain. To this aim, several organs of wild type and transgenic mice were measured. Although aP2-HMGA1 transgenic mice showed an increase in liver weight, it did not account for the whole body weight gain observed. No differences in the weight of other tissues such as muscle, heart, pancreas, spleen or kidneys were observed (Figure 11D).

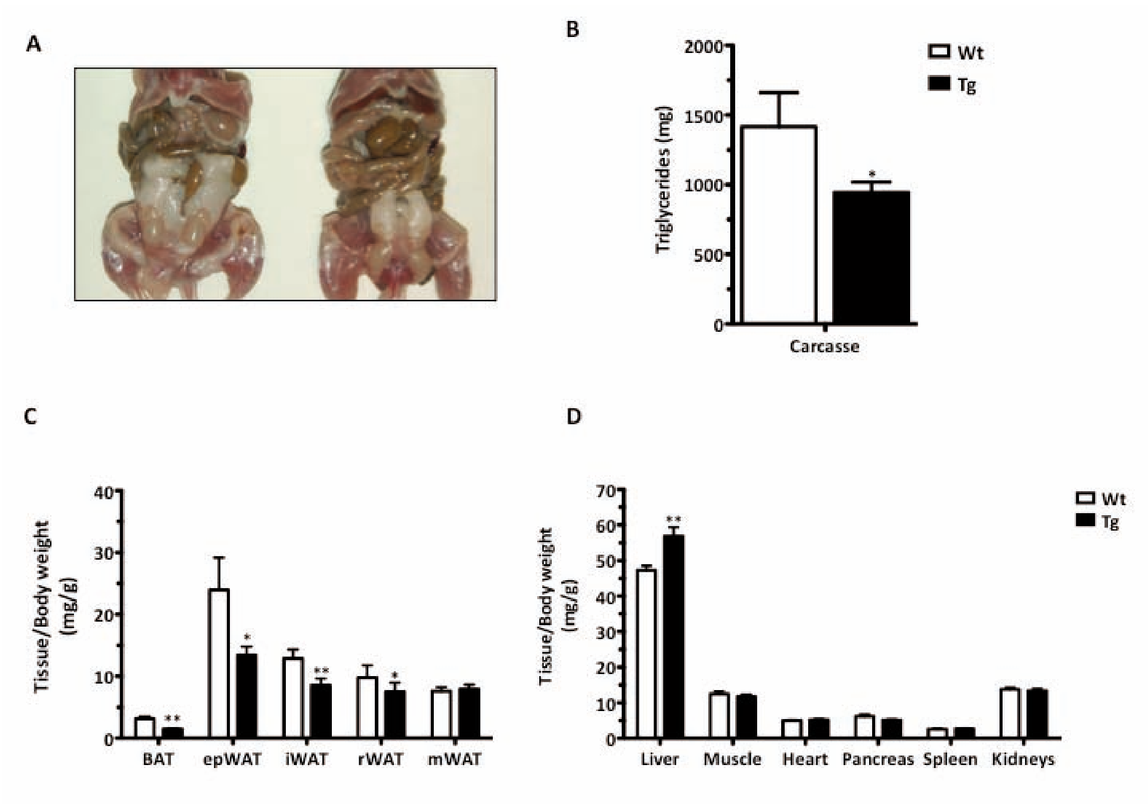

A
B
Triglycerides (mg)
2000
1500
1000
500
0
Wt
Tg
*
Carcasse
C
Tissue/Body weight (mg/g)
40
30
20
10
0
**
*
**
*
BAT
epWAT
iWAT
rWAT
mWAT
D
Tissue/Body weight (mg/g)
70
60
50
40
30
20
10
0
**
Wt
Tg
Liver
Muscle
Heart
Pancreas
Spleen
Kidneys

[illegible]

[illegible]

[illegible]

stained with hematoxylin/eosin showed that the epidermis and muscle layers of skin appeared normal (Figure 12C). However, increased expansion of the dermal layer was observed in aP2-HMGA1 transgenic mice. Notably, far fewer adipocytes were observed in the hypodermis layer of aP2-HMGA1 transgenic mice skin, confirming that subcutaneous fat depot was also smaller in these animals (Figure 12D). Other transgenic mice models in which adipose tissue was engineered also showed reduced intradermal adipose tissue or other abnormalities in skin structure and function, such as hair loss, epidermal hyperplasia, and abnormal sebaceous gland function have been reported (Bachman et al., 2002; Herrmann et al., 2003; Jong et al., 1998). In these mice models, the pool of stem cells of the skin was found to reside within the intradermal adipose tissue of the hypodermis. Thus, thickening of the dermis of aP2-HMGA1 transgenic mice may result from effects of HMGA1 in cell proliferation and/or apoptosis in this tissue.

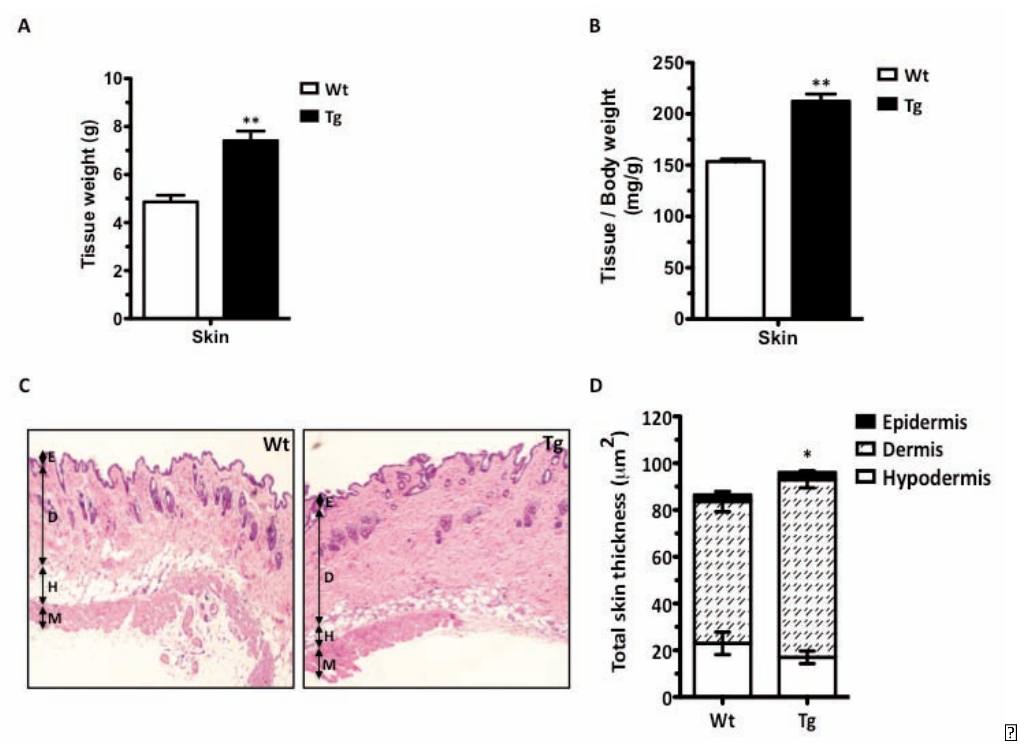
A
Tissue weight (g)
10
8
6
4
2
0
Skin
Wt
Tg
**
B
Tissue / Body weight (mg/g)
250
200
150
100
50
0
Skin
Wt
Tg
**
C
Wt
Tg
E
D
H
M
D
Total skin thickness (μm²)
120
100
80
60
40
20
0
Wt
Tg
*
Epidermis
Dermis
Hypodermis

observed. No differences between wild type and transgenic mice in fed glucose and in circulating insulin levels were found (Table 1).

Table 1. Circulating glucose and insulin levels.

	Wt	Tg
Fed glucose (mg/dL)	119 ± 3	123 ± 4
Fasting glucose (mg/dL)	70 ± 3	61 ± 2*
Fed insulin (ng/ml)	1 ± 0.6	1 ± 0.3

Circulating glucose and insulin levels in wild type (Wt) and transgenic (Tg) mice. Data are means ± SEM of at least 10 mice for each group. *$P \leq 0.05$ *vs.* wild type mice.

Whole-body insulin sensitivity of wild type and transgenic mice was measured by performing an insulin tolerance test. Initial glycaemia was very similar in both groups and decreased in parallel 30 minutes post-injection (Figure 13A). These results indicate that transgenic mice showed a normal hypoglycaemic response to insulin.

In order to determine whether aP2-HMGA1 transgenic mice presented a normal response to a glucose load, an intraperitoneal glucose tolerance test was performed. Initial glycaemia was very similar in both wild type and transgenic mice (Figure 13B). Moreover, 20 minutes after glucose infusion transgenic animals had lower glucose levels than transgenic mice. 120 minutes post-injection, glycaemia turned to basal levels in both groups in the same way. Overall, these results indicate that transgenic mice showed a normal hypoglycaemic response to insulin.

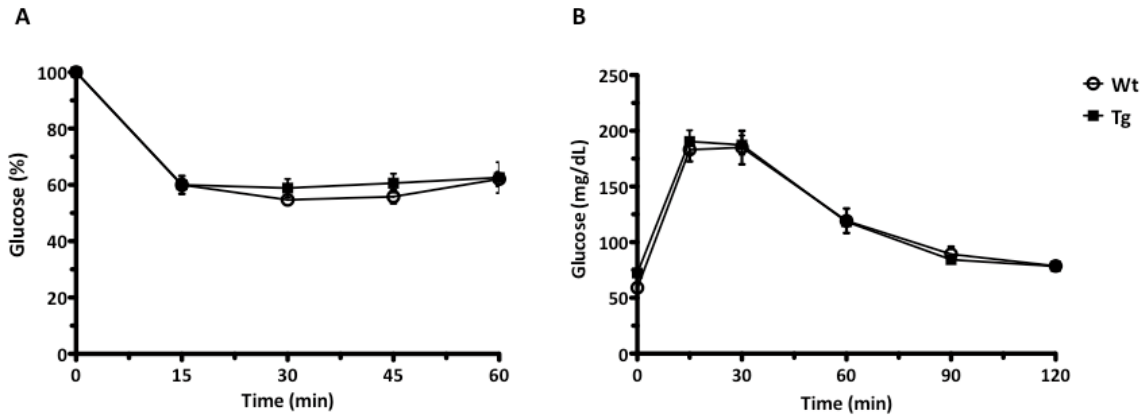

ÆYC EdmÉEOHYMOEH OHSALASVEOEEMEFH ESFMCEO É0E3 VlyPlné. PunhgSunÉvéuPl. TPVPgV6NK xa
éslPrabVnnsÁVyPX VE. sVl. gaP. nTXaYf nTP3E3 VlyPlné. PuaSTégPVéuPl. TPVPgV
X9axaYnnsÁVyPX VE. sVl. gaP. nTXaYf nTP3uéésgf yuPg(PlPVoP. eléf VbPV nGPnéeVbP
gf P. rf uVVbPVf Pgh snTVPs3VVlPf P. +É éeVuPgV9-f nTPeélPTbaléSy3

mfgÉgé S CNAOSAFOEFDAOYMSAOENS FMS HOPFCNFO H

ésPVPlf n PVbPPeTVéebmabuPGPugéeP)ylPggné. éeé é. TnlTSuV nafPV éunVPg sgPlSf bélf é. Pgf yunTV Psé. unyrsf PV éugf NgPlSf yl f PVPlg(PlPf PgSlPs3nyrsf PV éugf lPuV Psyl f PVPlgVégSTbg VnauTPlrsPgNdlPPeVl Tnsg sauTPléu(PlPlPsSTPsn 8Á 9Vl. gaP. nTf nTPn TéfylPngé. Vé(nsVyPf nTPX uP8Y3

éaf. nngrabVn Véyé\P. Vf TSl gPgéee. élf aSTégPVéuPl TP sngSungP. grVrGVl éeVl gaP. nTf nTPNuPGPugéeoPlgPlSf s nyéonPg(PlPPGaSV Ps3l. gaP. nTf nTPylPgP. VPslPsSTPsuPyVn NlPgrgVn s nyé. PTVnuPGPug(bP. Téfyl PsVéVbPnl(nsVyP rf gNyéggnuTé. VnSVnaVéf yléGPsauSTégP s uyrsf PV éugf X uP8Y3

Table 2. Serum parameters.

	Wild-type	Tg
Triglycerides (mg/dL)	128 ± 20	103 ± 15*
FFAs (mmol/L)	0.37 ± 0.03	0.36 ± 0.02
Glycerol (mM)	137 ± 3	108 ± 3*
Cholesterol (mmol/L)	3.2 ± 0.1	3.1 ± 0.06
Leptin (ng/mL)	2.8 ± 1	1.7 ± 0.4*
Resistin (ng/mL)	2.9 ± 0.4	1.6 ± 0.2*
Adiponectin (ng/mL)	2.5 ± 0.2	1.9 ± 0.1**

Serum parameters measured in serum from wild type (Wt) and transgenic (Tg) mice. Data are mean ± SEM of at least 10 mice for each group. $^{*}P \leq 0.05$ and $^{**}P < 0.01$ *vs.* wild type mice.

3.2.3. Energy metabolism

The regulation of body weight depends upon the balance between energy intake and expenditure. A widely used method for analysing energy expenditure is indirect calorimetry (Speakman, 2013). Because of the differences in weight gain and fat accumulation observed between wild type and aP2-HMGA1 transgenic mice, indirect calorimetry studies were performed. Continuous monitoring in individually housed mice was performed during a 24-hour period, and data from oxygen consumption, carbon dioxide production and locomotor activity were obtained (Figure 14).

Oxygen consumption and carbon dioxide production remained higher in aP2-HMGA1 transgenic mice when compared to wild type mice during either the light (basal or resting) or dark (higher activity) periods (Figure 14A and B), suggesting an increased metabolic rate in these mice. In accordance with these results, total energy expenditure was increased in aP2-HMGA1 transgenic mice related to wild type mice (Figure 14C). However, no changes in the respiratory quotient (RQ) between wild type

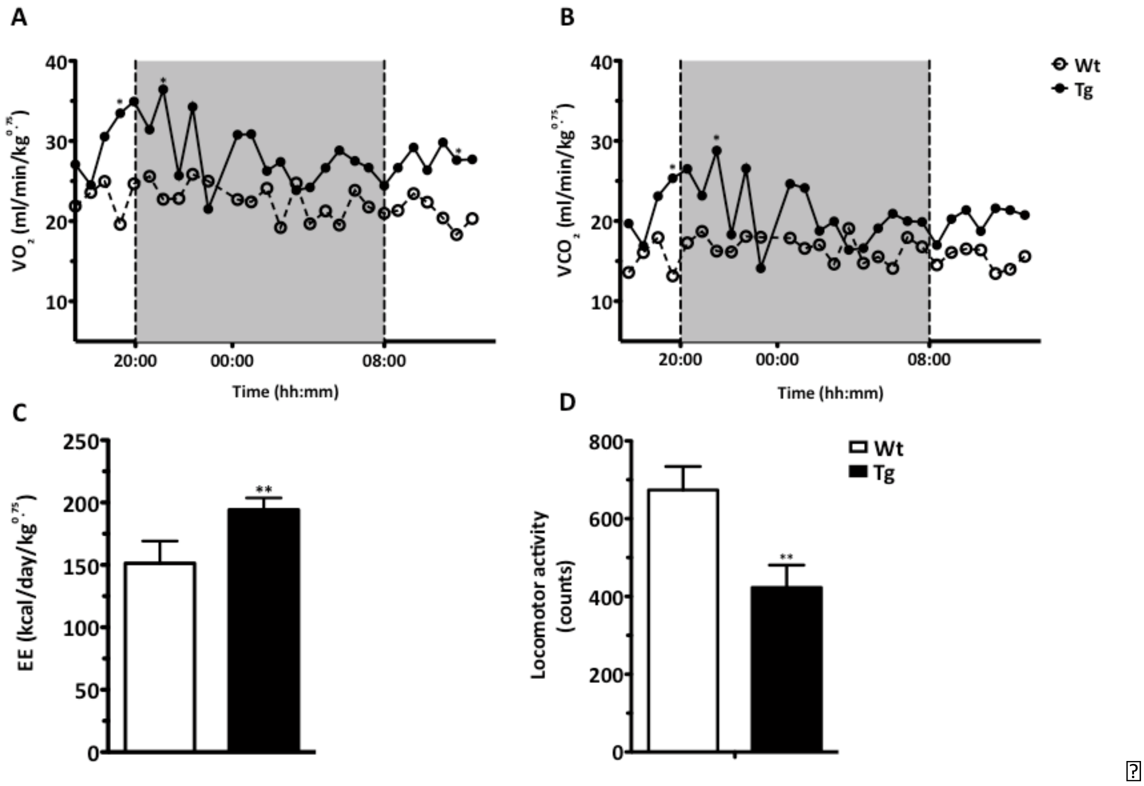
A
B
C
D
VO2 (ml/min/kg-0.75)
VCO2 (ml/min/kg-0.75)
Time (hh:mm)
20:00
00:00
08:00
Wt
Tg
EE (kcal/day/kg-0.75)
Locomotor activity (counts)

3.3. Study of white adipose tissue

As previously stated, weight of epididymal WAT from aP2-HMGA1 transgenic mice was significantly decreased in comparison to that of wild type mice (Figure 11C). Macroscopic examination of epididymal white adipose tissue showed that this depot was dramatically reduced in transgenic mice when compared to wild type mice (Figure 15A). Moreover, when normalized by tissue sample weight, triglyceride content was also significantly reduced in this depot in aP2-HMGA1 transgenic animals in comparison to wild type mice (Figure 15B).

3.3.1. Histological analysis of white adipose tissue

Histological and morphological analysis of white adipocytes of epididymal white adipose tissue from wild type and transgenic mice was performed. Histological slides stained with hematoxylin/eosin showed white adipocytes with a typical large unilocular lipid droplet in both wild type and aP2-HMGA1 transgenic mice. A slight decrease in the size of white adipocytes from aP2-HMGA1 transgenic mice was observed when compared to those from wild type (Figure 15C). Mean surface area was manually quantified by measuring adipocyte area. White adipocytes from aP2-HMGA1 transgenic mice showed lower mean surface area (3053 ± 40 μm^2) than that of wild type (3201±40 μm^2) (Figure 15D).

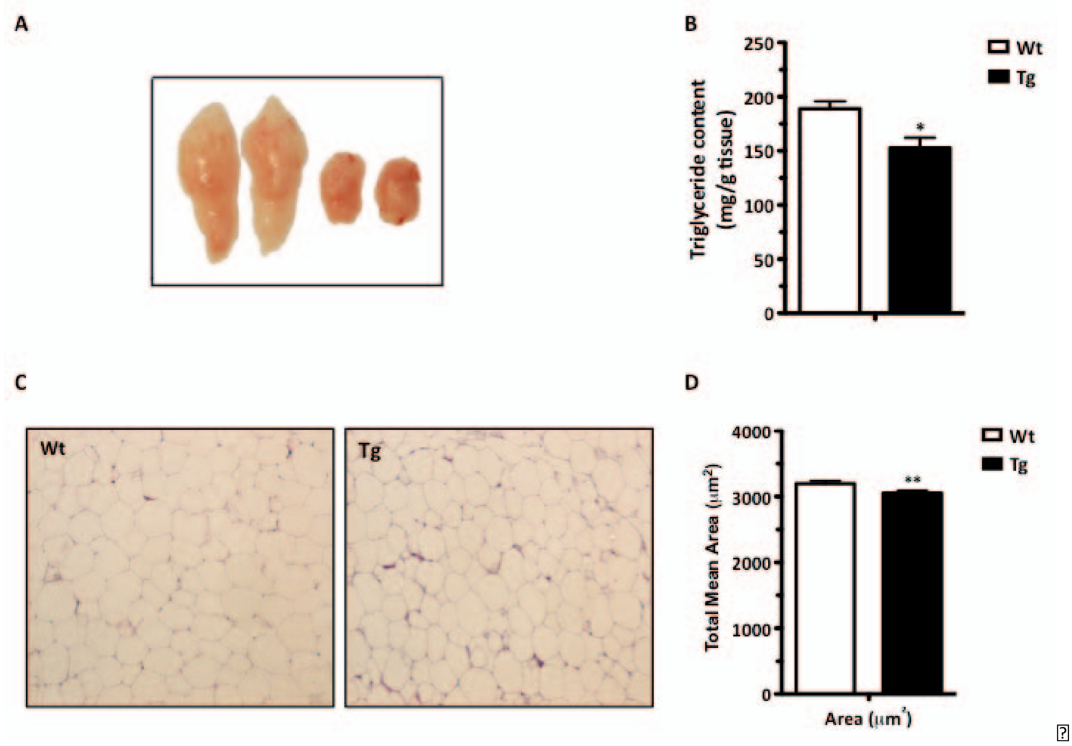

A
B
250
200
150
100
50
0
Triglyceride content
(mg/g tissue)
*
Wt
Tg
C
Wt
Tg
D
4000
3000
2000
1000
0
Total Mean Area (μm²)
**
Area (μm²)
Wt
Tg

metabolic process and cell differentiation were differentially expressed in aP2-HMGA1 transgenic mice (Table3).

Table 3. Functional analysis of epWAT gene expression. Significant gene ontologies.

Relevance	Genes	Hyp*	Annotations
1	43 genes	$3.12392e^{-06}$	GO:0006810: transport (BP)
2	17 genes	0.000180864	GO:0007155: cell adhesion (BP)
3	10 genes	0.00223739	GO:0006629: lipid metabolic process (BP)
4	14 genes	0.00233903	GO:0055085: transmembrane transport (BP)
5	9 genes	0.00245655	GO:0007067: mitosis (BP)
6	10 genes	0.00519566	GO:0051301: cell division (BP)
7	7 genes	0.0130988	GO:0016192: vesicle-mediated transport (BP)
8	13 genes	0.0118659	GO:0007049: cell cycle (BP)
9	7 genes	0.0111955	GO:0005975: carbohydrate metabolic process (BP)
10	3 genes	0.0341804	GO:0006461: protein complex assembly (BP)
11	12 genes	0.0470428	GO:0030154: cell differentiation (BP)

Second, we performed KEGG gene pathways analysis and we found that pathways related to VEGF signalling, cell adhesion molecules and Wnt signalling pathways were differentially expressed in aP2-HMGA1 transgenic mice (Table4).

Table 4. Functional analysis of epWAT gene expression. Significant gene pathways.

Relevance	Genes	Hyp*	Annotations
1	11 genes	0.000345649	(KEGG) 04145: Phagosome
2	9 genes	0.000682808	(KEGG) 04142: Lysosome
3	7 genes	0.000776076	(KEGG) 04520: Adherens junction
4	7 genes	0.000762664	(KEGG) 04370: VEGF signaling pathway
5	10 genes	0.00242663	(KEGG) 04510: Focal adhesion
6	8 genes	0.00264708	(KEGG) 04360: Axon guidance
7	10 genes	0.00328039	(KEGG) 04144: Endocytosis
8	11 genes	0.0035392	(KEGG) 04010: MAPK signaling pathway
9	8 genes	0.00375858	(KEGG) 04514: Cell adhesion molecules (CAMs)
10	8 genes	0.00445843	(KEGG) 04310: Wnt signaling pathway
11	5 genes	0.00429247	(KEGG) 04150: mTOR signaling pathway

Taken together these results show that aP2-HMGA1 transgenic mice presented alterations in the cell cycle, cell adhesion, VEGF or vascularisation and Wnt pathways suggesting impaired white adipose tissue development probably related to dysregulation of the adipocyte cell cycle.

3.3.3. Study of extracellular matrix components in white adipose tissue

Mature adipocytes and their progenitor cells (preadipocytes) exist enclosed by a three-dimensional (3D) network of extracellular matrix (ECM) proteins within the stromal-vascular fraction (Chun, 2012). ECM is crucial for maintaining the structural integrity of adipocytes and plays an important role in adipogenesis and whole tissue formation (Divoux and Clément, 2011).

Therefore, we performed immunohistochemical analysis of common ECM components in epWAT to validate previous results from array analysis where alterations in the gene expression of genes related to cell adhesion (or involved in the

adhesion to the ECM) were observed. According to microarray data, immunohistochemical detection of lamimin revealed higher levels of expression of this protein in transgenic mice than in wild type mice, with signal mainly confined to the basement membrane of white adipocytes. Interestingly, collagen IV and fibronectin expression were also higher in transgenic mice when compared to wild type mice (Figure 16A).

One of the distinctive features of adipose tissue is its unique plasticity to rapidly respond to nutrient availability. To fulfil this role, adipose tissue active and continuous remodelling is needed. Matrix metalloproteinases (MMPs) are important players in adipose tissue remodelling. Immunohistochemical evaluation of matrix metalloproteinases expression in epWAT showed that MMP-2 and MMP-9 expression was increased in transgenic mice in comparison to wild type mice (Figure 16B).

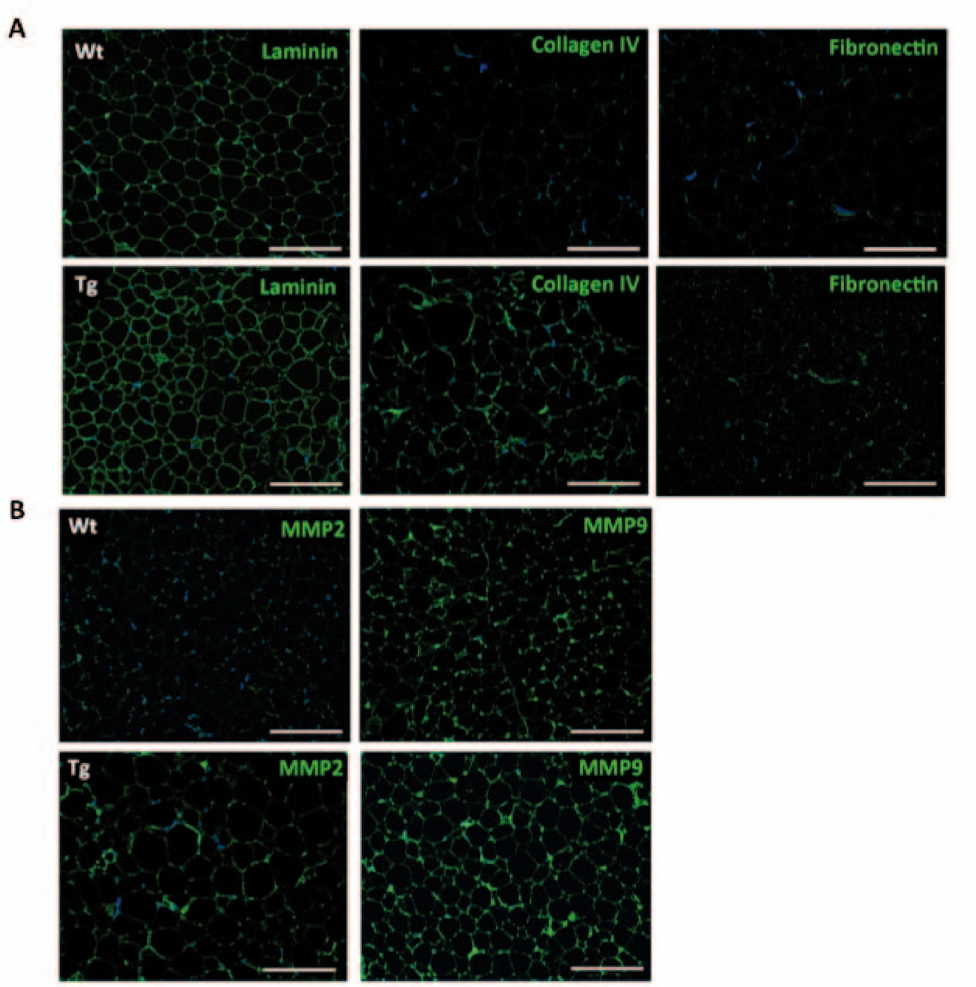

A
Wt
Laminin
Collagen IV
Fibronectin
Tg
Laminin
Collagen IV
Fibronectin
B
Wt
MMP2
MMP9
Tg
MMP2
MMP9

decreased in comparison to that of wild type mice (Figure 17C).

3.4.1. Histological analysis of brown adipose tissue

Macroscopic examination of interscapular brown adipose depots showed that this depot was dramatically reduced in transgenic mice when compared to wild type mice (Figure 1B). Interestingly, histological analysis showed that the small size multilocular lipid droplets characteristic of brown adipose tissue were larger in transgenic mice when compared to wild type mice (Figure 17A and 17B). Moreover, in some adipocytes lipid deposition appeared a unilocular lipid vacuole, typical of white adipocytes (Figure 17C).

When cell number was quantified in this depot by automatically measuring adipocyte nuclei (Song et al., 2010), a marked increase in cell number was observed in BAT from transgenic mice (Figure 17C). In addition, compared to wild type mice, transgenic mice showed increased amounts of DNA content in this fat depot (Figure 17D), indicating the presence of either greater amount of smaller cells or a higher amount of other cell types such as preadipocytes, macrophages or endothelial cells.

Since the expression of *Hmga1* was linked to that of *Pref-1* in BAT from wild type mice (Figure 2) and increased levels of *Pref*-1 expression were detected in the SVF of BAT from aP2-HMGA1 transgenic mice (Figure 9), we aimed to further characterize the stromal vascular fraction of BAT, which is enriched in preadipocytes. To this aim, preadipocytes within the SVF were separated from mature adipocytes by collagenase digestion of BAT from wild type and transgenic mice and manual quantification was carried out. aP2-HMGA1 transgenic mice showed significantly increased preadipocyte cell number per fat depot in comparison to wild type mice within the SVF from brown adipose tissue (Figure 17E).

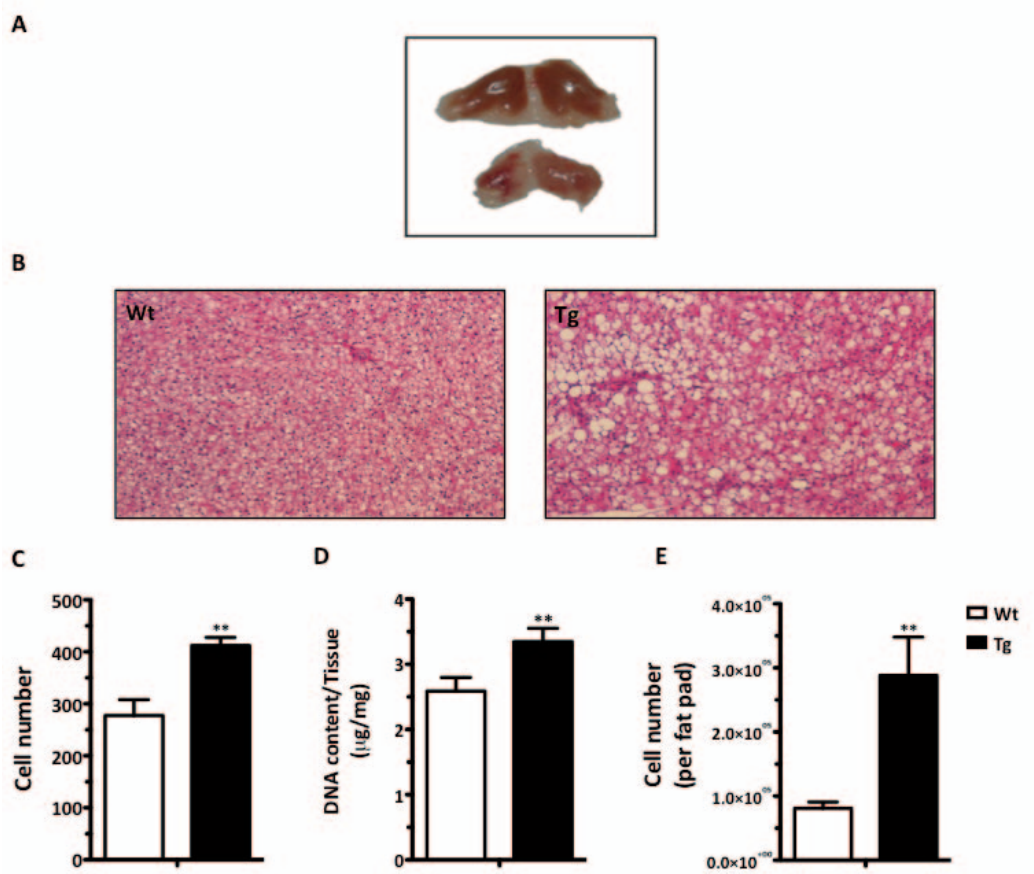
A
B
Wt
Tg
C
D
E
Cell number
0
100
200
300
400
500
**
DNA content/Tissue
(μg/mg)
0
1
2
3
4
**
Cell number
(per fat pad)
0.0×10+00
1.0×10
2.0×10
3.0×10
4.0×10
**
Wt
Tg

performed gene ontology (GO) analysis and we found that ontologies related to cell cycle, carbohydrate metabolic process, cell adhesion, lipid metabolic process, cell differentiation and mitochondrion organization were differentially expressed in aP2-HMGA1 transgenic mice (Table 5).

Table 5. Functional analysis of BAT gene expression. Significant gene ontologies.

Relevance	Genes	Hyp*	Annotations
1	402 genes	$1.51847e^{-53}$	GO:0006810: transport (BP)
2	108 genes	$4.89335e^{-33}$	GO:0006412: translation (BP)
3	123 genes	$7.09195e^{-17}$	GO:0007049: cell cycle (BP)
4	63 genes	$1.09303e^{-16}$	GO:0005975: carbohydrate metabolic process (BP)
5	113 genes	$1.15203e^{-15}$	GO:0007155: cell adhesion (BP)
6	58 genes	$4.17908e^{-14}$	GO:0016192: vesicle-mediated transport (BP)
7	68 genes	$1.18498e^{-13}$	GO:0006629: lipid metabolic process (BP)
8	70 genes	$2.83774e^{-10}$	GO:0051301: cell division (BP)
9	65 genes	$8.42455e^{-10}$	GO:0006397: mRNA processing (BP)
10	40 genes	$5.79931e^{-09}$	GO:0006457: protein folding (BP)
11	18 genes	$5.60978e^{-09}$	GO:0007005: mitochondrion organization (BP)
12	40 genes	$4.13769e^{-07}$	GO:0008283: cell proliferation (BP)

Second, we performed KEGG gene pathways analysis and we found that pathways related to oxidative phosphorylation, focal adhesion molecules and insulin signalling pathways were differentially expressed in aP2-HMGA1 transgenic mice (Table 6).

Table 6. Functional analysis of BAT gene expression. Significant gene pathways.

Relevance	Genes	Hyp*	Annotations
1	77 genes	$1.30972e^{-27}$	(KEGG) 05010: Alzheimer's disease
2	61 genes	$2.83964e^{-22}$	(KEGG) 00190: Oxidative phosphorylation
3	77 genes	$4.38035e^{-22}$	(KEGG) 04510: Focal adhesion
4	57 genes	$3.62964e^{-21}$	(KEGG) 04142: Lysosome
5	60 genes	$5.43993e^{-21}$	(KEGG) 04910: Insulin signaling pathway
6	68 genes	$2.13784e^{-19}$	(KEGG) 05016: Huntington's disease
7	97 genes	$4.50385e^{-19}$	(KEGG) 05200: Pathways in cancer
8	62 genes	$5.21831e^{-18}$	(KEGG) 04141: Protein processing in endoplasmic reticulum
9	70 genes	$4.06525e^{-16}$	(KEGG) 04810: Regulation of actin cytoskeleton
10	52 genes	$4.83863e^{-16}$	(KEGG) 05012: Parkinson's disease
11	41 genes	$1.56757e^{-15}$	(KEGG) 04666: Fc gamma R-mediated phagocytosis

Further analysis of the adipogenesis pathway showed that in aP2-HMGA1 transgenic mice this pathway was dysregulated. The expression of marker genes of preadipocytes such as *Dlk-1* (or *Pref-1*) was upregulated in aP2-HMGA1 transgenic mice (Figure 18). Upregulation of other genes involved in early stages of adipogenesis such as Kruppel-like factor 7 (*Klf-7)* and bone morphogenetic protein 1 (*Bmp-1)* was also observed in aP2-HMGA1 transgenic mice (Figure 18).

In contrast, the expression of genes involved in early differentiation such as *C/ebpα*, *C/epβ*, *Pparγ* and *Pparα* was downregulated in the BAT from aP2-HMGA1 transgenic mice. In accordance, the expression of marker genes involved in late differentiation such as *Fabp4* (or *aP2*), *Slc2a4* (or *Glut4*) and hormone sensitive lipase (*Lipe*) was also downregulated in the BAT from aP2-HMGA1 transgenic mice (Figure 18).

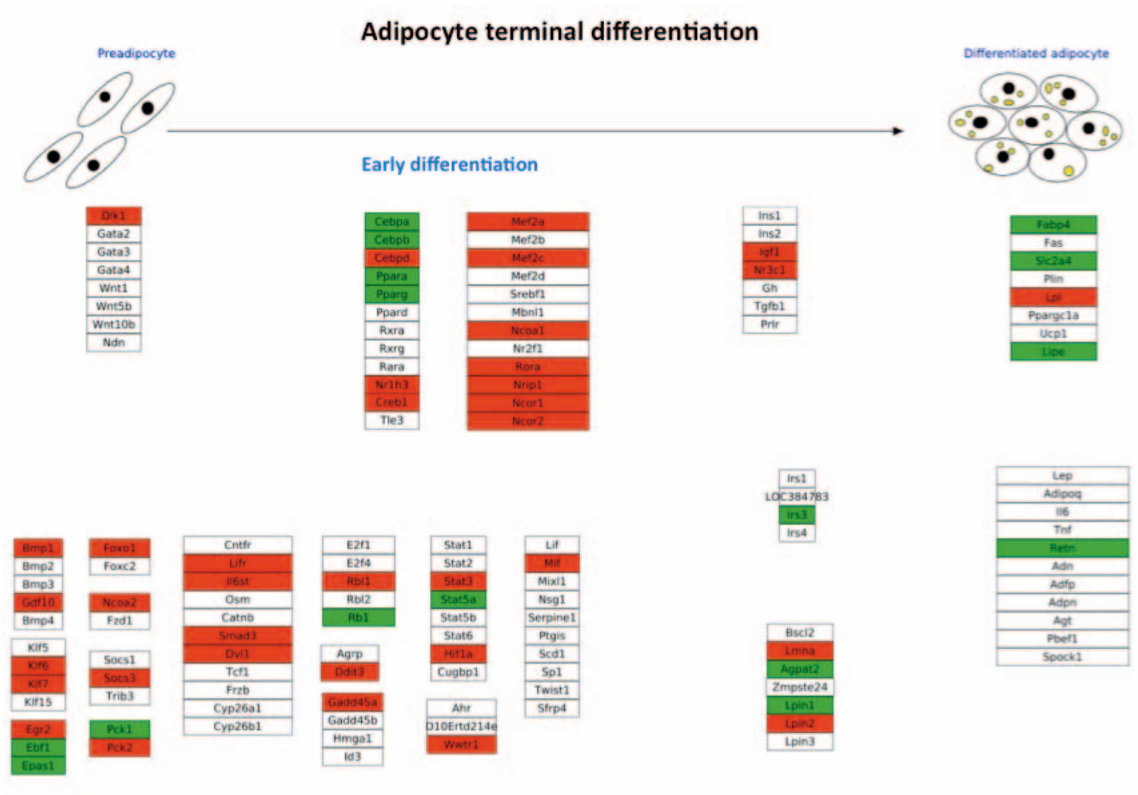

Adipocyte terminal differentiation
Preadipocyte
Differentiated adipocyte
Early differentiation
Dlk1
Gata2
Gata3
Gata4
Wnt1
Wnt5b
Wnt10b
Ndn
Cebpa
Cebpb
Cebpd
Ppara
Pparg
Ppard
Rxra
Rxrg
Rara
Nr1h3
Creb1
Tle3
Mef2a
Mef2b
Mef2c
Mef2d
Srebf1
Mbnl1
Ncoa1
Nr2f1
Rora
Nrip1
Ncor1
Ncor2
Ins1
Ins2
Igf1
Nr3c1
Gh
Tgfb1
Prlr
Fabp4
Fas
Slc2a4
Plin
Lpl
Ppargc1a
Ucp1
Lipe
Irs1
LOC384783
Irs3
Irs4
Lep
Adipoq
Il6
Tnf
Retn
Adn
Adfp
Adpn
Agt
Pbef1
Spock1
Bmp1
Bmp2
Bmp3
Gdf10
Bmp4
Klf5
Klf6
Klf7
Klf15
Egr2
Ebf1
Epas1
Foxo1
Foxc2
Ncoa2
Fzd1
Socs1
Socs3
Trib3
Pck1
Pck2
Cntfr
Lifr
Il6st
Osm
Catnb
Smad3
Dvl1
Tcf1
Frzb
Cyp26a1
Cyp26b1
E2f1
E2f4
Rbl1
Rbl2
Rb1
Agrp
Ddit3
Gadd45a
Gadd45b
Hmga1
Id3
Stat1
Stat2
Stat3
Stat5a
Stat5b
Stat6
Hif1a
Cugbp1
Ahr
D10Ertd214e
Wwtr1
Lif
Mif
Mixl1
Nsg1
Serpine1
Ptgis
Scd1
Sp1
Twist1
Sfrp4
Bscl2
Lmna
Agpat2
Zmpste24
Lpin1
Lpin2
Lpin3

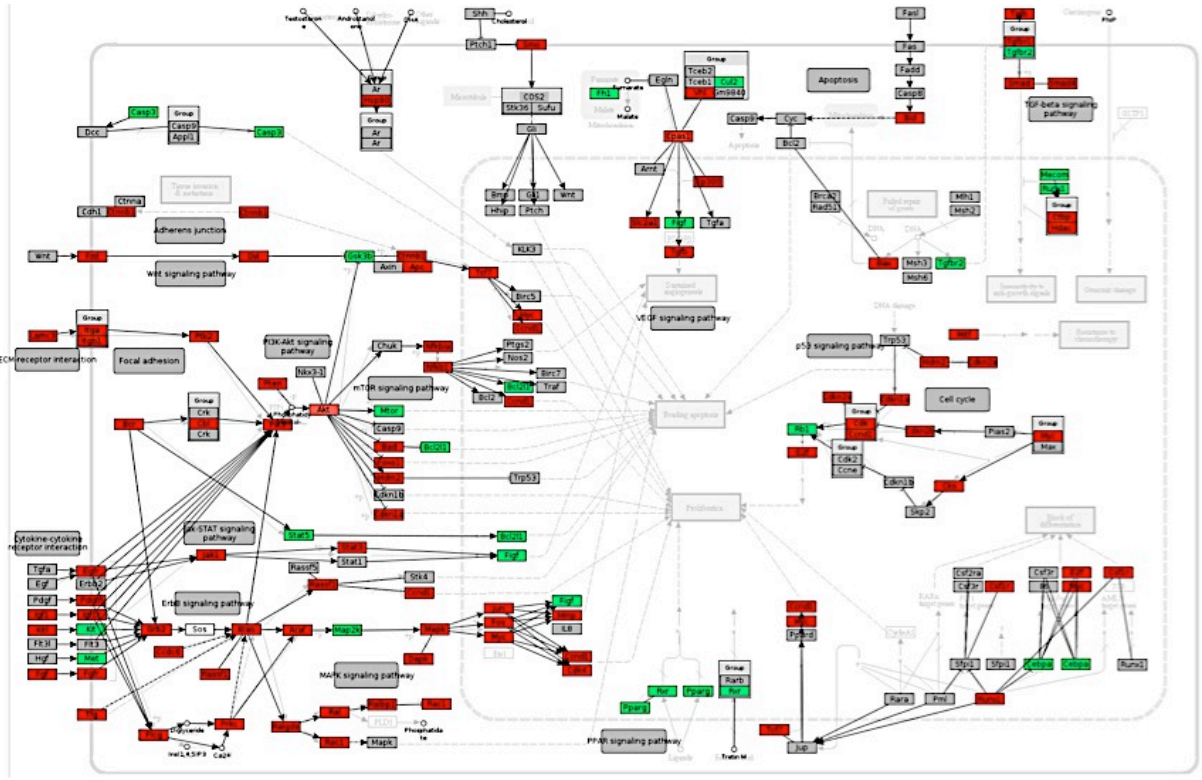

Figure 19. Integrative view of the dysregulated gene pathways in the BAT of transgenic mice. The schema summarizes the expression of genes involved in ECM receptor integration, PPAR signaling, senescence, cell cycle and Wnt signaling pathways.

3.4.3. Mitochondria functionality assessment

To confirm and extend these observations, we investigated the protein expression levels of some of the differentially expressed genes (Figure 20). As expected, compared to wild type mice aP2-HMGA1 transgenic mice had lower expression of proteins involved in adipogenesis such as C/EBPβ, PPARγ and PPARδ (Figure 20A and 20B).

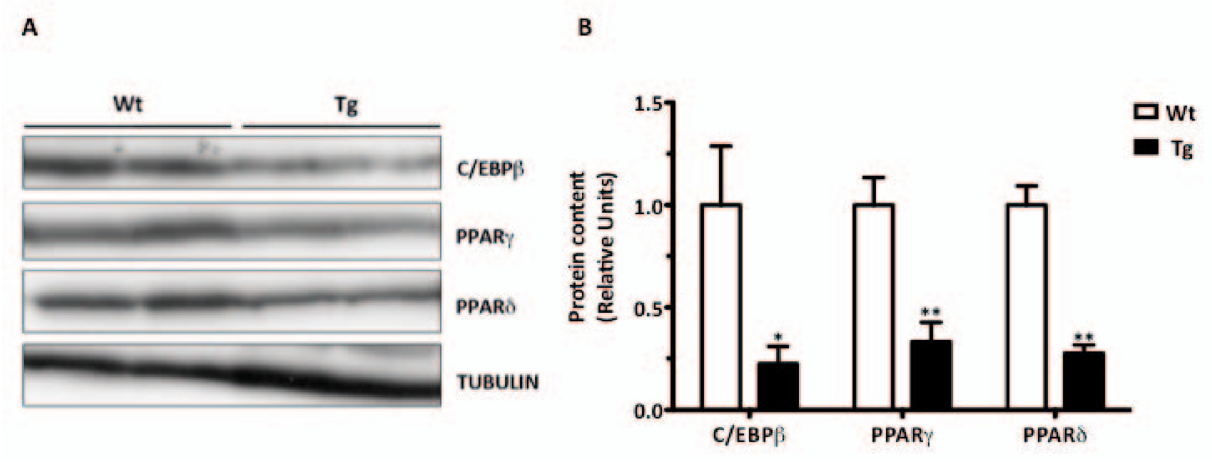

A
B
Wt
Tg
C/EBPβ
PPARγ
PPARδ
TUBULIN
Protein content
(Relative Units)
1.5
1.0
0.5
0.0
*
**
**
Wt
Tg
C/EBPβ
PPARγ
PPARδ

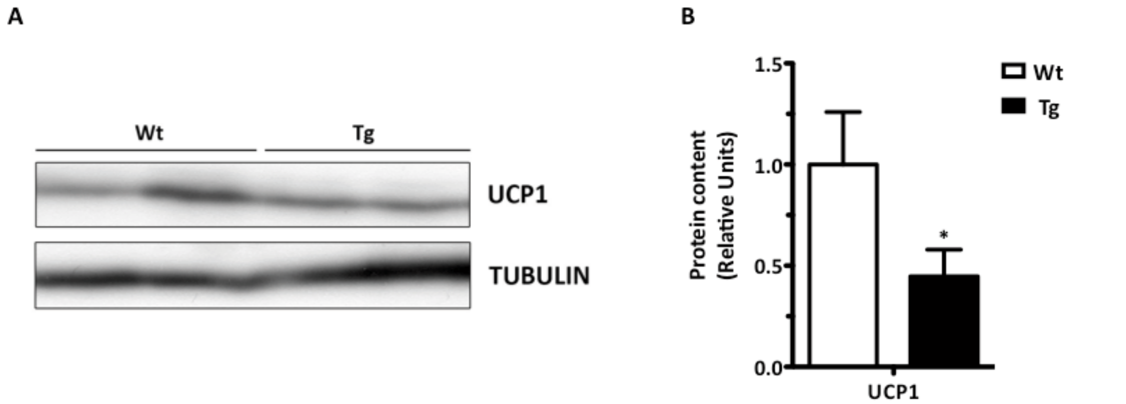
A
B
Wt
Tg
UCP1
TUBULIN
Protein content
(Relative Units)
1.5
1.0
0.5
0.0
*
UCP1
Wt
Tg

f oPl éé f nVéTbé. s lmu néaP. Pgmg3 VnGnM (g gma. meTl VuI lPs STPs n

Vl . gaP. nT f nTP (bP. Téf yl Ps Vé (nus M yP f nTP X naSl P 88 Y3 g Té. gPMSP. TP

eléf VbP s PTl Pg P ylé Vpn uPGPug s s PTl Pg Ps Téf yuP) VnGnM N

VnauI TPl ns P Té. VP. Vn eléf M gaP. nT f nTP h Tl Pg Ps PuW Ps Vé (nus M yP f nTP

X naSl P 88 YN SI VbPl Té. enl f n a brng Véuéan Tu u l gng éé gus Pg (bPl P bnabPl uny ns

s Pyég nVné. n M gaP. nT f nTP (g é gPl GPs X naSl P 9' Y3

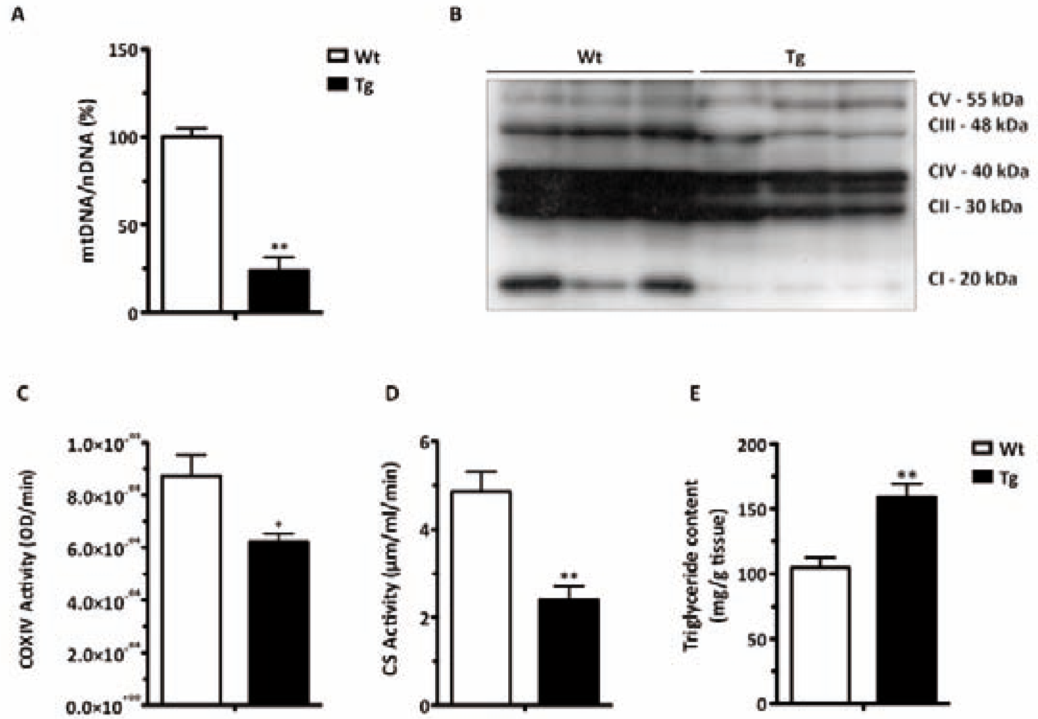

ÆYC gg CFUO ABFH SAHY DYO SAFO MSV O MHAHE 3 nVéTbé. s lmu Té. VP. Vn 3 3 PylPgP. VnGP éé f nVéTbé. s lmu Téf yuP) ylé Vpn g3 3 . íl f Vn Téf yuP) TVnGnM 3 3 nM VP gl . Vb gP TVnGnM 3 3 l mauI TPl ns P Té. VP. Vn 3 PgSuVg IP f P. é K s ne Pl P. V . nf ug P Tb alé Syg3 5 5 6 3 6 K . s 5 5 5 6 3 6 9 *d* (nus M yP f nTP3

bSgN eléf 8Á 9 M gaP. nT f nTP gbé (Ps ué (Pl f nVéTbé. s lmu

Té. VP. V s é) ns M nGP ybégybéll uW né. gSaaPg Vn. a VPl Ps VbPl f él PaSuW né. T y nM

éé VbPgP nf u g3

3.4.4. aP2-HMGA1 transgenic mice response to chronic cold exposure

Given that BAT from transgenic mice showed an altered pattern of gene and protein expression and lower mitochondrial content and oxidative phosphorylation capacity, we sought to determine whether this adipose depot remained functional. To this aim, we analysed the response of wild type and transgenic mice to cold exposure for 96 hours. Sensitivity to cold exposure was measured as the percentage of mice that entered hypothermia or as a 10º C reduction of core body temperature. Core body temperature was measured in the rectum of wild type and aP2-HMGA1 transgenic mice at the indicated time points using a digital thermometer. Mice were removed from the cold environment after a 10º C fall in rectal temperature otherwise they would die.

Initial body temperature measured at thermoneutrality (21º C or room temperature) showed no difference between wild type (37.62±0.27) and transgenic mice (37.59±0.21). During the first 12 hours no differences were observed in body temperature between groups. After 24 hours of cold exposure, wild type mice were gradually acclimatising to low temperature whereas aP2-HMGA1 transgenic mice showed more sensitivity to cold, as body temperature started to drop. However, at any of the time points studied, differences in core body temperature did not reach statistical significance (data not shown). After 72 hours, 40% of transgenic mice started to seriously reduce their body temperature and showed inability to maintain body temperature. Sixty per cent of transgenic mice entered hypothermia as a consequence of exposure to cold environment after 84h. By the end of the study (96h) 70% of aP2-HMGA1 transgenic mice had lowered their core body temperature 10º C. These data indicate that aP2-HMGA1 transgenic mice were unable to maintain core body

temperature when placed at 4º C, with loss of thermoregulatory control occurring within 96 h.

Taken together, these data indicate that HMGA1 blocks development and functionality of brown adipose tissue.

3.4.5. Study of extracellular matrix components in brown adipose tissue

Adipose tissue functionality is related to the equilibrated dynamics and proportion of its cellular components. Higher preadipocyte cell number (Figure 23E) and increased expression of preadipocyte marker genes (Figure 9A) in BAT of transgenic mice could indicate either a continuous adipocyte turnover or a remodelling process taking place. Therefore, we performed immunohistochemical analysis of common ECM components in BAT.

Masson's trichromic staining showed increased fiber deposition in BAT slides from transgenic mice in comparison to wild type mice (Figure 23A). As in white adipose tissue immunohistochemical detection of lamimin revealed similar pattern of expression of this protein in wild type and transgenic mice, with signal mainly confined to the basement membrane of brown adipocytes (Figure 23A). These findings indicate a loss of BAT structure in transgenic mice, suggesting an increased remodelling process in these mice.

Interestingly, fibronectin expression highly increased in transgenic mice when compared to wild type mice. However, collagen IV expression only mildly increased in transgenic mice (Figure 23B). Further detection of matrix metalloproteinases (MMPs) showed increased expression of MMP-2 and MMP-9 in BAT from aP2-HMGA1 transgenic mice in comparison to wild type mice (Figure 23B).

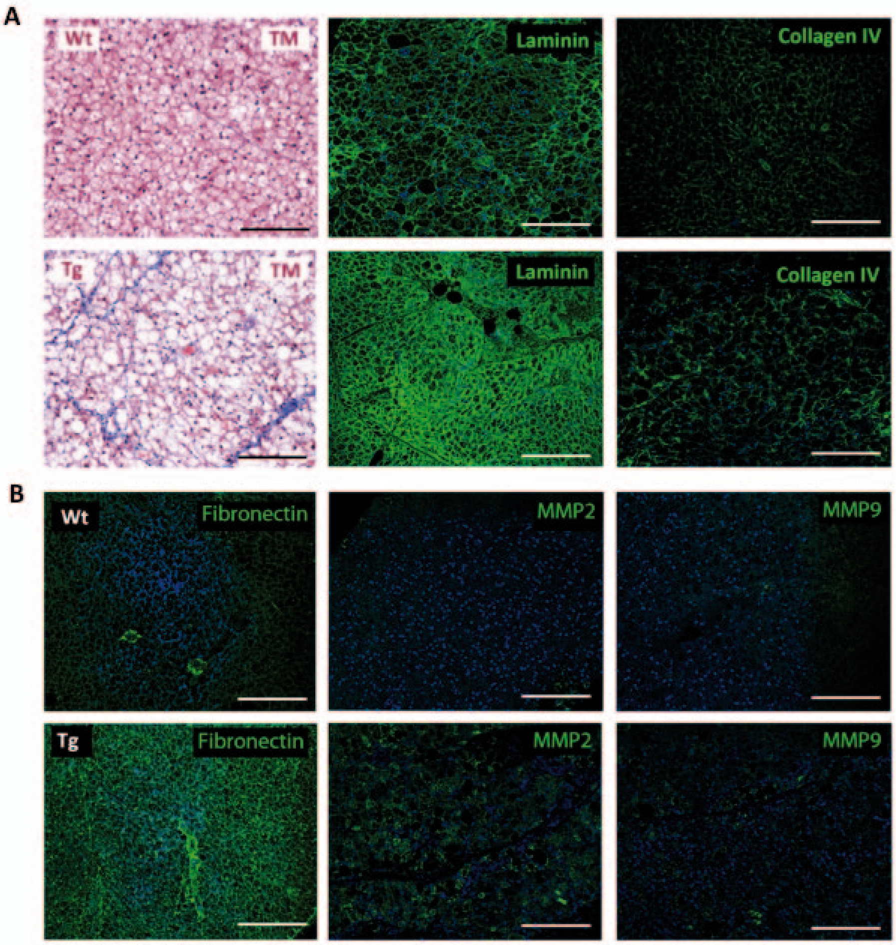

A
Wt
TM
Laminin
Collagen IV
Tg
TM
Laminin
Collagen IV
B
Wt
Fibronectin
MMP2
MMP9
Tg
Fibronectin
MMP2
MMP9

3.5. Study of the liver and skeletal muscle

One of the main metabolic complications of lipodystrophic mouse models is ectopic fat deposition, i.e. in those non-adipose tissues such as muscle and liver. As aP2-HMGA1 transgenic mice showed a lipodystrophic-like phenotype, we sought to determine whether fat accumulation was taking place in other important organs in glucose homeostasis, histological and gene expression analyses were performed in liver and skeletal muscle of wild type and transgenic mice.

3.5.1. Histological study of the liver

Histological sections from liver of wild type and transgenic mice, stained with haematoxylin/eosin showed no morphological differences between wild type and transgenic mice (Figure 24A).

3.5.2. Gene expression analysis of the liver

Next, quantitative gene expression analysis was performed in the liver from wild type and transgenic mice. The expression of representative genes involved in different lipid metabolism pathways was analysed. In transgenic mice, the expression of lipogenic genes, such as sterol regulatory element binding transcription factor 1 (Srebp-1c) (Figure 24B) or estrogen related receptor-a (Esrrα) (Figure 24C) was upregulated. In addition, the expression of genes involved in fatty acid oxidation such as uncoupling protein 2 (UCP2) (Figure 24D) or in cholesterol synthesis (or ketogenesis) such as 3-hydroxy-3-methylglutaryl-Coenzyme-A synthase 1(Hmgcs1) (Figure 24E) was also upregulated in the liver of transgenic mice in comparison to wild type mice.

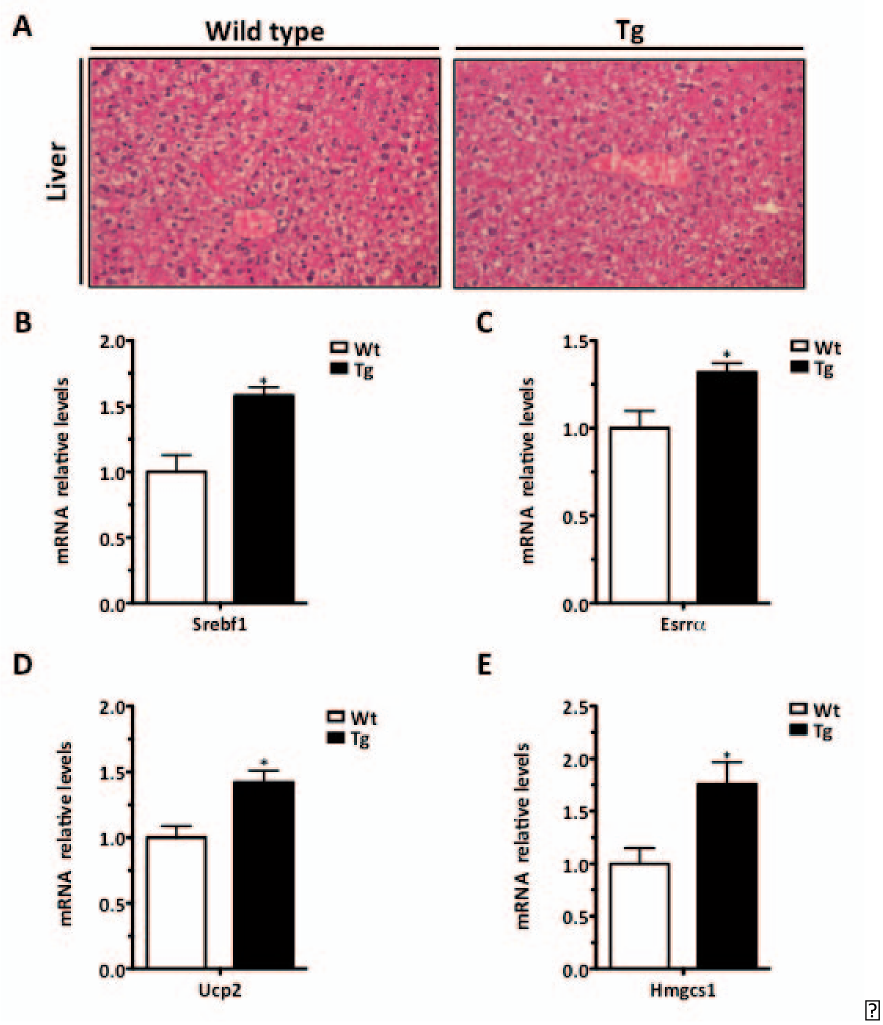

A
Wild type
Tg
Liver
B
mRNA relative levels
Srebf1
Wt
Tg
C
mRNA relative levels
Esrrα
Wt
Tg
D
mRNA relative levels
Ucp2
Wt
Tg
E
mRNA relative levels
Hmgcs1
Wt
Tg

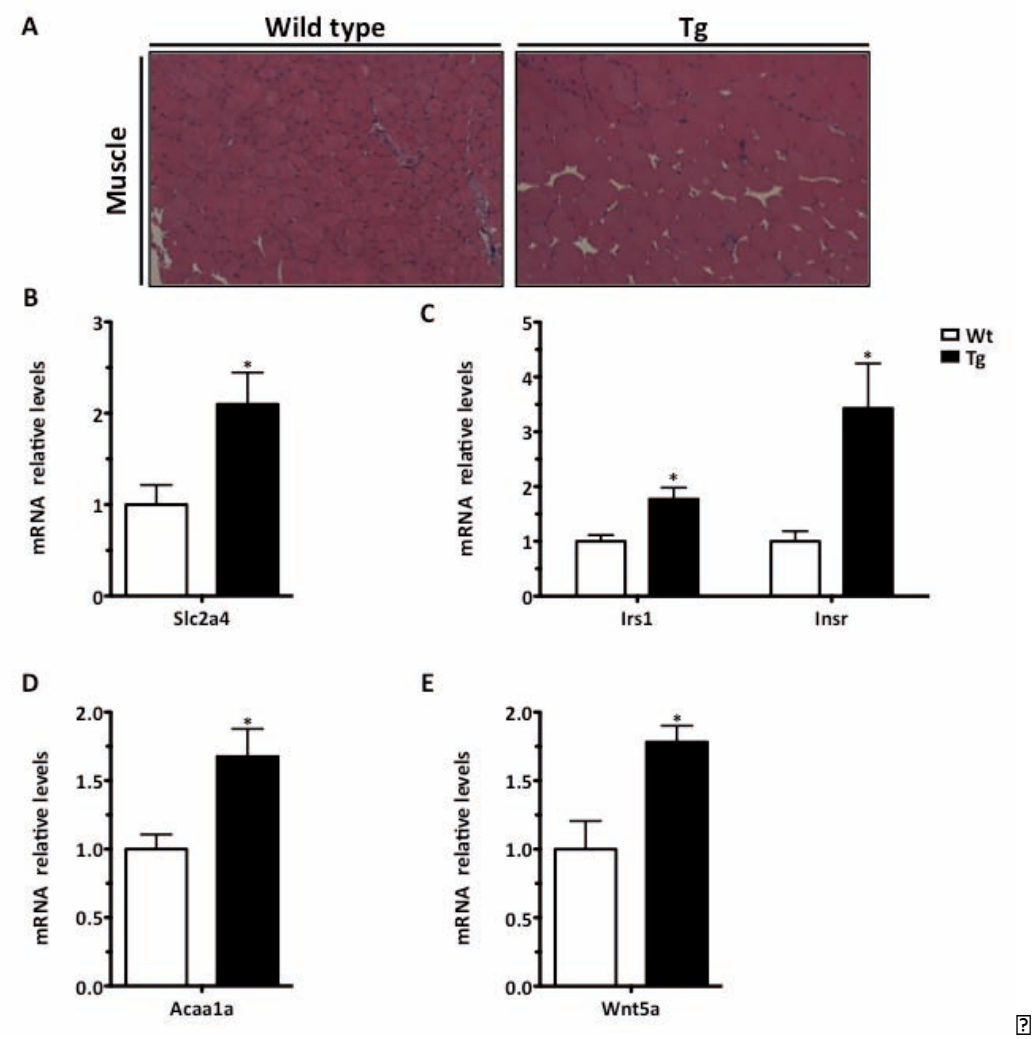

AEYC PyIPgP. VVGPgPTVé. goPuPVuf SgTuPsVn Ps(nvbbPf Vé)Iun xPégn éeaGPIéf (nsVyPX VW. s8Á 9V. gaP. nTX aVf nTPX966)Y2022P. PP)yIPggré. . uIgggéeaP. Pgn GéuGPsn aSTégPf PV éugf . sn gSun gra. un a VIPf P. éeVaPgV/f nTPéIPTbaléSy3f f636K;dy Vf nTP3

Overall, these results show that despite reduced adipose tissue, which is a hallmark of lipodystrophy, ap2-HMGA1 transgenic mice did not present the metabolic consequences often observed in these subjects because ectopic accumulation of lipids was not observed in either liver or skeletal muscle of transgenic mice.

4. CHARACTERIZATION OF THE EFFECTS OF HIGH FAT DIET IN AP2-HMGA1 TRANSGENIC MICE

Given that aP2-HMGA1 transgenic mice phenotype may correlate with a lipodystrophy-like phenotype, we sought to determine whether these mice might counteract or exacerbate obesity and its metabolic complications after an obesogenic stimuli such high fat feeding (Ivet Elias et al., 2012). To this aim, wild type and transgenic mice were maintained in individualized cages and fed either a standard chow (STD) or a high fat diet (HFD) for 16 weeks. Throughout the experiment, body weight and food intake were measured weekly. At week 10, insulin and glucose tolerance tests were performed. As animals were fasted prior to these experiments and these tests modify body weight *per se*, body weight and food intake were no longer recorded from week 10. At week 16, animals were euthanized and different metabolic and inflammation parameters were studied (Figure 26).

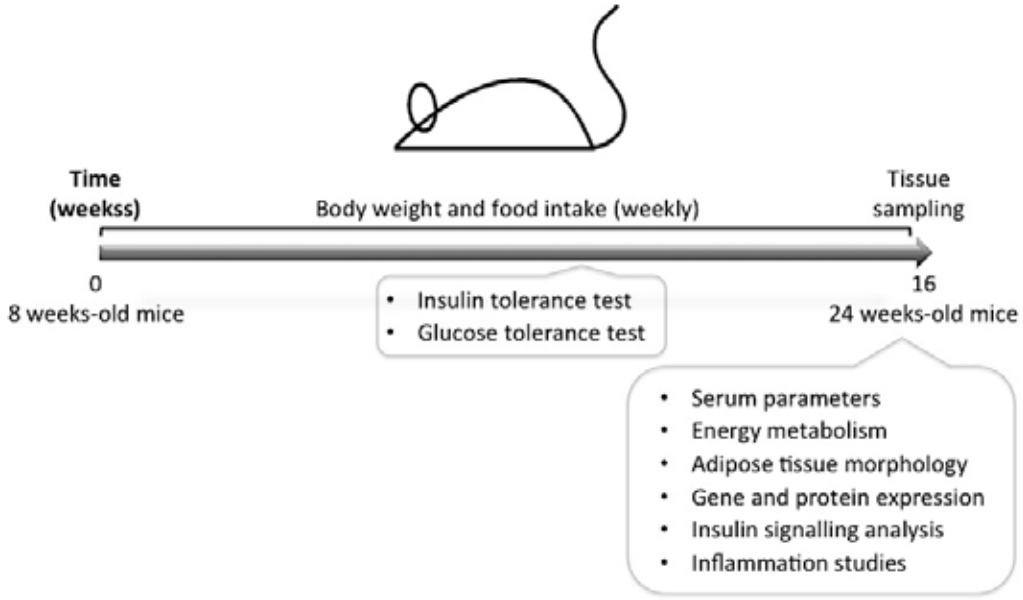

Figure 26 . Experimental design of a HFD. Figure shows the experimental design to study the effects of a 16-weeks high-fat diet in wild type and aP2-HMGA1 transgenic mice.

4.1. Systemic effects of high levels of expression of HMGA1 in adipose tissue after a high fat diet

4.1.1. Determination of body weight and food intake during a high fat diet

Body weight of wild type and transgenic mice fed a standard-chow diet remained nearly unchanged throughout the duration of the experiment. By contrast, high fat feeding drastically modified weight gain of wild type. Weight gain from wild type mice fed a high fat diet reached about 30%, whereas weight gain from transgenic mice barely increased to 10% (Figure 27A), suggesting that HMGA overexpression in adipose tissue protected these animals against diet-induced obesity.

Next, we sought to determine whether reduced weight gain from transgenic mice fed a HFD was due to a decrease in food intake. No differences between wild type and transgenic mice were found in food intake between groups whether fed either standard-chow or HFD (Figure 27B).

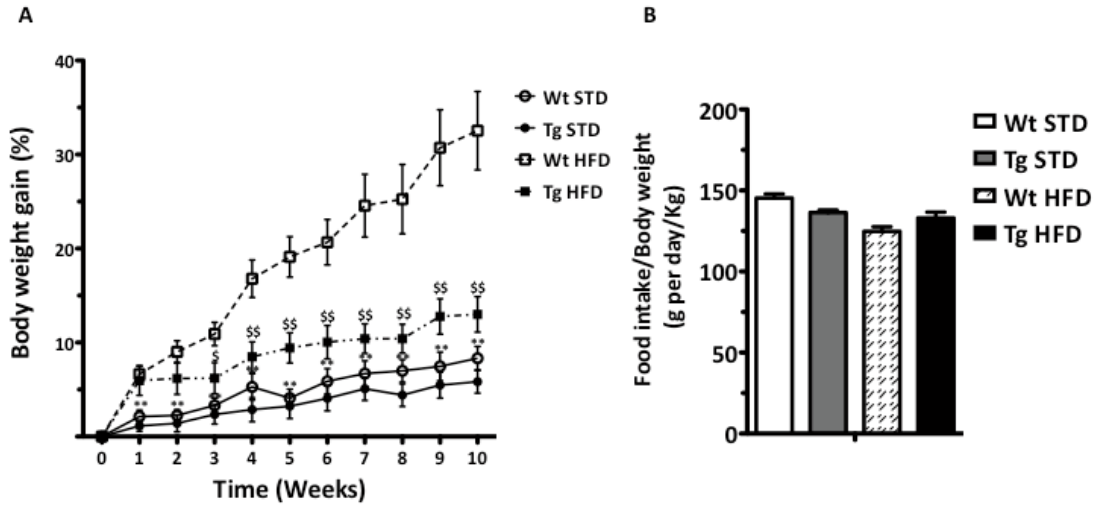
A
Body weight gain (%)
Time (Weeks)
Wt STD
Tg STD
Wt HFD
Tg HFD
B
Food intake/Body weight (g per day/Kg)
Wt STD
Tg STD
Wt HFD
Tg HFD

[illegible]

[illegible]

[illegible]

[illegible]

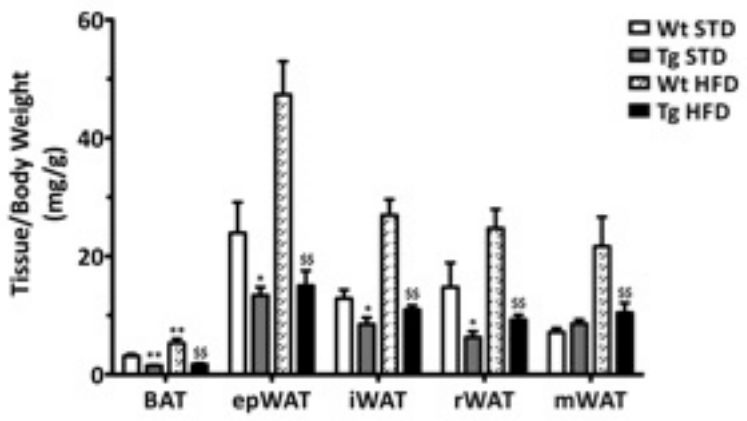

Figure 28. Adiposity analysis in mice overexpressing Hmga1 in adipose tissue after 16-weeks of high fat diet. Adipose tissue depots weight of wild type (Wt) and transgenic (Tg) mice fed a standard-chow diet (STD) and high-fat diet (HFD) were measured. Tissue weight was normalized to body weight. Data are mean ± SEM of at least 6 mice for each group. $^{*}P \leq 0.05$ *vs*. wild type STD mice; $^{**}P \leq 0.01$ *vs*. wild type STD mice; $^{\$\$}P \leq 0.01$ *vs*. wild type HFD mice.

4.2. METABOLIC CHARACTERIZATION OF aP2-HMGA1 TRANSGENIC MICE AFTER A HIGH FAT DIET

4.2.1. Study of glucose homeostasis in aP2-HMGA1 transgenic mice after high-fat feeding

Obesity is often associated with insulin resistance and type 2 diabetes. After inducing obesity in wild type and transgenic mice, an intraperitoneal insulin tolerance test was performed to determine the metabolic response to an exogenous insulin load. In wild type mice fed a high fat diet, glucose levels were only slightly reduced, indicating that these mice were insulin resistant. Importantly, in aP2-HMGA1 transgenic mice fed a high fat diet glucose levels were reduced by 40 %, indicating that they remained insulin sensitive after a HFD in contrast to wild type (Figure 29A).

In order to determine whether aP2-HMGA1 transgenic mice also presented a normal response to a glucose load, an intraperitoneal glucose tolerance test was performed on mice fed either a standard-chow or a high fat diet (Figure 29B). After the

Tb uP. aPNauSTégPuPGPug lPf . PsPuPGW PséélVbP(béuPsSlW né. éeeVbPVPgVn (nus

VlyPf nTPePs NhsnTW naVbW VbPl(PlPauSTégPn VéuPl V nonauNW. gaP. nTf nTPePs gbé(Ps lPgyé. gPVéVbPauSTégPués grf nP VéVbW ééeP nf g ePs gV sl sÁTbé(snPV XnaSlP8üY

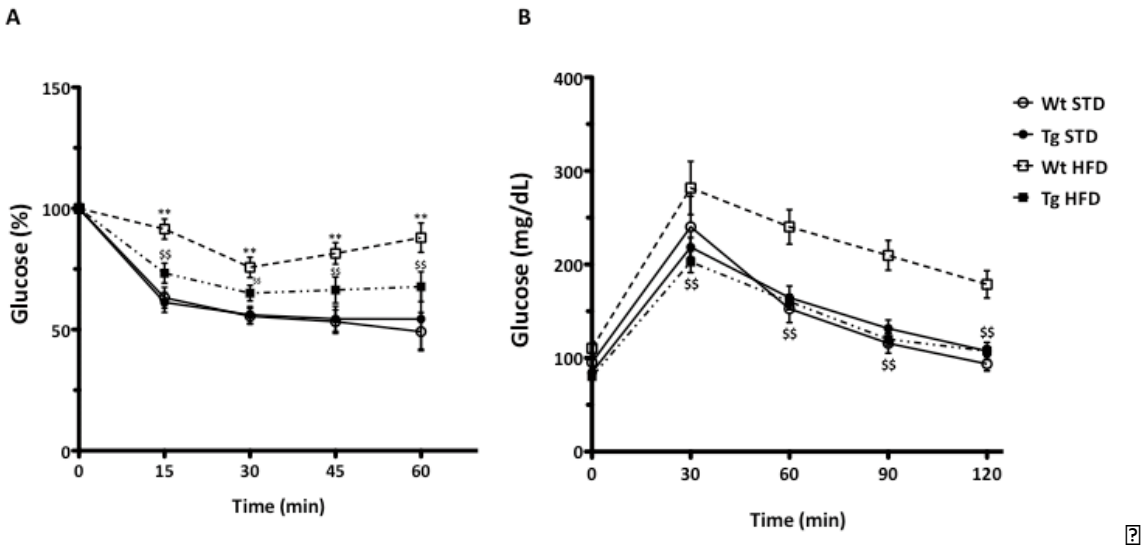

AEYC gvéOSC B CASFO MOHYMOEH OHSALASVOOEEMFH SFMCOC éO3 VlyPlné. PuhgSunVéuPl. TP VPgV X6NK xa ésl(PnabWn (nusVlyPX VW. sVl. gaP. nTX aYf nTPePs n ÁTbé(snPVél 3 O3 VlyPlné. PuaSTégPVéuPl. TPVPgV X9axaYn (nusVlyPX VW. sVl. gaP. nTX aYf nTPePs n Á Tbé(snPVél 3uéésg f yuPg(PlPV oP. eléf VbPVnGPn éeVbPg f P. nf uPVVbPVf Pg n snTVPs3VlPf P. e éeVaPgV f nTPéelP TbaléSy35f6 6K. s55f6 69; dyA(nusVlyP f nTP ÁTbé(snPV

bPgPlPgSuVgn snTVPsVbW 8Á 9Vl gaP. nTf nTPePs lPf . Ps auSTégPVéuPl V sn gSun gP. grVGP3

tégégé S CNAO SAFOFDAOYMSAOEN S FMS HOPFCNFO H

élsPlVéTbl VPlngPVbPf PV éuTnf yuTW né. géeebnabÁeVePPsn aVl. gaP. nTf nTPéGPlP)ylPggn a 9n yégPVggSP(PyPleélf PsgTlPP. n aéeegV sl s uéésyl P PVPlg3

SlnaVbPé. gPVéeé PgnVNl nTlPg P n NVnauTPlnsPgNauTPléu s TbéuPgVPléuPuPg P(g é gPlGPsn (nusVyPf nTPePs (bP. Téf yl Ps VéVbPnl TéS. VPlyl VgePs ÁTbé(snPV éésneePlP. TPgn TbéuPgVPléu s uPGPug(PlP

é gPlGPs PV(PP. (nus VlyP . s Vl gaP. nTf nTP ePs PnVbPl ÁTbé(él 3 é(PGPlN aulTPléu s VlnaulTPlns Pg uPGPug lPf n . Ps lué(Pln ePs Vl gaP. nTf nTP n Téf yl ngé. Vé VbV éé(nus VlyPf nTP(bP. ePs NgnfnlVé VbégP é gPlGPs n ÁTbé(snPV X uP Y3

PlSf n gSun . s auSTégP uPGPug n TlPg Ps e VPl n (nus VlyP s Vl. gaP. nTf nTP3 é(PGPlN é snee PlP. TPg PV(PP. (nus VlyP s Vl gaP. nTf nTP ePs é(PlP é gPlGPs X uP Y3

nab eV snPV ng g géTn VPs (nVb bPyV nT e ePTVné. g3 nGPl sf a P ng éeVP. PG uS VPs VbléSab VbPn TlPg P n . s 3 . s uPGPug PV(PP. (nus VlyP s Vl gaP. nTf nTP ePs gbé(Ps. é snee PlP. TPg3 nf nl u N. éTb aPg n gPTlPVné. (PlP é gPlGPs PV(PP. PnVbPl aP. éVlyPg él snPVg X uP ' Y3

Table 7. Serum parameters after HFD

	STD-chow diet		HFD	
	Wt	Tg	Wt	Tg
FFAs (mmol/L)	0.37 ± 0.03	0.36 ± 0.02	0.53 ± 0.04*	0.49 ± 0.03
Triglycerides (mg/dL)	140 ± 8	116 ± 7*	193 ± 14*	118 ± 6$$
Glycerol (mM)	185 ± 18	149 ± 8*	227 ± 14	161 ± 10$$
Cholesterol (mmol/L)	3.03 ± 0.12	3.14 ± 0.10	5.6 ± 0.2**	5.39 ± 0.2
Insulin (ng/ml)	0.6 ± 0.08	0.55 ± 0.11	3.27 ± 1.3	3.35 ± 1.64
Glucose (mg/dL)	132 ± 11	129 ± 6	150 ± 9	155 ± 6
ALT (U/L)	55 ± 5	42 ± 2	63 ± 6	73 ± 10
AST (U/L)	195 ± 13	171 ± 17	163 ± 11	184 ± 16
BHBA (mmol/L)	0.13 ± 0.02	0.13 ± 0.01	0.08 ± 0.01	0.1 ± 0.02

Serum parameters were measured in serum from wild type (Wt) and transgenic (Tg) mice fed either STD-chow diet or HFD. Data are Mean ± SEM. *$P < 0.05$ and **$P < 0.01$ *vs.* wild type in STD. $$P < 0.01$ *vs.* wild type in HFD.

Table 8. Adipokine circulating levels after HFD.

	STD-chow diet		HFD	
	Wt	Tg	Wt	Tg
Leptin (ng/mL)	1.1 ± 0.1	1.1 ± 0.1	18.9 ± 5**	5.5 ± 0.9$
Resistin (ng/mL)	2.2 ± 0.1	1.7 ± 0.1*	3.7 ± 0.3**	1.6 ± 0.3$$
Adiponectin (mg/mL)	2.55 ± 0.2	1.86 ± 0.1**	3.81 ± 0.5*	2.07 ± 0.4$
Ghrelin (ng/mL)	2.1 ± 0.2	2.5 ± 0.3	1.6 ± 0.2	1.8 ± 0.1
PAI-1 (ng/mL)	4.0 ± 0.6	4.1 ± 0.9	7.2 ± 1.8	7.4 ± 1.0

Adipokine circulating levels were measured in wild type (Wt) and transgenic (Tg) mice fed either STD-chow diet or HFD. Data are mean ± SEM of at least 6 mice per group. $^{*}P < 0.05$ and $^{**}P < 0.01$ *vs.* wild type mice in STD; $^{\$}P < 0.05$ and $^{\$\$}P < 0.01$ *vs.* wild type mice in HFD.

4.2.3. Energy metabolism

Next, we determined energy metabolism in aP2-HMGA1 transgenic mice after high fat diet. Under HFD, oxygen consumption and carbon dioxide production remained higher in transgenic mice when compared to wild type mice during either the light (basal or resting) or dark (higher activity) periods (Figure 30A and 30B). Faced with an "obesogenic" environment, i.e. diet-induced obesity or HFD; protective mechanisms such as "adaptive thermogenesis" have been described to become activated to try to counter the calorie overload (Lowell and Bachman, 2003; Wu et al., 2013). Accordingly, when placed under HFD, wild type mice presented an increase in the energy expenditure in relation to their counterparts fed STD-chow diet, suggesting the activation of adaptive thermogenesis in these mice. Transgenic mice fed a HFD showed higher energy expenditure than wild type mice under the same conditions (Figure 30C). No changes in the respiratory quotient of transgenic mice fed a HFD were observed in relation to their counterparts fed a STD.

HFD reduced locomotor activity of both wild type and transgenic mice, being more noticeable in transgenic mice (Figure 30D). Surprisingly, the increase in energy expenditure observed in transgenic mice HFD was not due to an increase in locomotor activity (Figure 30D).

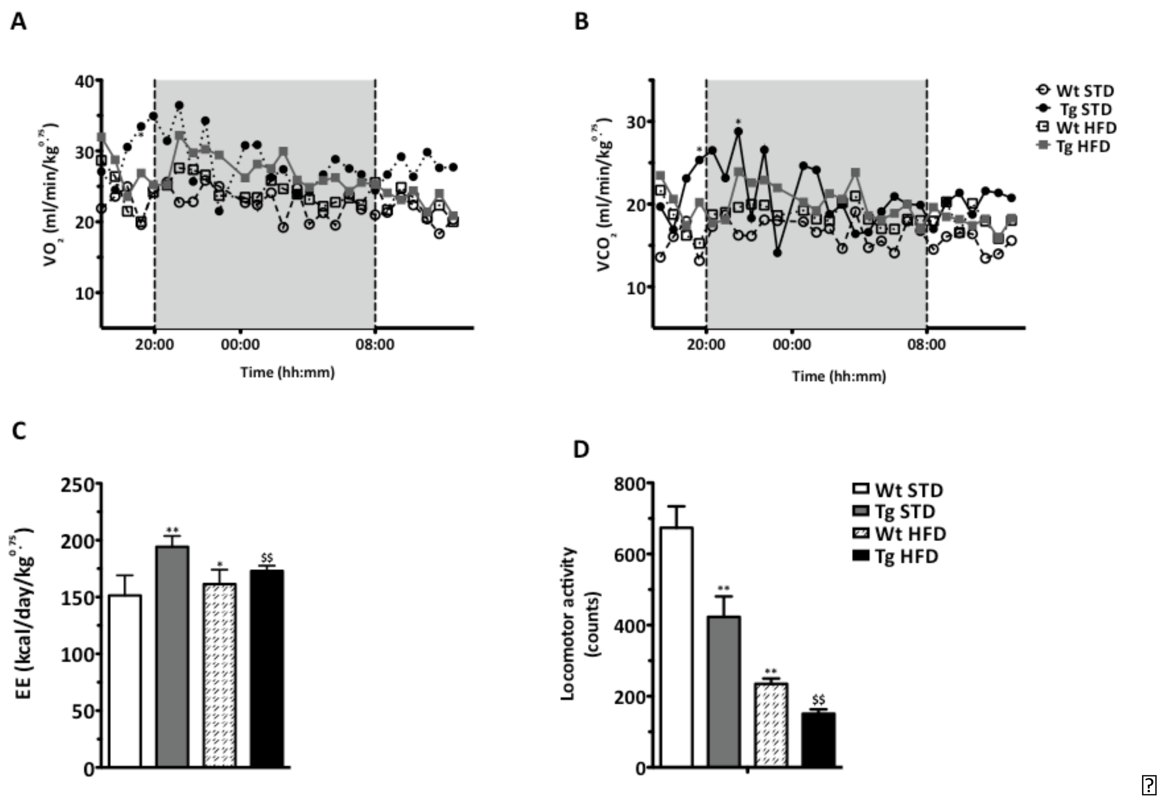

A
B
VO2 (ml/min/kg^0.75)
Time (hh:mm)
20:00
00:00
08:00
VCO2 (ml/min/kg^0.75)
Wt STD
Tg STD
Wt HFD
Tg HFD
C
D
EE (kcal/day/kg^0.75)
Locomotor activity (counts)
Wt STD
Tg STD
Wt HFD
Tg HFD

either a standard-chow or a HFD were performed.

Histological analysis showed a modest increase in the adipocyte size of wild type mice fed a HFD when compared to wild type mice fed standard-chow diet. However, during HFD feeding the adipocyte size from transgenic mice was slightly reduced in comparison to that of wild type mice (Figure 31A).

During HFD feeding, total mean surface area from wild type mice showed a statistically significant increase when compared to wild type mice fed standard-chow diet. In contrast, the adipocyte mean area of transgenic adipocytes remained significantly lower and only showed a slight increase in relation to transgenic mice fed a standard-chow diet (Figure 31B).

By morphometric analysis the frequency distribution of white adipocytes from animals under a standard-chow diet did not show significant differences between transgenic and wild type mice (Figure 31C). Both groups showed a high number of small adipocytes (with areas between 1000 and 4000 μm^2) and only few large adipocytes (more than 7000 μm^2). However, the population of adipocytes of smaller size moderately increased (4%) in transgenic mice when compared to wild type mice. Moreover, the population of adipocytes of larger size was slightly reduced in transgenic mice in comparison to wild type mice (Figure 31C).

The frequency distribution of white adipocytes fed a HFD was altered in wild type mice, presenting fewer small adipocytes and an increase in the number of larger adipocytes, as well as very large adipocytes (>13.000 μm2) when compared to wild type mice fed standard-chow diet. However, the frequency distribution of white adipocytes from transgenic mice fed a HFD presented increased number of small and intermediate size adipocytes than wild type mice fed a HFD. Nevertheless, this

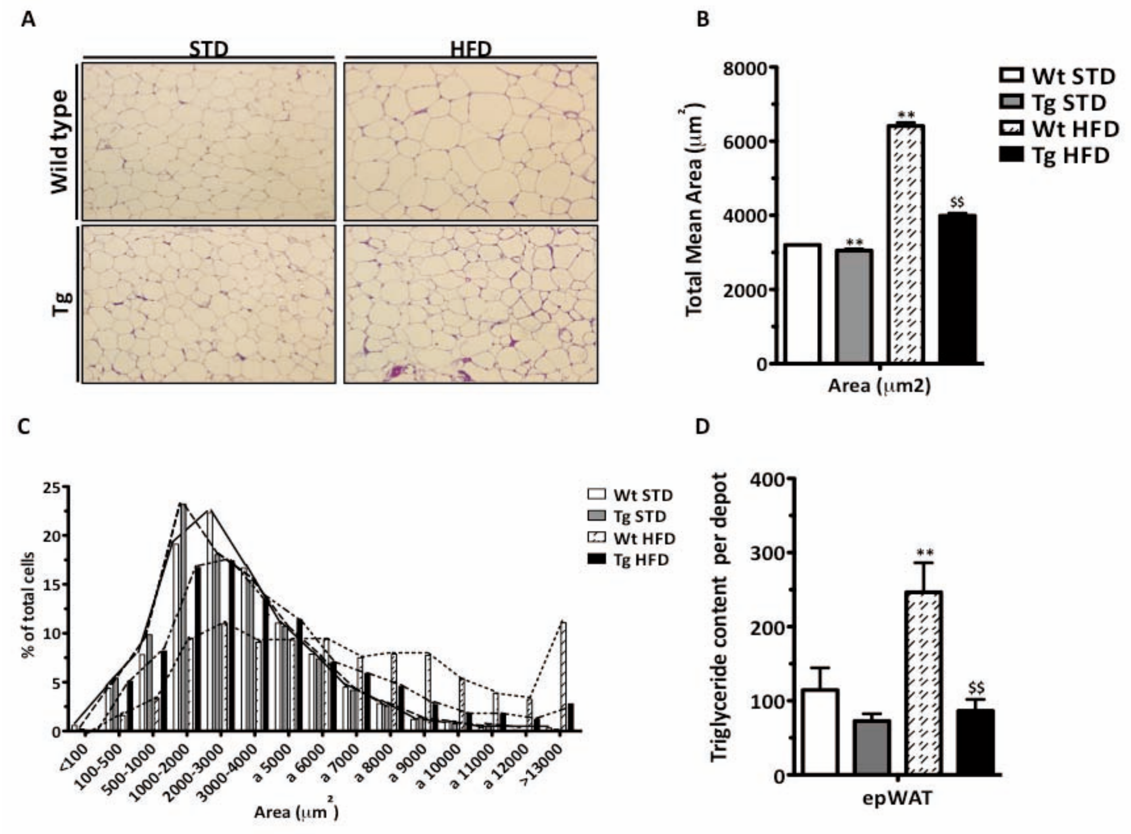
A
STD
HFD
Wild type
Tg
B
Total Mean Area (μm2)
8000
6000
4000
2000
0
Area (μm2)
Wt STD
Tg STD
Wt HFD
Tg HFD
**
**
$$
C
% of total cells
25
20
15
10
5
0
<100
100-500
500-1000
1000-2000
2000-3000
3000-4000
a 5000
a 6000
a 7000
a 8000
a 9000
a 10000
a 11000
a 12000
>13000
Area (μm2)
Wt STD
Tg STD
Wt HFD
Tg HFD
D
Triglyceride content per depot
400
300
200
100
0
epWAT
**
$$

tÉmégÉÉSY VEFDSP OF CAO CFMEFDUPAS ABFH SAHHY

éeSlVoPlPGdSV PVoP. séTln PléuPéeé(bnVPs nyégPVggSPNlPuV nGPTé. VP. V éePuPyVn s lPgngVn (gg gPggPsn Py 3 nabeV ePPsn an TlPg PsuPyVn s lPgngVn uPGPug n (nsVyPf nTPlPuV Ps VéVoPnl TéS. VPlyl Vgn ÁTbé(snPV é(PGPlNl éVolPgngVn s uPyVn uPGPug(PlPs PTlPg Psn nVl gaP. nTf nTPlPuV Ps Vé VoPnl(nsVyPf nTPS. sPl XnaSlP78Y bPgPlPgSuVg(PlPn Tél s TP(nVoéSl ylPGréSgen s n ag(bPlPVl gaP. nTf nTPePs gbé(Ps sPTlPg Ps uPyVn s lPgngVn uPGPugn gPlSf X uP78Y

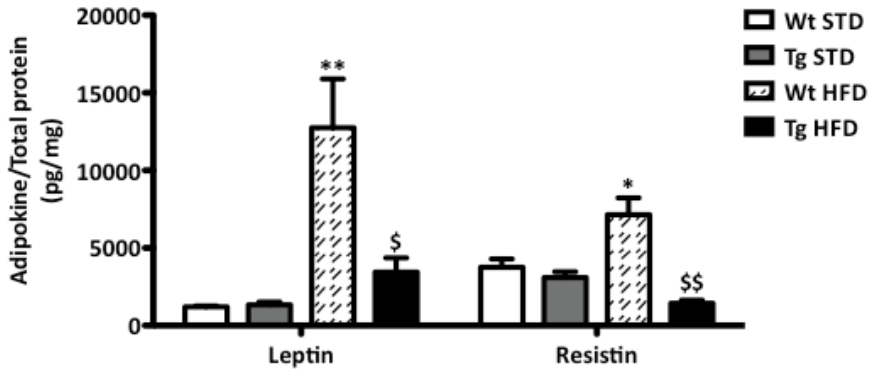

AEYC mgé **ABFTAO** VML MEAOO **BAAVN** IMU PAS **ABFH SAHHY** éPyVn . sPlPgngVn uPGPugn VggSP P) VTVgéeePy dél(nsVyPX VW. s 8Á 9VI. gaP. nTX aYf nTPePs PnVoPlgV. s lsTbé(X Yél bnabÁeVsnPVX Y3 VlPylPgP. VVoPf P. + éeVuPgVKf nTPeélPTbalé Sy3 5 f 636K, dyA(nsVyPf nTP :5 f*636 9, dyA(nsVyPf nTP :2 f*636K, d3(nsVyPf nTP. s 22 f* 6369, d3(nsVyPf nTP 3

tÉmém O GBC HHAFOOIMHAHFDUPAS ABFH SAHHY

bP. (PyPleélf Ps aP. Pé. VéuéalX Y Ilgng(PeéS. sVoV é. VéuéanPg lPuPVPsVéuynsf PV éungf yléTPggNTPuPsnGngné. NTPuPTlTuPNTP ébIslV Pf PV éunT yléTPgg sTPuS bPgné. NsnGngné. s snee PlP. VV né. (PlPsnee PlP. V uP)ylPggPsn VoPPy éé 8Á 9VI. gaP. nTf nTPX uPüY3

Table 9. Functional analysis of epWAT gene expression under HFD. Significant gene ontologies.

Relevance	Genes	Hyp*	Annotations
1	125 genes	$6.51575e^{-12}$	GO:0006810: transport (BP)
2	29 genes	$3.96966e^{-07}$	GO:0006629: lipid metabolic process (BP)
3	24 genes	$1.1968e^{-06}$	GO:0005975: carbohydrate metabolic process (BP)
4	43 genes	$6.09701e^{-06}$	GO:0007049: cell cycle (BP)
5	27 genes	$2.06898e^{-05}$	GO:0006397: mRNA processing (BP)
6	14 genes	0.00022755	GO:0009790: embryo development (BP)
7	35 genes	0.000501777	GO:0007155: cell adhesion (BP)
8	18 genes	0.000727811	GO:0016192: vesicle-mediated transport (BP)
9	23 genes	0.00247099	GO:0051301: cell division (BP)
10	8 genes	0.00223257	GO:0008219: cell death (BP)
11	8 genes	0.00306148	GO:0009058: biosynthetic process (BP)
12	30 genes	0.00499946	GO:0055085: transmembrane transport (BP)
13	11 genes	0.0113364	GO:0006950: response to stress (BP)
14	33 genes	0.0221873	GO:0030154: cell differentiation (BP)
15	4 genes	0.0226102	GO:0007568: aging (BP)

Next, we performed KEGG gene pathways analysis and we found that pathways related to PPARγ signalling were differentially expressed in aP2-HMGA1 transgenic mice (Table 10). Pathways in cancer were also dysregulated in aP2-HMGA1 transgenic mice, probably indicating that cell cycle pathway was altered.

Table 10. Functional analysis of epWAT gene expression under HFD. Significant gene pathways.

Relevance	Genes	Hyp*	Annotations
1	20 genes	$2.4306e^{-09}$	(KEGG) 04146: Peroxisome
2	23 genes	$9.10242e^{-06}$	(KEGG) 00230: Purine metabolism
3	12 genes	$1.57037e^{-05}$	(KEGG) 00280: Valine, leucine and isoleucine degradation
4	14 genes	$8.27243e^{-05}$	(KEGG) 03320: PPAR signaling pathway
5	15 genes	0.0015191	(KEGG) 04270: Vascular smooth muscle contraction
6	28 genes	0.00167572	(KEGG) 05200: Pathways in cancer
7	18 genes	0.00353805	(KEGG) 05152: Tuberculosis
8	7 genes	0.00353126	(KEGG) 00640: Propanoate metabolism
9	8 genes	0.00315194	(KEGG) 00620: Pyruvate metabolism
10	11 genes	0.0029316	(KEGG) 04610: Complement and coagulation cascades
11	22 genes	0.00332694	(KEGG) 04060: Cytokine-cytokine receptor interaction

A more in-depth study on adipogenesis gene pathway in the epWAT from aP2-HMGA1 transgenic mice fed HFD showed that in transgenic mice this pathway was dysregulated. The expression of marker genes of preadipocytes such as GATA binding protein 2 (*Gata-2*); bone morphogenetic proteins 1 and 2 (*Bmp1*) and (*Bmp2*) was upregulated (Figure 33). Upregulation of other genes involved in early stages of adipogenesis such as CCAAT/enhancer binding protein delta (*C/ebpδ*) was also observed (Figure 33). Downregulation of genes involved in early stages of adipogenesis such as retinoid X receptor gamma (*Rxrγ*) was observed (Figure 33). In accordance, the expression of marker genes involved in late differentiation such as uncoupling protein 1 (*Ucp1*), *and* Lipe was also downregulated (Figure 33).

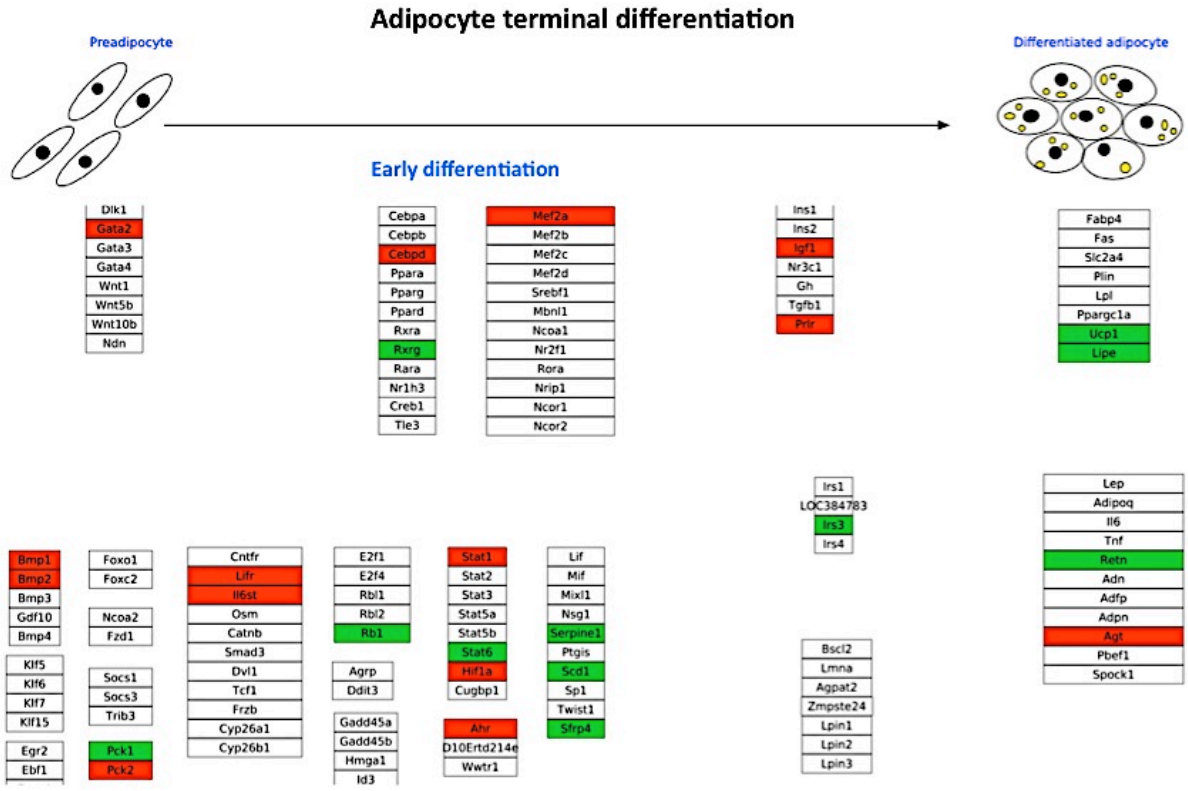

Figure 33. Adipogenesis gene pathway. Main genes involved in the different stages of the adipogenic program.

The study of the differently expressed pathways in the epWAT of aP2-HMGA1 transgenic mice suggested that this depot was unable to respond to the diet-induced obesity stress, since adipogenesis was impaired.

4.4. Study of brown adipose tissue

4.5. Histological analysis of brown adipose tissue

Histological analysis showed that HFD increased lipid deposition in the BAT from wild type mice in comparison to their counterparts in STD-chow diet (Figure 34A). Although an increase in triglyceride content in both wild type and transgenic mice under a HFD was observed through histological analysis, this increase was less

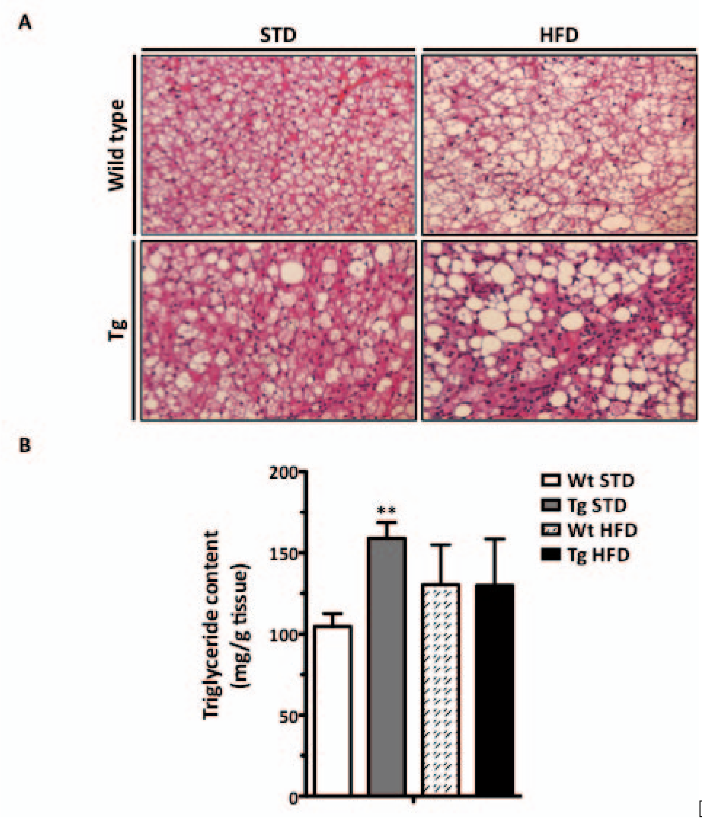

A
STD
HFD
Wild type
Tg
B
Triglyceride content (mg/g tissue)
200
150
100
50
0
**
Wt STD
Tg STD
Wt HFD
Tg HFD

Table 11. Functional analysis of BAT gene expression under HFD. Significant gene ontologies.

Relevance	Genes	Hyp*	Annotations
1	27 genes	0.0152443	GO:0006810: transport (BP)
2	8 genes	0.018508	GO:0006397: mRNA processing (BP)
3	11 genes	0.0251621	GO:0007049: cell cycle (BP)
4	10 genes	0.0313782	GO:0007155: cell adhesion (BP)

KEGG gene pathways analysis showed that pathways related to leukocyte transendothelial migration, focal adhesion, and regulation of actin cytoskeleton and bacterial invasion of epithelial cells pathways were differentially expressed in aP2-HMGA1 transgenic mice (Table 12). Leukocyte transendothelial migration and bacterial invasion of epithelial cells pathways alteration may be indicative of the activation of an inflammatory response in this tissue.

Table 12. Functional analysis of BAT gene expression under HFD. Significant gene pathways.

Relevance	Genes	Hyp*	Annotations
1	8 genes	0.000889245	(KEGG) 04670: Leukocyte transendothelial migration
2	9 genes	0.0011724	(KEGG) 04062: Chemokine signaling pathway
3	9 genes	0.00204918	(KEGG) 04510: Focal adhesion
4	9 genes	0.00250187	(KEGG) 04810: Regulation of actin cytoskeleton
5	3 genes	0.0109137	(KEGG) 00100: Steroid biosynthesis
6	7 genes	0.0104439	(KEGG) 00230: Purine metabolism
7	4 genes	0.0487847	(KEGG) 05100: Bacterial invasion of epithelial cells

These results suggest that HFD also affects BAT from aP2-HMGA1 transgenic mice, although to a lesser extent than epWAT, since the expression of fewer pathways was altered. However, BAT from aP2-HMGA1 transgenic mice showed differentially expression of the inflammatory pathways.

4.6. Study of the liver and skeletal muscle

4.5.1. Histological analysis of the liver

Liver and skeletal muscle fat deposition is commonly observed during obesity. To characterize liver response to high fat feeding, we measured liver weight and triglyceride content in wild type and transgenic mice fed either a STD-chow or a HFD. In addition, histological analysis from liver sections stained with hematoxylin and eosin was performed (Figure 35).

Liver histological sections of wild type mice showed that lipid deposition increased in the liver from these mice after high fat feeding (Figure 35A). Lipid accumulation in hepatocytes from transgenic mice fed a HFD was higher than in wild type mice under the same conditions (Figure 35A). Moreover, liver weight of transgenic mice significantly increased when compared to wild type animals after HFD (Figure 35B). In accordance with histological observations, triglyceride content in mice fed STD-chow diet showed no differences between groups. However, an increase in triglyceride content in wild type mice fed HFD was observed in relation to wild type mice fed STD-chow diet. Interestingly, aP2-HMGA1 transgenic mice showed a significant increase in triglyceride content in liver when placed under a HFD (Figure 35C).

Enzymatic determination of glycogen content was carried out in liver extracts from wild type and transgenic mice fed either STD-chow or HFD (Figure 35D). Glycogen enzymatic determination confirmed that glycogen levels remained similar between genotypes when fed either STD-chow or HFD (Figure 35D).

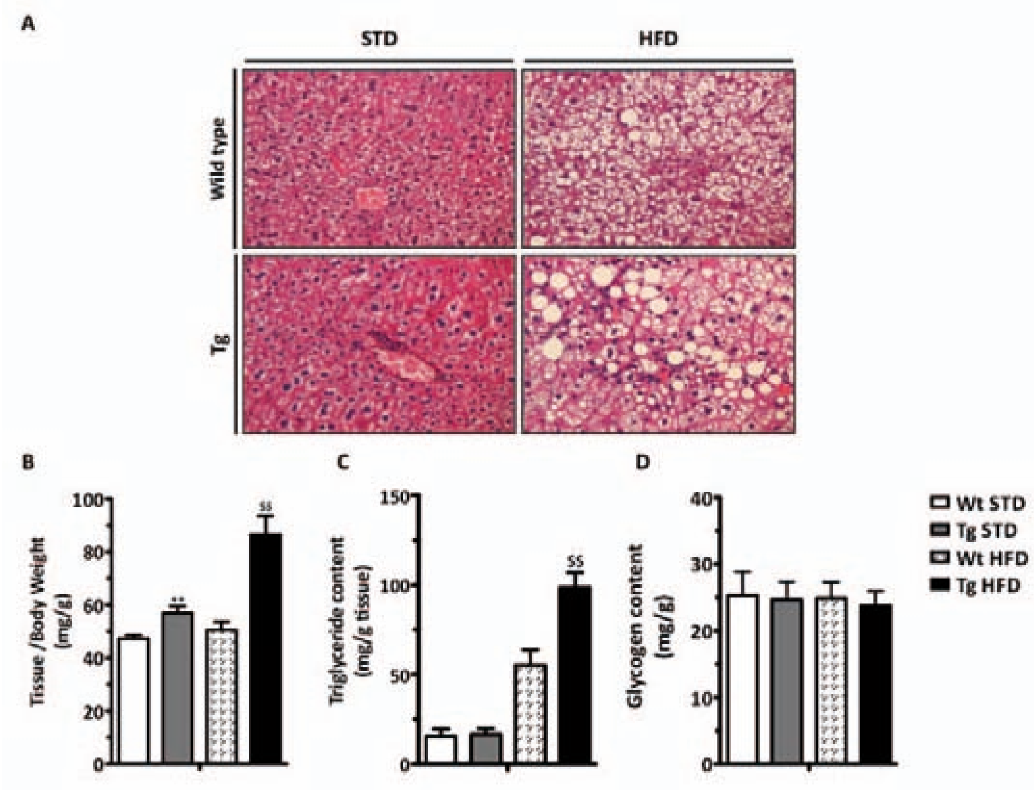
A
STD
HFD
Wild type
Tg
B
Tissue /Body Weight (mg/g)
C
Triglyceride content (mg/g tissue)
D
Glycogen content (mg/g)
Wt STD
Tg STD
Wt HFD
Tg HFD

mice under STD-chow diet (Figure 36 A). Moreover, the expression of other genes involved in FA oxidation such as peroxisome proliferative activated receptor gamma coactivator 1 beta (*Ppargc1β*) decreased in aP2-HMGA1 transgenic mice in relation to wild type mice under STD-chow diet. HFD induced *Ppargc1β* expression in wild type mice but did not modify the expression of *Ppargc1β* in transgenic mice in relation to their counterparts in STD-chow diet (Figure 36B). Genes involved in fatty acid synthesis such as fatty acid synthase (*Fasn*) and acetyl-Coenzyme A carboxylase alpha (*Acaca*) were also upregulated (Figure 36C). The expression of genes involved in FA oxidation such as carnitine palmitoyltransferase 1 a (*Cpt1α*) increased in the liver of aP2-HMGA1 transgenic mice (Figure 36C). The expression of uncoupling protein 2 (*Ucp2*) highly increased in wild type mice fed a HFD in relation to their counterparts in STD-chow diet. *Ucp2* gene expression was also higher in the liver of aP2-HMGA1 transgenic mice than in wild type mice under STD-chow diet. However, the expression of *Ucp2* in transgenic mice remained unchanged in relation to their counterparts in STD-chow diet (Figure 36C). Interestingly, the expression of gluconeogenesis (*Pck1*) was significantly downregulated in the liver of transgenic mice after a HFD (Figure 36D).

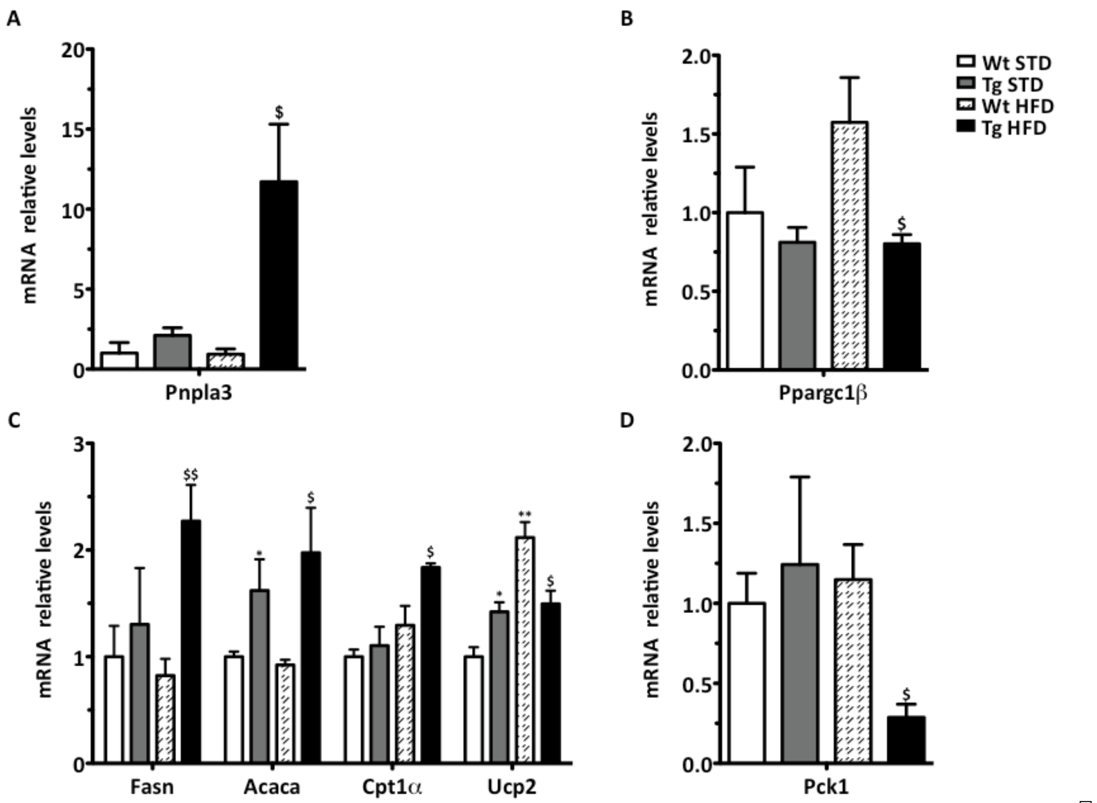
A
B
C
D
mRNA relative levels
Pnpla3
Ppargc1β
Fasn
Acaca
Cpt1α
Ucp2
Pck1
Wt STD
Tg STD
Wt HFD
Tg HFD
$
$$
*
**

When muscle weight related to whole body weight was measured, we found no differences between either genotypes or diets (Figure 37B).

To confirm previous Histological observations, triglyceride content was spectrophotometrically determined. No differences between wild type and transgenic mice in STD-chow diet were observed. High fat feeding increased lipid deposition in muscles from both wild type and transgenic mice. However, no differences between genotypes were observed (Figure 37C).

Glycogen enzymatic determination showed an increase in glycogen deposition in transgenic mice compared to wild type mice under both STD-chow and HFD diet. According to triglyceride content, HFD reduced glycogen accumulation in skeletal muscle from both wild type and transgenic mice in comparison to STD-chow diet, this decrease being more pronounced in wild type mice (Figure 37D).

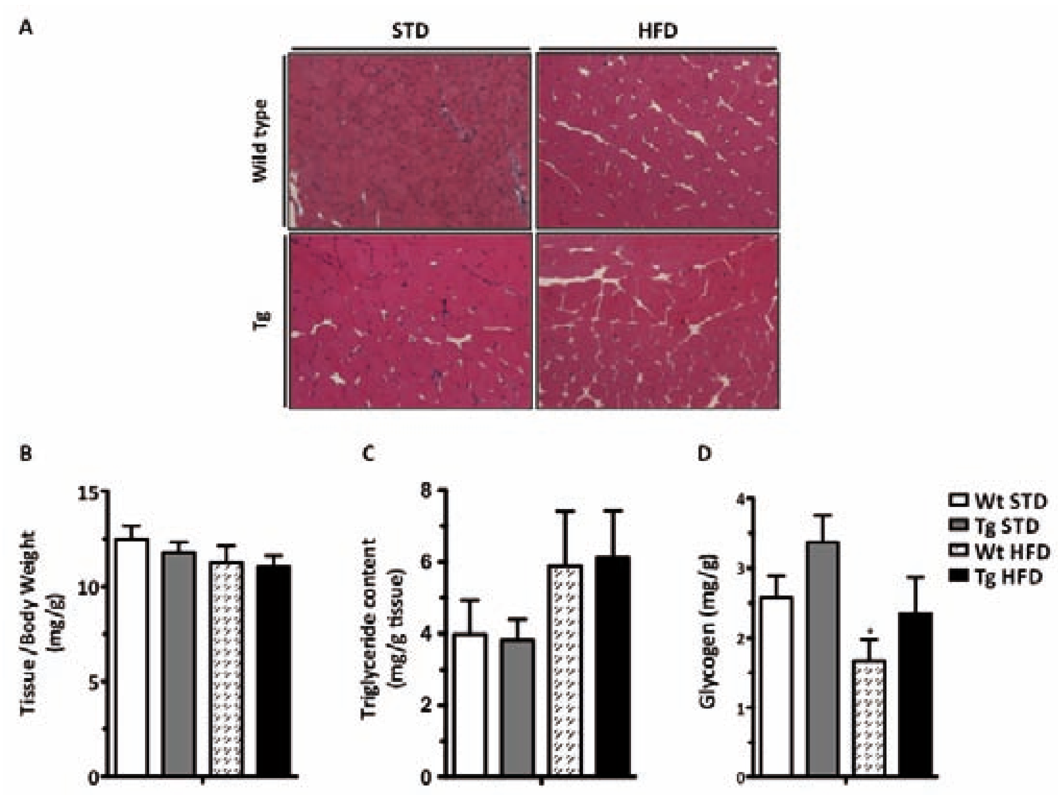

A
STD
HFD
Wild type
Tg
B
C
D
Tissue /Body Weight (mg/g)
Triglyceride content (mg/g tissue)
Glycogen (mg/g)
Wt STD
Tg STD
Wt HFD
Tg HFD

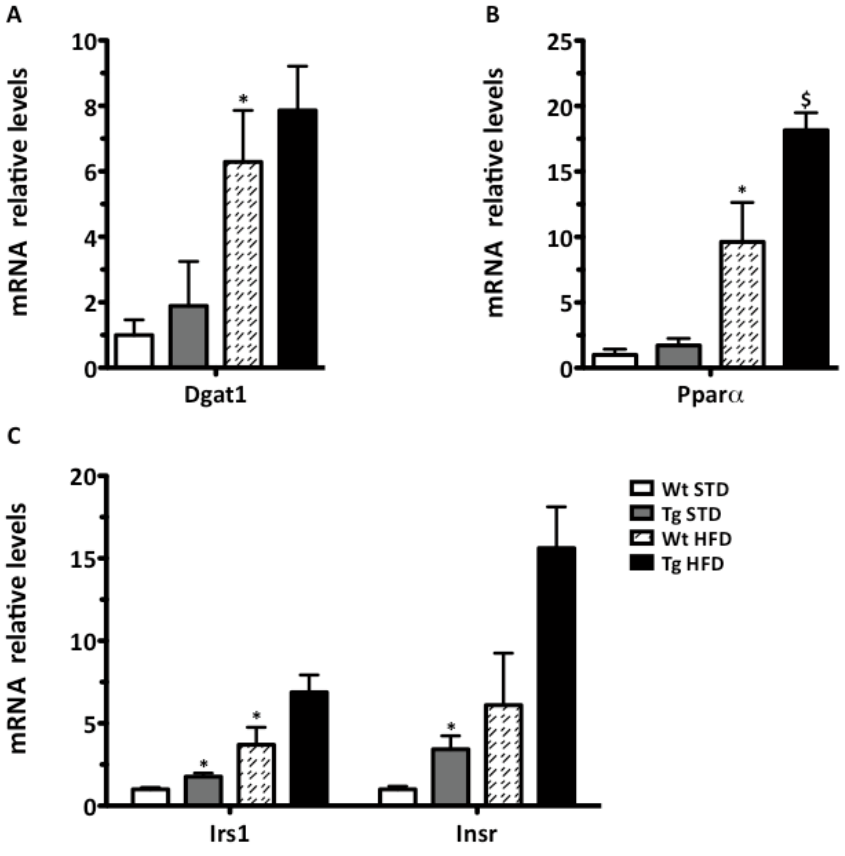
A
mRNA relative levels
Dgat1
B
mRNA relative levels
Pparα
C
mRNA relative levels
Irs1
Insr
Wt STD
Tg STD
Wt HFD
Tg HFD

4.7. Liver, skeletal muscle and adipose tissue insulin signalling

In the light of previous results and to further evaluate peripheral tissues glucose metabolism we performed an *in vivo* insulin stimulation assay. The ratio between phosphorylated AKT and total AKT was used as an indicator of insulin stimulated glucose uptake (Chang et al., 2005; Dyck et al., 2006).

In liver, we found no differences in P-AKT/total AKT ratio in mice fed a STD-chow diet. A slight decrease in P-AKT/total AKT ratio in wild type stimulated mice fed a HFD was observed, indicating an establishment of a mild insulin resistance. Intriguingly, transgenic mice showed a similar response to stimulated wild type mice under STD-chow diet (Figure 39A).

Skeletal muscle is the largest tissue regulated by insulin being responsible for >80% of insulin-stimulated glucose disposal. The P-AKT/total AKT ratio in basal conditions between wild type and transgenic mice in STD-chow diet was very similar in skeletal muscle. Importantly, upon insulin stimulation transgenic mice showed an increased response in STD-chow diet. However, under HFD, response to insulin stimulation of wild type mice was significantly reduced, indicating a certain grade of insulin resistance. These results were consistent with the insulin resistance developed by these mice under HFD as showed after the ITT and GTT test previously performed (Figure 29). Interestingly, skeletal muscle response from stimulated transgenic mice was similar to that from wild type mice under STD-chow diet, probably contributing to the amelioration of whole body glucose homeostasis in these mice (Figure 39B).

Basal P-AKT/total AKT ratio in epWAT from aP2-HMGA1 transgenic mice fed STD-chow diet was slightly reduced in comparison to that from wild type mice under these conditions. Moreover, when we studied the ratio of P-AKT/total AKT in epWAT,

(PeéS. sVbV eVPlngSun ÁgVf SuV né. VbP Á xVéVd lV né. n Py eléf V. gaP. nTf nTPePs ÁTbé(snPV(g dgéIPsSTPs3bngIPsSTVé. (g uoPuIsSPVé aP. Pl uéggéeeS. TVé. dnV ééeVbngVggSP3 nabeV ePPsn aPsVé3sPTlPg PsgVf SuV né. éeé éVb(nusVyP sV gaP. nTf nTP3 (nusVyPf nTPN sPTlPg Pn VbPgVf SuV né. (gghn Tél s TP(nVbVbPngSun IPgngV TP3sPGPuéyPsS. sPlVbPgPTé. snVé. gX naSlP 8üY3 uVbéSab ué(PlPsIPgyé. gPVéngSun n Téf ylngé. Vé ÁTbé(snPV Té. snVé. g (ggé gPlGPsNgVf SuV né. n V gaP. nTf nTPePs IP bPs f égV gnf nP uPGPug Vé VbégP ée gVf SuV Ps V gaP. nTf nTPePs ÁTbé(snPV XnaSlP 7ü YN Ig gé Té. Vn SVn aVéauSTégPf PV éugf n VbPgPf nTP3

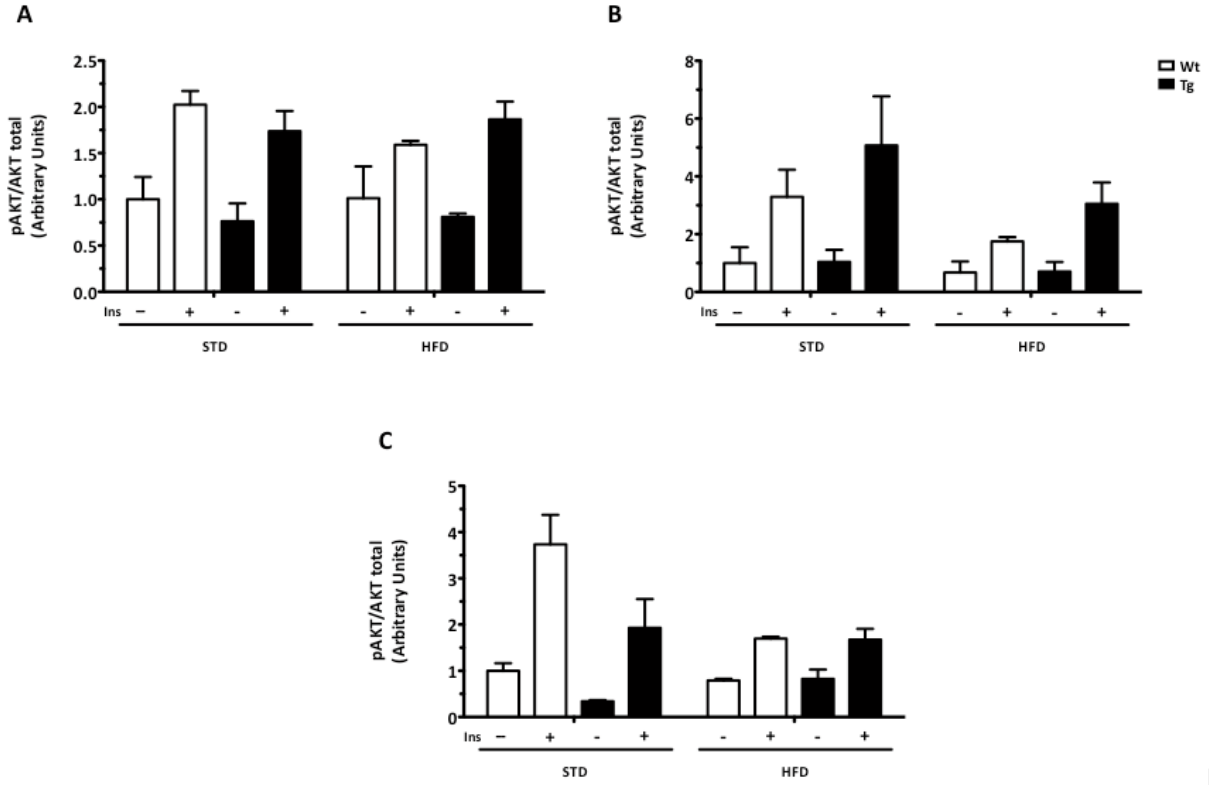

AEYC nvéSY VF DSP AOHYMO2HEO MDEBSPU VAOeML CO3(goPuPV uf SgTuPO3. s sryégPVggSPO3 . Pugbé(VbP lVé PV(PP. Á . sVéV uNTuTSuPVPs I sP. gnVéf PVIéeIPylPgP. V VGP uéVg PeélP . s eVPlngSun gVf SuVné. n gV. s lsÁTbé(X Y . s ÁePs X Yf nTP3

4.8. Study of inflammation in white adipose tissue of aP2-HMGA1 transgenic mice

It has been described that in obesity there is an increase in macrophage infiltration and cytokine production in adipose tissue that can lead to insulin resistance (Schenk et al., 2008). Furthermore, during the onset of obesity in humans, dead adipocytes attract macrophages to their surroundings, where they reabsorb lipid remnants. This biological process results in characteristic morphological elements termed crown-like structures that are positive for MAC-2 (Saverio Cinti et al., 2005; I Murano et al., 2009).

4.8.1. Study of the presence of inflammatory cell infiltrates in white adipose tissue

First, immunohistochemistry against the macrophage marker MAC-2 (Dong and Hughes, 1997; Solinas et al., 2007) was performed in epWAT of both wild type and transgenic mice fed either a standard-chow or a HFD. In neither slides from wild type or transgenic mice under STD were detected MAC-2 positive cells (Figure 40A). However, there was a dramatic increase of typical crown-like structures in both groups when fed a HFD, being more pronounced in wild type mice. Interestingly, transgenic mice presented higher amount of MAC-2 positive cells when placed under a HFD in comparison to STD (Figure 40A).

With the objective of determining the presence of activated macrophages within the infiltrates previously observed in epWAT from wild type and transgenic mice fed a HFD, flow cytometry analysis was carried out (Figure 40B and Figure 40C).

Confirming immunohistochemical observations, FACS analysis showed increased percentage of activated macrophages in wild type mice fed a HFD in

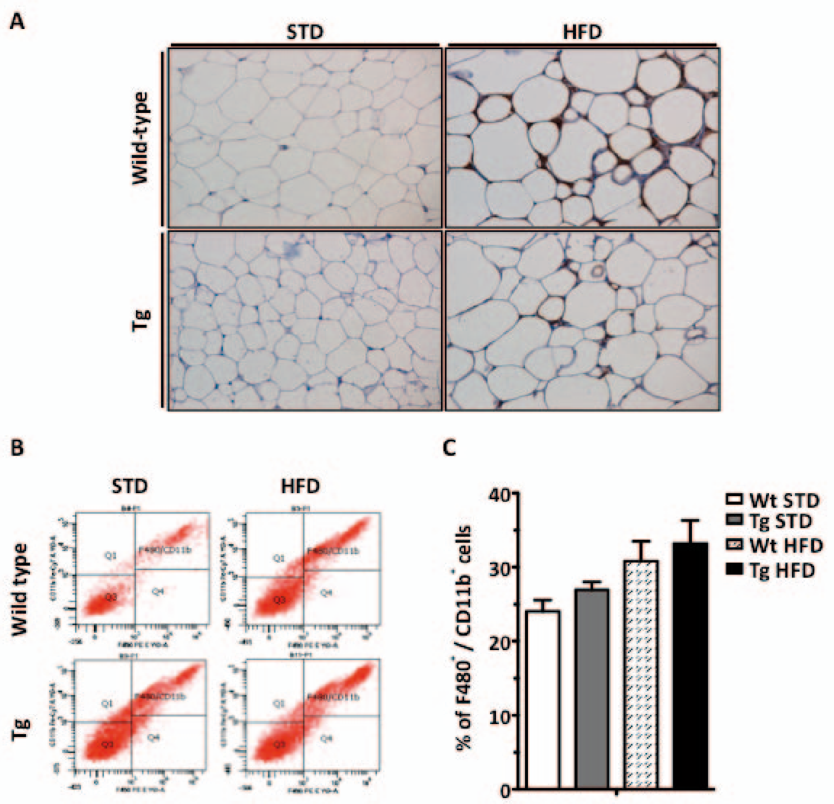
A
STD
HFD
Wild-type
Tg
B
STD
HFD
Wild type
Tg
Q1
Q3
Q4
F480/CD11b
C
Wt STD
Tg STD
Wt HFD
Tg HFD
% of F480+ / CD11b+ cells
0
10
20
30
40

than wild type mice. The increased macrophage content in epWAT of aP2-HMGA1 transgenic mice prompted us to characterize the repertoire of the infiltrate.

With the objective of characterizing the repertoire of the infiltrate, activation of specific markers for classically activated (or M1) or alternatively activated" (or M2) macrophages was assessed (Figure 41).

We analysed the double expression of CD11b and CD11c as markers of "classically activated" (M1) macrophages. No differences were observed in double-labelled cells between wild type and transgenic mice when fed a STD. Under high fat feeding, both groups showed a slight increase in the percentage of double positive cells (Figure 40A and Figure 41B), indicating a mild activation of the infiltrated macrophages.

On the other hand, we analysed the double labelling for CD11b and MGL1 as markers of "alternatively activated" (M2) macrophages. The percentage of double positive cells remained virtually unchanged between genotypes in STD-chow diet. High fat feeding increased the percentage of double positive cells in both wild type and transgenic mice, not showing differences between genotypes under this condition. Interestingly, a significant increase in M2 macrophages in wild type under HFD was observed in relation to that of wild type mice fed STD-chow diet (Figure 41C and Figure 41D).

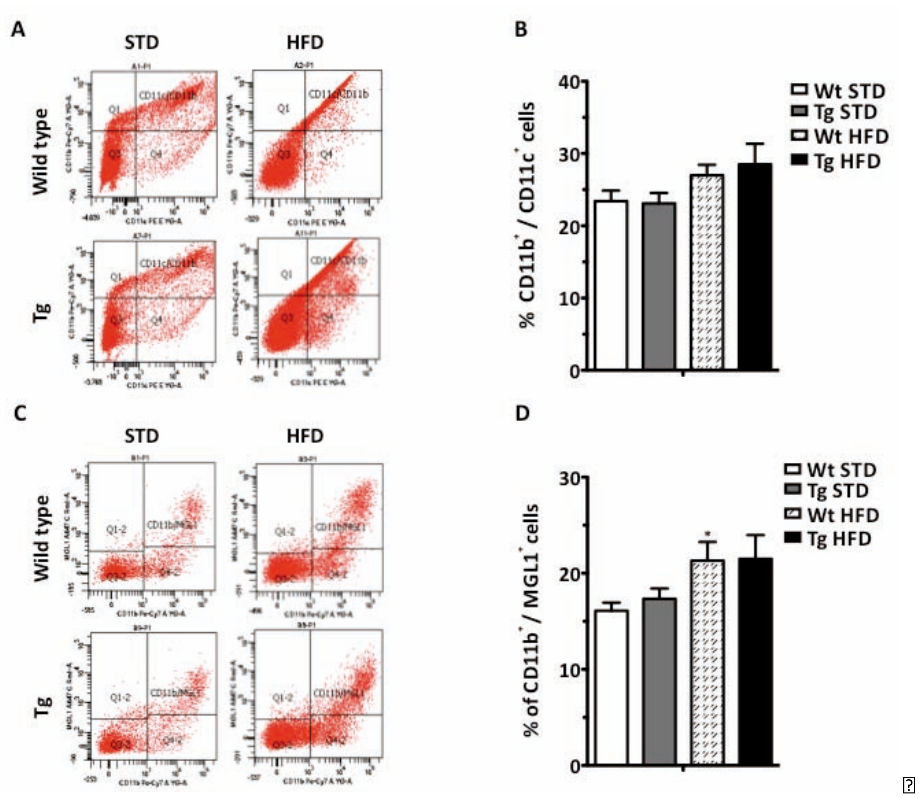

A
STD
HFD
Wild type
Tg
B
% CD11b+ / CD11c+ cells
Wt STD
Tg STD
Wt HFD
Tg HFD
C
STD
HFD
Wild type
Tg
D
% of CD11b+ / MGL1+ cells
Wt STD
Tg STD
Wt HFD
Tg HFD

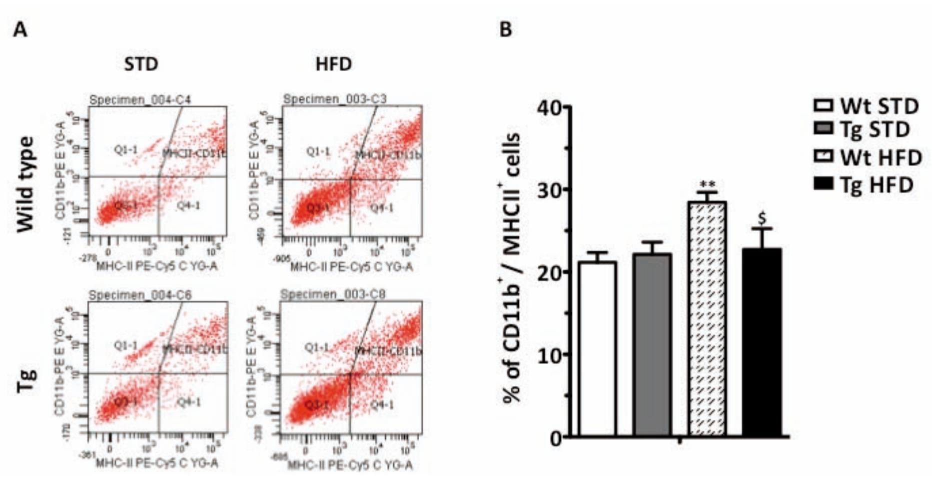
A
STD
HFD
Wild type
Tg
Specimen_004-C4
Specimen_003-C3
Specimen_004-C6
Specimen_003-C8
Q1-1
MHCII-CD11b
Q3-1
Q4-1
CD11b-PE E YG-A
MHC-II PE-Cy5 C YG-A
B
Wt STD
Tg STD
Wt HFD
Tg HFD
% of CD11b+ / MHCII+ cells
**
$
0
10
20
30
40

4.8.3. Determination of pro-inflammatory cytokine concentrations in white adipose tissue

Adipose tissue and resident macrophages are the source of a number of secreted proteins, such as proinflammatory cytokines involved in adipogenesis and insulin resistance (Chazenbalk et al., 2011; Galic et al., 2010). Moreover, increased adipose mass associated with obesity has been linked with a low-grade, chronic inflammatory response characterized by altered production of adipokines and increases in biological markers of inflammation, such as tumour necrosis factor-α (TNFα), interleukin-6 (IL-6), monocyte-chemoattractant protein-1 (MCP-1) or plasminogen activated inhibitor (PAI-1).

To further characterise the grade of inflammation in aP2-HMGA1 transgenic mice after HFD we measured some adipokines and biological markers of inflammation in epWAT tissue extracts (Figure 43).

IL-6, MCP-1 and TNFα levels remained unchanged during STD-chow diet between wild type and transgenic mice. As expected IL-6, MCP-1, TNFα and PAI-1 levels increased in both wild type and transgenic mice after HFD. Consistent with decreased inflammatory state, inflammatory cytokine expression of IL-6, MCP-1, TNFα and PAI-1 was reduced in epWAT of transgenic mice fed a HFD related to their wild type counterparts (Figure 43A and Figure 43B).

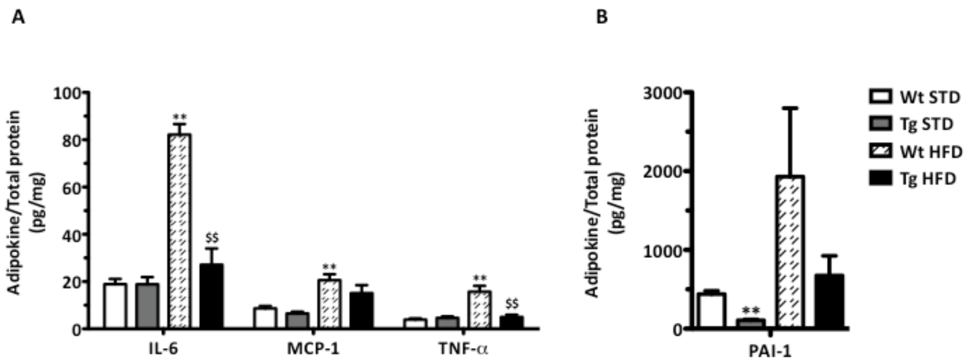
A
B
Adipokine/Total protein (pg/mg)
100
80
60
40
20
0
**
$$
IL-6
MCP-1
TNF-α
3000
2000
1000
PAI-1
Wt STD
Tg STD
Wt HFD
Tg HFD

5. DISCUSSION

In this study, in order to elucidate the role of HMGA1 during adipose tissue development and its implications in obesity and related diseases, we generated transgenic mice specifically overexpressing HMGA1 in adipose tissue. Previous observations *in vitro* and *in vivo* have shown that HMGA1 proteins are active players in adipose tissue differentiation and growth (Bianchi and Agresti, 2005; Raymond Reeves, 2010). In this regard, whereas suppression of HMGA1 proteins function increases growth rate and impairs adipocytic differentiation in 3T3-L1 cells (R M Melillo et al., 2001), transgenic mice carrying a truncated (dominant negative) HMGA1 gene are overweight and accumulate abundant ectopic fat (Monica Fedele et al., 2011). Transgenic mice over-expressing HMGA1 in the adipose tissue showed impaired adipose tissue development and thus, lower adiposity than wild type mice. When fed a HFD, transgenic mice showed increased metabolic rate and did not present a pathogenic inflammatory profile. Therefore, transgenic mice were protected against diet-induced obesity and remained insulin sensitive and glucose tolerant.

HMGA1 proteins have been described as crucial effectors in glucose homeostasis control. Active variants of HMGA1 gene have been associated with insulin resistance and T2D (Chiefari et al., 2013), and *Hmga1*$^{-/-}$ mice (which lack these proteins since early embryonic development) showed marked insulin resistance and diabetes (Foti et al., 2005). However, aP2-HMGA1 transgenic mice showed similar glucose tolerance and insulin sensitivity to wild type mice.

Adipocyte functionality is lost during the onset of insulin resistance and obesity, and has been related to impaired transcriptional regulation of the key factors that control adipogenesis. Balanced adipogenesis and adipocyte turnover within fat depots, and balance between BAT and WAT fat depots directly affects systemic energy balance

and may contribute to the development of obesity (Koppen and Kalkhoven, 2010; Smorlesi et al., 2012; Peter Tontonoz and Bruce M Spiegelman, 2008). During the onset of obesity, body weight and adipose tissue mass increases. High-fat feeding did not increase either body weight or the adipose tissue mass of transgenic mice. Adipose tissue usually expands its mass given its relatively high proliferative through hyperplasia and hypertrophy (Jo et al., 2009; Tang and Lane, 2012). The balance between the two is crucial for the development of obesity. In the SVF of epWAT and BAT from aP2-HMGA1 transgenic mice the expression of *Pref-1* was higher than in wild type, indicating more preadipocytes, perhaps indicative of hyperplasia and of the potential for adipose expansion.

Another mechanism of increasing adipose tissue mass is through hypertrophy (Jo et al., 2009; Tang and Lane, 2012). Moreover, the normal population of mature adipocytes in white adipose tissue contains cells of very variable sizes. Morphometric analysis of white adipocytes showed that adipocytes from aP2-HMGA1 transgenic mice had a lower mean area than wild type mice under both STD and HFD. As observed in wild type mice under HFD, diet-induced obesity increased the sizes of adipocytes, thereby decreasing the heterogeneity of the adipocyte population (R M Melillo et al., 2001). When compared with wild type mice fed HFD, the size frequency distribution of the adipocyte population of aP2-HMGA1 transgenic mice was altered, remaining virtually unchanged relative to that of wild type fed STD. These results suggest a shift towards a population of adipocytes of smaller size. Adipocytes of smaller sizes have been associated with an ameliorated glucose metabolism profile (J Hoffstedt et al., 2010), which would account for the improved metabolic performance of the aP2-HMGA1 transgenic mice.

Adipose tissue is a dynamic endocrine organ that communicates with other tissues (Guilherme et al., 2008). The extraordinarily dynamic behaviour of adipose tissue and of adipocytes in particular, relies on their ability to secrete a wide range of adipokines (Frühbeck and Salvador, 2004), that is critical for regulating whole-body metabolism in both health and disease (Waki and Peter Tontonoz, 2007). However, as adiposity increases, the ability of adipocytes to function as endocrine cells and secrete adipokines is impaired (Cao, 2010). Thus, dysregulation of adipokines is now recognized as an important factor in the pathogenesis of obesity and insulin resistance (Guilherme et al., 2008). Plasma leptin, adiponectin, resistin and IL-6 concentrations were lower in aP2-HMGA1 transgenic animals when compared to wild type mice. Traditionally, a strong negative correlation between plasma adiponectin concentration and fat mass has been established. Transgenic mice over-expressing HMGA1 in the adipose tissue showed significantly lower circulating adiponectin concentrations that correlated with lower fat mass. Long-term studies have recently demonstrated that there is a drop on adiponectin concentration before the onset of diabetes, suggesting that hypoadiponectinemia contributes to the development of insulin resistance and diabetes (Frühbeck and Salvador, 2004; Waki and Peter Tontonoz, 2007). However, aP2-HMGA1 transgenic mice showed similar glucose tolerance and insulin sensitivity to wild type mice in STD and improved insulin sensitivity and glucose tolerance under HFD.

In the event of adipose tissue expansion such as that observed in obesity, increased macrophage infiltration has been reported (Smorlesi et al., 2012). This macrophage infiltration and subsequent low-grade inflammation is usually coincident with the appearance of metabolic complications related to obesity (Schipper et al.,

2012). Transgenic mice over-expressing HMGA1 in the adipose tissue presented high macrophage infiltration in the epWAT, although no increase of proinflammatory cytokines was observed. The increased macrophage recruitment observed in the epWAT of aP2-HMGA1 transgenic mice could be due to clearance of dead cells resulting from a remodelling process. In this regard, immunohistochemical analysis of white adipocytes revealed an active remodelling of this tissue in transgenic mice. Together with the decrease in the population of larger adipocytes previously observed, these results pointed at a possible inability to accumulate triglycerides, and limitations to expand, of the white adipose tissue from aP2-HMGA1 transgenic mice fed a HFD.

The inability of the white adipose tissue to expand would explain the lower mass of the fat depots in aP2-HMGA1 transgenic mice and therefore, could be indicative of early-onset of lipodystrophy. Lipodystrophy is commonly characterized by loss or redistribution of fat tissue (Garg and Agarwal, 2009). This lipodystrophic state that presented in aP2-HMGA1 transgenic mice was more pronounced on feeding a HFD. During a regime intended to produce diet-induced obesity, the lack of extra-fat accumulation in adipose depots may result in an increase in fat deposition in other peripheral tissues. However, no ectopic fat accumulation in the skeletal muscle of aP2-HMGA1 transgenic mice was observed. In contrast, a shift of TG storage towards BAT was also observed in these conditions. In addition, there was more TG deposition in the liver of aP2-HMGA1 transgenic mice when fed the HFD. In this regard, lipodystrophic diabetes is normally associated with fatty liver (Savage, 2009). As aP2-HMGA1 transgenic mice showed fatty liver but decreased fat mass on high fat feeding, we expected them to develop hyperinsulinemia and glucose intolerance (Rodeheffer et al., 2008). However, aP2-HMGA1 transgenic mice did not develop hyperinsulinemia

and presented improved glucose tolerance and insulin sensitivity under high-fat feeding. Increasing evidence dissociates fatty liver and diabetes (Z. Sun and M. a Lazar, 2013), for example, several mouse models such as CPT-1a$^{+/-}$ (Nyman et al., 2011), HDAC3$^{-/-}$ (Z. Sun et al., 2012), PCK1$^{+/-}$ (Gómez-Valadés et al., 2008) or PCK$^{-/-}$ (Burgess et al., 2007) have been described that even presenting fatty liver remained insulin sensitive or glucose tolerant. In addition, although lipodystrophy models usually present hyperphagia (Savage, 2009), aP2-HMGA1 transgenic mice showed similar food intake than wild type mice, suggesting no compensatory response.

High-fat feeding did not increase either body weight or the adipose tissue mass of aP2-HMGA1 transgenic mice, despite similar food intakes to wild type mice. Low fat accumulation in the adipose tissue of aP2-HMGA1 transgenic mice could be explained by an increase in energy expenditure. Surprisingly, transgenic mice over-expressing HMGA1 in the adipose tissue did show a 27% increase in whole body energy expenditure compared to wild type mice, despite exhibiting decreased locomotor activity. Moreover, insulin signalling in skeletal muscle from aP2-HMGA1 transgenic mice was improved in relation to wild type mice under HFD, showing similar responses to wild type mice fed the standard diet. Furthermore, an increased in gene expression of genes involved in fatty acid oxidation was observed in aP2-HMGA1 transgenic mice. In agreement, no ectopic fat accumulation in the skeletal muscle of aP2-HMGA1 transgenic mice was observed. Increasing evidence shows the importance of the interplay between skeletal muscle and BAT in the process of “non-shivering” thermogenesis (Leslie P Kozak, 2013; Sahoo et al., 2013). These results suggested that muscle may be responsible of the higher metabolic rate observed in aP2-HMGA1 transgenic mice through “non-shivering” thermogenesis.

Thus, energy homeostasis may depend upon both the interaction between skeletal muscle and the WAT/BAT ratio (Leslie P Kozak and Young, 2012; Smorlesi et al., 2012). Severe structural and morphological changes such as large lipid droplets and increased expression of proteins involved in remodelling were evidenced in brown adipose tissue sections from aP2-HMGA1 transgenic mice in comparison to wild type mice. In addition, BAT from aP2-HMGA1 transgenic mice contained more larger lipid droplets, more typical of WAT, both under STD or HFD conditions. Some authors have recently proposed that after continued exposure to an ‘‘obesogenic environment,’’ BAT can transform into WAT (Ishibashi and Seale, 2010). In this context, it has been proposed that this process occurs through direct transformation of adult cells via a physiologically reversible transdifferentiation that involves genetic reprogramming of adult cells as well as tissue reorganization. These processes may contribute to the phenotype observed in the BAT of aP2-HMGA1 transgenic mice. In addition, HFD, which is known to activate thermogenesis in BAT in mice in order to counteract diet-induced obesity (Ivet Elias et al., 2012), did not alter the genetic expression pattern in BAT of aP2-HMGA1 transgenic mice towards an activation of genes involved in adaptive thermogenesis.

Gene expression analyses showed that BAT from aP2-HMGA1 transgenic mice does not express either white or brown adipocyte gene markers. Moreover, the expression of genes implicated in adipogenesis, cell cycle and adipocyte differentiation were dysregulated in BAT and WAT from aP2-HMGA1 transgenic mice when compared with wild type animals. Depletion of *Prdm16* in primary brown fat cell precursors causes a near-total loss of brown fat features (Kajimura et al., 2010, 2008; Seale et al., 2008). Moreover, activation of *Pparg2* by Prdm16 implies the expression of other specific

markers for brown fat cells such as *Pgc1-α* and *Cidea*. Furthermore, BAT from PRDM16-deficient mice exhibits an abnormal morphology (Kajimura et al., 2008). These observations were consistent with our findings, since the morphological changes observed in BAT were accompanied by downregulation of genes involved in brown adipocyte differentiation as well as genes involved in lipid metabolism. In addition, aP2-HMGA1 transgenic mice showed a marked decrease in the expression of mitochondria specific genes. Moreover, the expression of other genes implicated in the mitochondrial biogenesis and metabolism were also significantly downregulated in aP2-HMGA1 transgenic mice.

Impaired BAT specific gene expression program in aP2-HMGA1 transgenic mice had two consequences: First, aP2-HMGA1 transgenic mice showed higher amounts of lipid deposition in BAT, that were related to the almost complete absence of an uncoupling mechanism to dissipate the proton-motive force across the mitochondrial membrane (Enerbäck et al., 1997). Impaired BAT activity through decreased thermogenesis is believed to have an important role in the development of obesity in mice (Leslie P Kozak, 2013). In this way, UCP1 inhibition or absence in aP2-HMGA1 transgenic mice should result in the development of obesity. Even though early studies with UCP1 knock-out mice failed to demonstrate an obesogenic effect (Enerbäck et al., 1997), recent data show that UCP1 ablation does induce obesity and abolishes diet induced thermogenesis but only if mice are housed at thermoneutrality (30 ºC) (Feldmann et al., 2009). When housed at 21ºC, aP2-HMGA1 transgenic mice showed almost total UCP1 ablation and were protected against diet-induced obesity. Second, as a consequence of the dramatically low UCP1 expression and low citrate synthase and mitochondrial complex IV activities, aP2-HMGA1 transgenic mice were cold intolerant. In agreement,

most transgenic mouse models with genetically ablated BAT are cold intolerant (Longo et al., 2004) and are prone to develop obesity (M Carmen Carmona et al., 2005). In this regard, aP2-HMGA1 transgenic mice were cold intolerant but remained protected against diet-induced obesity.

It has been proposed that impairment of the expression of genes that are required for mitochondrial function are a characteristic in pre-diabetic and age-related insulin resistance processes, and may indicate a connection between mitochondrial dysfunction and metabolic disease (Jacene and Wahl, 2009; Stefan et al., 2009; K. Sun et al., 2011b). However, aP2-HMGA1 transgenic mice remained glucose tolerance and insulin sensitivity even under an obesogenic stimuli such as high-fat feeding, indicating that adipose tissue HMGA1 overexpression did not severely alter glucose metabolism.

The presence of lipid-filled cells within the interscapular BAT observed in aP2-HMGA1 transgenic mice are characteristic of a number of mouse models in which development or function of brown adipose tissue has been disrupted (Bachman et al., 2002; Enerbäck et al., 1997; Longo et al., 2004; Moitra et al., 1998). Together with increased preadipocyte number and active remodelling observed in the BAT from aP2-HMGA1 transgenic mice, increased lipid deposition could be indicative of impaired adipogenesis in this tissue. In addition, high expression of the preadipocyte marker gene expression (*Pref-1*) was observed in the stromal vascular fraction of BAT from aP2-HMGA1 transgenic mice, which could also be indicative of impaired terminal differentiation of this tissue.

Impaired terminal differentiation process of adipocytes has been claimed to be responsible for lower fat mass of both WAT and BAT (Longo et al., 2004). Accordingly, the lower fat depot mass observed in aP2-HMGA1 transgenic mice may be due to

impaired differentiation of adipocytes. High mobility group –AT-hook-1 proteins influence expression of other genes in a cell type specific manner (Shah et al., 2012). Overexpression of HMGA1 prevented terminal differentiation in myocytes and osteocytes keeping cells in a in a less differentiated or stem cell-like state (Ismail et al., 2012). As these cell types derived from a common mesenchymal origin as adipocytes, it could be possible that high HMGA1 levels may prevent complete adipocyte differentiation. Expression of HMGA1 was time-related to that of the preadipocyte marker gene *Pref-1* in the epWAT and BAT from wild type mice, decreasing its levels as differentiation progressed. These results suggest that downregulation of the expression of both *Pref-1* and HMGA1 may be necessary for complete adipocyte terminal differentiation (Armengol et al., 2012; Carvajal et al., 2002; Shah et al., 2012).

During adipogenesis, adipocytes undergo different phases, which include, growth phase, growth arrest, clonal expansion and differentiation (Algire et al., 2012; Symonds, 2012). Growth arrest, where adipocytes retire from the cell cycle before undergoing final differentiation, is a key step in adipogenesis (Lefterova and M. A. Lazar, 2009). Gene expression analysis of epWAT and BAT from aP2-HMGA1 transgenic mice showed downregulation of the genes involved in the final steps towards specific differentiation. Moreover, overexpression of genes involved in cellular senescence such as p16 (Cdkn2a), p53 or retinoblastoma (Rb) was observed. In parallel, the activation of Wnt signalling pathway was also observed.

Cellular senescence was originally defined as the state of proliferative arrest that accompanies the replicative exhaustion of cultured human cells. Senescent cells remain permanently insensitive to mitogenic signals, owing to the combined action of p53, p16 (Cdkn2a)-Rb tumour suppressor networks. These pathways are frequently

disabled in cancer processes (Masashi Narita et al., 2006). The increase in the gene expression of p16 (Cdkn2a), p53 or retinoblastoma (Rb) in the BAT from aP2-HMGA1 transgenic mice suggests that adipocytes from these mice remain arrested during growth arrest phase of adipogenesis, resulting in impaired final differentiation.

High mobility group –AT-hook-1 proteins are known to be active players in the formation of the enhanceosome during active replication (Carvajal et al., 2002). As in replication, senescence is related to global changes chromatin through the formation of the enhancesome (M Narita, 2007), which in this case could lead to the upregulation of senescence-associated genes such as p16 or Rb.

In human and rodent fat, at least two populations of preadipocytes have been described. The first being more capable of extensive replication, differentiation and adipogenic transcription-factor expression. The second, being more prone to undergo apoptosis (Tamara Tchkonia et al., 2013). Histological analysis of BAT from aP2-HMGA1 transgenic mice showed lipid-filled cells more characteristic of white adipose tissue, in addition to typical brown adipocytes, suggesting the presence of two adipocyte populations. Together with gene expression analyses where the expression of preadipocyte marker genes such as (*Pref-1*) and genes involved in senescence was higher, these results reinforce the idea of the existence of two active adipocyte populations within the adipose tissue from aP2-HMGA1 transgenic mice. One of the populations differentiates normally, whereas the other remains arrested during the first phases of adipocyte differentiation. This later population could eventually overexpress genes involved in senescence processes and thus, in aging.

It has been described that preadipocytes can undergo cellular senescence, particularly with aging and obesity (Minamino et al., 2009; Tamara Tchkonia et al.,

2013). Moreover, when senescent cells are eliminated from older mice, age-related fat-tissue loss is delayed or prevented, confirming the relevance of senescent cells to related fat-tissue dysfunction (Baker et al., 2011; Tamara Tchkonia et al., 2013). Thus, taking into account the lack of adipose tissue of aP2-HMGA1 transgenic mice and the increased number of preadipocytes observed, senescence might be occurring in the brown adipocytes of aP2-HMGA1 transgenic mice. Senescent cells have been described to secrete proinflammatory cytokines, chemokines and extracellular matrix proteases (Tamara Tchkonia et al., 2013). However, although the expression of proteins involved in ECM remodelling was increased in aP2-HMGA1 transgenic mice, the concentration of proinflammatory cytokines remained lower related to that of wild type mice.

As stated above, HMGA1 proteins are directly involved in gene expression regulation through enhanceosome formation. However, HMGA1 action is dependent on cellular context (Hock et al., 2007). Previous studies link the HMGA gene family to oncogenesis and show that high levels of HMGA1 proteins can promote proliferation, transformation and tumourigenesis (R Reeves, 2001b; Sgarra et al., 2004). Through their implication in the regulation of senescence, Masashi Narita et al. 2006 demonstrated that HMGA1 proteins might be both pro- and anti-oncogenic depending on the cellular context. In accordance, as implicated in the formation of higher protein complexes, HMGA1 have been reported to participate in replicative senescent. This type of senescence has been proposed to participate in beneficial processes such as limitation of tumourigenesis (Kuilman et al., 2010). In this regard, although HMGA1 was originally characterised as an oncogene, we did not observe a higher incidence of tumours in aP2-HMGA1 transgenic mice.

The results presented in this thesis show that overexpression of HMGA1 in adipocytes results in impaired development of adipocytes. It is possible that HMGA1 could act by either increasing the precursor (or preadipocyte) pool or increasing adipocyte turnover; however, given that HMGA1 is reported to maintain a certain level of stem cell-like characteristics and inhibit apoptosis, the mostly likely mechanism is that HMGA1 inhibits development of adipocytes in a stage later to adipocyte commitment and previous to differentiation.

In summary, overexpression of HMGA1 in adipose tissue from aP2-HMGA1 transgenic mice prevented the development of this tissue, leading to a certain degree of lipodystrophy. High levels of HMGA1 expression resulted in altered size frequency distribution of the adipocyte population of transgenic mice. Moreover, dysregulation of gene pathways involved in cell cycle and adipogenesis was observed in both epWAT and BAT from aP2-HMGA1 transgenic mice, suggesting that expansion, differentiation and/or both processes were impaired in the adipose tissue of these mice. High levels of HMGA1 led to structural changes in brown adipose tissue as well as an altered expression pattern of genes involved in BAT development and mitochondrial biogenesis. Impaired BAT development resulted in an almost complete loss of functionality and thus, to an abnormal TG accumulation in this tissue. However, the systemic metabolic profile of aP2-HMGA1 transgenic mice was improved, since aP2-HMGA1 transgenic mice were protected against diet-induced obesity and its metabolic complications. Thus, HMGA1 participates in the regulation of the adipose mass through the regulation of the cell cycle during the adipogenic process.

6. CONCLUSIONS

1. The specific overexpression of HMGA1 in adipose tissue led to lower adiposity in transgenic mice. Moreover, lower adiposity did not affect glucose metabolism of transgenic mice. In addition, serum parameters involved in lipid metabolism and adipokine secretion were lower in transgenic mice.
2. Lower fat accumulation of transgenic mice resulted from greater energetic metabolism as these mice presented higher oxygen consumption and carbon dioxide production, as well as increased energy expenditure. However, this increase in energetic metabolism was not due to an increase in locomotor activity.
3. The overexpression of HMGA1 in white adipose tissue showed no structural or morphological changes. However, differences in frequency distribution of adipocyte cell surface of white adipose tissue were observed between wild type and transgenic mice indicating a possible impairment of white adipocyte differentiation.
4. In brown adipose tissue, HMGA1 overexpression led to structural and morphological changes in transgenic mice. These changes were further translated into differential expression pattern of genes involved in specific brown adipocyte differentiation program, mitochondrial biogenesis and function as well as genes involved in lipid metabolism, leading to a decrease in thermogenic capacity of this tissue.
5. The expression of preadipocyte marker genes was higher in the SVF of both epWAT and BAT from transgenic mice, suggesting that an hyperplasia process was taking place in these tissues. Moreover, gene expression analysis of white and brown adipose tissue of transgenic mice showed dysregulation of gene pathways involved in fatty acid and insulin metabolism, cell cycle, and adipogenesis; further

suggesting impaired adipocyte differentiation in the adipose depots of transgenic mice.

6. In contrast to wild type mice, transgenic mice fed a high fat diet were protected against diet-induced obesity, remaining insulin sensitive and glucose tolerant.
7. Despite being neither obese nor insulin resistant, aP2-HMGA1 transgenic mice presented high macrophage infiltration in epWAT. Despite presenting higher macrophage infiltration than wild type mice, transgenic mice showed decreased antigen presentation capacity, in parallel to a reduced expression of the proinflammatory cytokines IL-6, MCP-1 and TNF-α.
8. Finally, these results indicate that the overexpression of HMGA1 in adipose tissue leads to increased protection against insulin resistance and obesity by altering adipose tissue development and adipogenesis.

7. MATERIALS AND METHODS

1. MATERIALS

1.1. Animals

aP2HMGA1 mice were generated *de novo* for the realization of this work. The colony was generated from hybrid strain C57Bl6/SJL (The Jackson Laboratory, Bar Harbor, Maine, USA) with the microinjection technique.

Mice were kept in a specific pathogen-free facility (SER-CBATEG) under controlled temperature and light conditions, light-dark cycle of 12 h (lights on at 8:00 a.m.). Mice were fed ad libitum with a standard chow diet (2018S Teklad Global, Harlan Teklad, Madison, Wisconsin, USA) or high fat diet (TD88137 Teklad Global, Harlan Teklad, Madison, Wisconsin, USA).

Unless otherwise indicated, animals aged 6-months-old were used for the realization of this work.

When stated, animals were anaesthetized by means of inhalational anaesthetics with isoflourane (IsoFlo®, Esteve, Barcelona, Spain) and euthanized by decapitation. Blood and tissues of interests were taken between 09:00 and 11:00 hours, immediately frozen in liquid N_2 and kept at −80°C until analysis. In the experiments described below, heterozygous male mice were used. Littermates were used as wild type for the transgenic animals. The Ethics and Experimental Animal Committee of the Universitat Autònoma de Barcelona (UAB) approved all experimental procedures involving mice.

1.2. Working reagents

All molecular biology reagents were obtained from the commercial manufactures Roche (Roche Diagnostics Corp., IN, USA), Invitrogen Corporation (now Life

Technologies) (San Diego, CA, USA), Bio-Rad Laboratories (Hercules, CA, USA), Amersham Biosciences (Piscataway, NJ, USA), Sigma (St.Louis, MO, USA), Promega Corporation (Madison, WI, USA), Millipore (Millipore™ Corp., Billerica, MA, USA), Abcam (Abcam, Cambridge, UK), Qiagen (Qiagen, Hilden, Germany) and QBiogene (QBiogene Inc, CA, USA). Cell culture medium and antibiotics were obtained from PAA (Pasching, Austria) and serum from Gibco (Invitrogen, Life Technologies).

1.3. Bacterial strains and plasmids

The bacterial strain used to obtain the aP2HMGA1 plasmid construct was the *E. Coli* DH5α strain (Invitrogen, Live Technologies). All used plasmids contained the ampicillin resistance gene for selection, and therefore, the bacterial culture was grown in LB medium (Miller's LB Broth, Conda, Madrid) in the presence of 50 µg/ml of ampicillin. When cells were grown on a solid medium, 2% agar was added to the LB medium.

1.4. DNA probes

The probe used to detect the presence of the transgene in the genomic DNA of aP2HMGA1 transgenic mice by souther blotting corresponed to a 6.8 kb *Kpn*I—*Kpn*I fragment from the digestion of the plasmid *paP2-HMGA1-SV40* used for oocite microinjection. To detect HMGA1 transcripts in different tissues a 623 bp corresponding to mouse HMGA1 cDNA was used.

1.5. Oligonucleotides

The oligonucleotides used for Real Time PCR analysis are summarized in the following table:

	Forward primer	Reverse primer
Hmga1	CAGGAAAAGGATGGGACTGA	CACTTCACTGGGCTCTTTCTG
Rplp0	TCCCACCTTGTCTCCAGTCT	ACTGGTCTAGGACCCGAGAAG

For liver and muscle gene expression analysis, specific RealTime Ready custom qPCR assays were design (Roche Diagnostics GMBH, Germany)

1.6. Antibodies

The specification of the antibodies and reagents used for the detection of proteins by immunohistochemistry, Western Blot and Flow Cytometry are summarized in the following table:

Table. Antibodies

Antibody	Reactivity	Species	Supplier	Dilution
Western-Blot				
Primary antibodies				
HMGA1a/HMGA1b (ab4078)	Human, Zebrafish	Rabbit	Abam	1:100
PPARd (ab23673)	Human, mouse, rat, pig and sheep	Rabbit	Abcam	
PPARg (ab5907)	Human, mouse, rat and dog	Rabbit	Abcam	
UCP1 (ab10983)	Human, mouse and rat	Rabbit	Abcam	
C/EBPb (C-19) sc-150	Mouse, rat and human	Rabbit	Santa Cruz Biotech.	
PGC1-a (H-300) sc-13067	Mouse, rat and human	Rabbit	Santa Cruz Biotech.	1:500
MitoProfile®total OXPHOS Rodent WB antibody cocktail (ab110413)	Mouse, rat, cow and human	Mouse	Abcam	
Tubulin (ab4078)	Human, mouse, rat, chicken and cow	Rabbit	Abcam	1:100
Secondary antibodies				
Anti-Rabbit IgG-HRP	Rabbit	Swine	Dako-Cytomation	1:10000
Anti-Mouse IgG-HRP	Mouse	Sheep	Amersham	1:10000

Antibody	Reactivity	Species	Supplier	Dilution
Immunohistochemistry				
Primary antibodies				
Anti-Mac2		Rat	Cederlane	
Secondary antibodies				
Biotinilated anti-Rat IgG		Rabbit	Dako Cytomation	
Antibody		**Species**	**Supplier**	
Flow Cytometry				
PE Anti-mouse CD11b (557397)		Rat	BD Pharmigen	
PE/Cy7 Anti-mouse CD11b (101216)		Rat	Biolegend	
PE Anti-mouse CD11c (557401)		Hamster	BD Pharmigen	
FITC Anti-mouse F4/80 (123107)		Rat		
AlexaFluor 488 Anti-mouse CD301 (MGL1) (MCA2391A488T)		Rat	AdB Serotec	
PE/Cy5 Anti-mouse I-A/I-E (107611)		Rat	Biolegend	

2. METHODS

2.1. Basic DNA techniques

2.1.1. Plasmid DNA preparation

Minipreparations of plasmid DNA were performed using the alkaline lysis protocol originally described by Birnboim and colleagues (Birnboim and Doly, 1979). When higher amounts of plasmid DNA were needed, the EndoFree Plasmid Mega Kit (Qiagen, Hilden, Germany) was used. In this case, up to 2.5 mg of DNA could be obtained from each individual preparation.

2.1.2. DNA digestion with restriction enzymes

Each restriction enzyme required specific reaction conditions of pH, ionic strength and temperature. Therefore, in each case, the manufacturer's instructions were followed (New England Biolabs, Roche, Promega or Fermentas). In general, DNA was digested using 1-4 units of the enzyme per µg of DNA. Digestions were carried out for 2-3 h in the specific buffer and the digestion products were analysed in agarose

gels.

2.1.3. Ligation of DNA fragments

The bacteriophage *T4 DNA ligase* was used for the ligation reactions, following the manufacturer's instructions (New England Biolabs Inc, UK, Ltd). The reaction was carried out in the presence of the ligation buffer with ATP for 2-3 h at 16º C.

2.1.4. Transformation of competent E. coli

Plasmid DNA can be introduced into competent bacteria by heat shock transformation. In this technique, competent cells were thawed on ice just before the moment of use and up to 5 μl of the DNA ligation reaction or control DNA was added directly to the cells. Cells and DNA were mixed and incubated on ice for 30 minutes. After that, a heat-shock of 30 seconds in a 42º C water bath was applied, and cells were immediately returned to ice for 2 minutes. 1 ml of LB was added to the tubes and cells were incubated at 37º C for 1 h with moderate shaking. Following this, 100 μl of the suspension was plated in LB plates with the appropriate antibiotic (ampicillin) and incubated at 37º C overnight.

2.1.5. DNA resolution and purification

Electrophoresis through agarose gels was the standard method used to separate, identify and purify DNA fragments. One per cent agarose gels were used to resolve DNA fragments between 0.5-7 Kb. The location and relative size of DNA within the gel was determined by staining the gel with low concentrations of the fluorescent dye ethidium bromide, which intercalates between the two strands of DNA. The presence of DNA was visualized with low wavelength ultraviolet (310 nm) light using a transilluminator and a camera system (Syngene). This technique allows detection down to 5 ng of DNA. The relative sizes of DNA fragments were calculated comparing

the location of the DNA band with the bands of the GeneRuler™ 1kb DNA ladder (Fermentas).

Gels were prepared dissolving 1% agarose in 1x TAE electrophoresis buffer (Tris-acetate pH 8.3, 40 mM and EDTA 1 mM) containing 0.5-µg/ml-ethidium bromide. Samples were loaded in 10x loading dye (Fermentas) and electrophoresed in 1x TAE electrophoresis buffer at 60-90 volts. To extract and purify a DNA fragment from the agarose gel, the GeneJET™ Gel Extraction kit (Fermentas) was used, following manufacturer's instructions. DNA was then quantified by measuring the absorbance at 260 and 280 nm in a NanoDrop™ 1000 Spectrophotometer (Thermo Scientific, USA).

2.2. Transgenic mice generation by oocyte microinjection

To obtain aP2HMGA1 transgenic mice, the Unitat d'Animals Transgènics (UAT) of CBATEG used the DNA microinjection technique. A 480 bp *Hinc*II—*Pvu*II fragment containing a small region of the coding sequence of the mouse HMGA1 gene was introduced downstream of the *aP2* promoter gene at a *Sma*I site in the *paP2-SV40* plasmid. The resulting plasmid was designated *paP2-HMGA1-SV40*. A 6.8 kb *Kpn*I—*Kpn*I fragment, containing the entire *aP2-HMGA1* chimeric gene was purified by electroelusion and microinjected into male pronuclei of fertilized oocytes obtained from C57Bl6/SJL females. After microinjection, oocytes were transferred into CD1 females. Obtained transgenic mice were crossed with wild-type C57Bl6/SJL mice in order to establish the heterozygous transgenic line aP2HMGA1.

2.3. Genotyping of transgenic mice

At 3-4 weeks of age, mice were tested for the presence of the transgene aP2HMGA1 by Southern blot.

2.3.1. Isolation of genomic DNA

To obtain genomic DNA an adaptation of the method by de Wet was used (De Wet et al., 1987). DNA was extracted from a tail sample of approximately 0.5 cm obtained from animals aged 3-4 weeks. The tissue was digested overnight at 56º C in a 0.1% W/V proteinase K (Roche Diagnostics) buffered solution (TESNA: 100 mM Tris-HCl pH 8.5; 5 mM EDTA pH 8; 0.2% W/V SDS; 200 mM NaCl; 1 mg/ml Proteinase K). This incubation allows the digestion of the tissue by proteinase K and the release of the genomic DNA from the cells. The homogenised solution was clarified by addition of an excess of salt and genomic DNA was purified by precipitation with isopropanol. To do so, 250 μl of a saturated NaCl solution was added to 700 μl of digestion mixture and centrifuged for 15 minutes at 12000 g. The supernatant was recovered and genomic DNA was precipitated with the addition of 500 μl of isopropanol and then centrifuged for 15 minutes at 12000 rpm. Precipitated DNA was rinsed with a 70% V/V ethanol solution and resuspended in the appropriate volume of deionized water (approximately 50 μl) previously heated to 65º C to facilitate solubilisation of the DNA. Finally, the concentration of DNA in the different samples was determined by measurement of the absorbance at 260 nm using a Thermo Scientific NanoDrop™ 1000 Spectrophotometer.

2.3.2. DNA analysis by Southern blot

2.3.2.1. Digestion and electrophoresis of genomic DNA

10 μg of genomic DNA were digested overnight at 37º C with the restriction enzyme *EcoR*I. Then, 10x-loading dye (50% V/V Glycerol; 100 mM EDTA; 1% W/V SDS; 0.1% W/V Bromophenol blue) was added to the digested genomic DNA and loaded on

a 1% agarose/TAE as well as gel GeneRuler™ 1kb DNA ladder (Fermentas). Samples were allowed to run for 4-5 hours under 50-60 volts. After electrophoresis, the gel was treated prior to the transfer of the DNA to the blot. The treatment consisted of 0.25N HCl for 15 minutes to allow depurinization of DNA and to favour the transfer of high molecular-weight fragments; 15 minutes in alkaline solution (1.5 M NaCl; 0.5 M NaOH) to denature DNA and facilitate the transfer, and 30 minutes in neutralizing solution (1 M Tris; 3 M NaCl) to neutralize the pH and confer again a negative electrical charge to DNA.

2.3.2.2. Blotting of the genomic DNA

Blotting was carried out using positively charged nylon membranes (Roche Diagnostics, USA) and the Turboblotter® system (Schleicher & Schuell, Keene, New Hampshire). This system allows the transfer of DNA to the membranes by capillary action in high ionic strength buffer SSC 10x (1.5 M NaCl; 0.15 M sodium citrate pH 7.4) through absorbent papers (GB002 and GB004, Schleicher & Schuell, Keene, New Hampshire) during a minimum period of 2 hours. The blot was then irradiated with 120000 μJ of ultraviolet light during 25-50 seconds in a UV-Stratalinker 1800 (Stratagene, La Jolla, CA, USA) to immobilize the DNA in the nylon membrane by generation of covalent bonding.

2.3.2.3. Prehybridization and hybridization of membrane

The blot was pre-hybridized for 2 hours at 65º C in rotational agitation in a prehybridizaation/hybridation solution (0.25 mM Na_2HPO_4 pH 7.2; 10% W/V SDS; 1 mM EDTA; 0.5% W/V Blocking Reagent). This solution contains proteins, SDS and

ssDNA to block free binding sites and reduce subsequent non-specific binding. Hybridization was carried out overnight at 65º C with a specific probe for HMGA1.

2.3.2.4. Radioactive detection of the transgene

The commercial kit Ready-to-Go™ DNA Labelling Beads [α-P^{32}]-dCTP (3000 Ci/mmol; Amersham Biosciences Corp., Arlington Heights, Ill., USA) was used to label the probe following the manufacturer's instructions. Briefly, 25 ng of the probe were boiled for 5 minutes in a final volume of 45 μl to denature DNA, and quickly placed in ice for 2 minutes to avoid renaturalization. The denatured DNA solution was then added to a lyophilized mixture containing dATP, dGTP, dTTP and the Klenow fragment of the *E. coli* DNA polymerase provided by the manufacturer. Next, 5 μl of [α-P^{32}]-dCTP (3000 Ci/mmol; Amersham Corp., Arlington Heights, Ill., USA) was added and the mixture was incubated for 15 minutes at 37º C. This technique allows the synthesis of DNA probes uniformly labelled and with a high specific radioactivity. The non-incorporated radioactive nucleotides were separated from the labelled probe with Sephadex G-50 gel filtration columns (Probe Quant G-50 Micro Columns, Amersham Pharmacia Biotech). This step helps to reduce the non-specific or background radioactive signal. After the addition of the labelled probe (3-5.106 cpm/ml) to the hybridization solution, the hybridization was carried out overnight at 65º C with rotational agitation.

2.3.2.5. Membrane washes and developing

The following morning, several washes of the blot were performed to rinse excessive or non-specifically bound probe. These consisted of 3 consecutive washes with progressively higher stringency: two 10-minute washes at room temperature with a low-astringency buffer solution (SSC 2x; 0.1% W/V SDS) and a final 15-minute wash

at 65º C with a high-astringency buffer solution (SSC 0.1x; 0.1% W/V SDS).

Finally, blots were exposed to a photographic film (Eastman KODAK Company, New York, USA) to obtain the differential bands signal that allowed the genotyping of the animals.

2.3.3. Polymerase Chain Reaction (PCR)

Isolated genomic DNA was diluted to obtain approximately 40 ng of DNA and a standard PCR was used to amplify a band of 350 bp specific for the transgene and a band of 528 bp present in all mice. The sequence of oligonucleotide primers were:

aP2 Forward	TTT TGA CAG TCA AAA CAG GAA CC
aP2 Reverse	ACC TGG AGG GAT CAC GAG CTT G
Hmga1 Reverse	CCA ACA CCA GAA ATA GCC CCG AC

Time and temperature conditions were the following:

1. 4 minutes at 94º C
2. 32 cycles of:
   - 30 seconds at 94º C: *denaturalisation*
   - 25 seconds at 60º C: *annealing*
   - 35 seconds at 72º C: *elongation*
3. 1 minute at 72º C
4. Hold at 4º C

Finally, the resulting DNA fragments were run on a 1% agarose gel with ethidium bromide. The relative sizes of DNA fragments were calculated comparing the

location of the DNA band with the bands of the GeneRuler™ 500 bp DNA ladder (Fermentas).

2.4. Basic RNA techniques

2.4.1. Isolation of total RNA

For total RNA extraction, sample tissues were rapidly removed after sacrificing the animal and then snap frozen in liquid nitrogen. Frozen samples were homogenized in 1 mL of either Qizol® Lysis Reagent (Qiagen, Hilden, Germany) or Trizol® Reagent (Invitrogen, Carlsbad, CA, USA) with a Polytron® type tissue homogenizer. In this method, RNA isolation from other cell components is based on a phenol-chloroform extraction from the tissue homogenate using guanidine thiocyanate as a ribonuclease inhibitor. The fraction corresponding to RNA was extracted by addition of 0.2 ml of chloroform and further purified using adsorption columns for RNA purification, RNeasy® Mini Kit (Qiagen, Hilden, Germany), following the manufacturer's instructions. All samples were treated on-column with DNase I (RNase-Free DNase Set for on-column sample treatment, Qiagen) and, after rinsing with the buffer provided by the manufacturer, eluted from the column with 35 μl of RNase-free deionized water. Quantity and quality of RNA samples was determine by measurement of the absorbance at 260 nm using a NanoDrop™ 1000 Spectrophotometer (Thermo Scientific, USA). Finally, RNA samples were electrophoresed on a 1% agarose gel containing 2.2 mol/L formaldehyde.

2.4.2. Analysis of RNA expression by Northern blot

2.4.2.1. Electrophoreesis of RNA

For HMGA1 RNA detection, RNA was mixed with the appropriate volume of denaturing loading buffer (2% V/V deionised formamide; MOPS/EDTA 10x; 6.75% V/V 37% formaldehyde; 5.4% V/V glycerol; RNase-free sterile deionized water and Bromophenol blue as a dye. Filtered with a 0.22 nm filter) and heated at 65º C for 15 minutes, after which it was immediately placed in ice to prevent renaturalization. The denaturalized RNA samples were then loaded and run in sterile electrophoresis buffer (MOPS buffer pH 7: 0.2 M MOPS; 50 mM sodium acetate; 10 mM EDTA) for 3-4 hours at 60 V in denaturing agarose gels (1% W/V agarose; 10x MOPS buffer; 2.2 M formaldehyde). Given the conditions of the electrophoresis, the RNA keeps denaturalized allowing the separation of the different mRNA depending on their molecular weight. To prevent enzymatic degradation of RNA by ribonucleases, all the solutions were prepared with RNAse-free water and were autoclaved and filtered. Following steps (transference of RNA to nylon membranes and radioactive detection) are carried on following the same protocol described for DNA analysis by Southern Blot, without gel pre-treatment.

2.4.3. cDNA synthesis: two-step retrotranscription

1 µg of total RNA was retrotranscribed to first-strand cDNA using the Transcriptor First Strand cDNA Synthesis Kit (Roche) following manufacturer's instructions. Oligo-dT and random hexamer oligonucleotides were used as primers for the reaction in the presence of Protector RNase inhibitor.

$$\text{Fold difference} = 2^{-\Delta\Delta C_t}$$

$$\Delta C_{t\ \text{sample}} - \Delta C_{t\ \text{calibrator}} = \Delta\Delta C_t$$

$$C_{t\ GOI^s} - C_{t\ norm^s} = \Delta C_{t\ \text{sample}}$$

$$C_{t\ GOI^c} - C_{t\ norm^c} = \Delta C_{t\ \text{calibrator}}$$

2.4.5. AFFYMETRIX® GENECHIP® gene expression analysis

To prepare total RNA for microarray analysis, we used 100 mg of interscapular brown adipose tissue (BAT) and epididymal white adipose tissue (epWAT) from wild type and transgenic mice fed standard chow or high fat diet. We used the recommended Affymetrix protocol for RNA extraction (Expression Analysis Technical Manual; http://www.affymetrix.com). Briefly, each sample was homogenised Qiazol® lysis reagent (Qiagen, Hilden, Germany) before precipitation and column purification using RNeasy® Micro Kit (Qiagen). On-column DNase I digestion was carried out (Qiagen). All following steps were performed by Progenika (Bilbao, Spain; http://www.progenika.com/). cRNA biotinylated was synthetise from 300 ng of RNA from each sample using *GeneChip 3' IVT Express kit* (Affymetrix, 3_ivt_express_kit_manual) following manufacturer's recomendations. Quantification and integrity of the biotinylated cRNA was checked using a Thermo Scientific NanoDrop™ 1000 Spectrophotometer and a Bioanalyzer (Agilent Technologies,).

Labelled cRNA samples were hybridised to HT MG-430 PM array plate using a GeneTitan (Affimetrix®) platform. HT MG-430 PM array plate allows processing of 24 samples at a time, each of them desing's is identical to GeneChip Mouse Genome 430A 2.0 arrays (Affymetrix). The software used for microarray and data processing was Affymetrix GeneChip Command Console Software (AGCC 2.0, Affymetrix®) and Expression Console™ (EC 1.1, Affymetrix®).

Bioinformatics and normalisation using Robust Multichip Averaging were performed using GeneSpring GX v.7.3.1 (Agilent; http: //www.agilent.com), dChip (http: //www.dchip.org), as well as Affy and affyPLM (BioConductor; http: //www.bioconductor.org). The final gene list contained only those probe-sets with a P

< 0.05. For further analysis of the data, we used several free software tools such as R (http://www.r-project.org/), Bioconductor (http: //www.bioconductor.org), Cytoscape (http://www.cytoscape.org/) or TMEV (http://www.cytoscape.org/). Functional analysis was done using the online tools Incromap (http://www.ra.cs.uni-tuebingen.de/software/InCroMAP/), GeneCoDis3 (http://genecodis.cnb.csic.es) and David (http://david.abcc.ncifcrf.gov/) .

For statistical analysis of microarray data we considered Hyp* value as statistically significant. For its calculation p value was computed using hypergeometric distribution and corrected for multiple hypothesis testing using the false discovery rate (FDR) method of Benjamini and Hochberg (Klipper-Aurbach et al., 1995).

2.5. Basic protein analysis by Western blot

Western blot analysis from tissue samples was performed by standard procedures.

2.5.1. Total protein extraction

Frozen tissues samples were homogenized in 1 ml of a protein homogenization buffer (50 mM Tris-HCl pH7.5, 0.27 M sucrose, 1 mM EGTA, 1 mM EDTA, 50 mM NaF, 10 mM Na β-glycerolphosphate, 5 mM Ppi, 1% Triton X-100. Just before use, protease inhibitors were added to the buffer, one tablet per each 10 ml of buffer, Complete Mini EDTA-free protease inhibitor cocktail tablets, Roche Diagnostics GMBH, Germany) and kept in ice thereafter. Extracts were centrifuged for 5 minutes at 12.000 x g at 4º C to precipitate cellular debris.

2.5.2. Bradford method for protein quantification

For the measurement of protein concentration in different extracts, an aliquot of the samples was assayed for protein concentration by the Bradford method as

described by the manufacturer (Bio-Rad protein assay; Bio-Rad, Hercules, CA). Briefly, this method is based on the shift in the colour of Coomassie brilliant blue dye when complexed with proteins. This colour shift produces a change in the absorbance maximum from 495 to 595 nm. Appropriate volumes of the protein extracts were diluted to 800 μl in deionized water, to which 200 μl of the Bradford reagent (Bio-Rad Protein Assay, Bio-Rad) was added. The same reaction was performed with different amounts (0-20 μg) of bovine serum albumin (BSA) to obtain the standard curve. After adding the Bradford reagent, samples were mixed and incubated for 5 minutes before measuring their absorbance at 595 nm in a spectrophotometer. The protein concentration of the samples was determined by interpolation of their absorbances into the calculated standard curve.

2.5.3. Electrophoresis in polyacrylamide gels (SDS-PAGE)

Protein expression was analyzed by electrophoresis of the differen protein extracts in two-phase polyacrylamide gels under denaturating conditions with SDS (Laemmli, 1970). The SDS-PAGE polyacrylamide gels were made of two different gels. The upper gel was the *stacking gel* (pH 6.8: 0,5 M Tris-Cl, 0.4% W/V SDS), which with its low concentration of polyacrylamide (3.9%) allowed the proteins to stack together into a tightly packed band before entering the other gel. The bottom gel was the *resolving gel* (pH 8.8: 1.5M Tris-Cl, 0.4% W/V SDS), which was composed of different percentages of polyacrylamide gels depending of the protein of interest (acrylamide-bisacrylamide 30%, BioRad) and allowed the separation of proteins according to their molecular weights.

Protein extracts were mixed with a 1/5 volume of a Laemmli loading buffer (20 mM phosphate buffer pH=7.0; 30 % V/V Glycerol; 4 % SDS; 2 % V/V 2-β-

mercaptoetanol and bromophenol blue as a dye) and denaturalized at 95° C for 3 minutes, before being loaded into the SDS-PAGE gel. Electrophoresis was carried out in electrophoresis buffer (5 mM Tris; 192 mM glycine; 0.1% SDS W/V) at 50 V while samples were migrating in the stacking gel. Once samples entered the resolving gel, potency was increased to 100 V. Pre-stained molecular weight markers were run on the same gel to facilitate band identification (Spectra Multicolor Broad Range Protein Ladder, Fermentas).

2.5.4. Blotting of proteins to membranes and immunodetection

Electrotransference of proteins from the polyacrylamide gel to PVDF membranes (Immobilon-P Transfer Membranes, Millipore) was performed with Mini Trans-Blot® Electrophoretic Transfer Cell (Bio-rad) at 100 V for 2 hours at 4° C in electrotransference buffer (25 mM Tris, 150 mM glycine, 20% V/V Methanol). After transference, membranes were stained with Ponceau dye to evaluate protein quality and loading differences between samples. Afterwards, membranes were washed with TBS-T 0.05% (25 mM Tris-HCl, 137 mM NaCl 0.05% Tween20) to completely remove Ponceau dye and subsequently blocked for 1 hour in agitation at room temperature with TBS-T with 5 % bovine serum albumin (BSA) or with 5% W/V dry skimmed milk, depending on each antibody's preferences. Later, membranes were incubated with appropriate primary antibodies, summarized in *Section 1.6,* diluted in TBS-T-BSA overnight at 4° C in agitation. Membranes were then washed with TBS-T (3 rapid rinses and then 2 washes of 10 minutes each) to eliminate excess of antibody. Blots were incubated for 2 hours at room temperature with the corresponding peroxidase-conjugated secondary antibodies (summarized in *Section 1.6*) diluted at 1:10000 in TBS-T-BSA. Finally, the membranes were washed again with TBS-T, adding a final 5-

minute rinse with TBS (25 mM Tris-HCl, 137 mM NaCl).

Immunodetection was performed using Immobilon Western Blot Chemiluminiscence Kit (Millipore) following manufacturer's instructions. Then, the ECL-treated membrane was exposed to a photographic film and developed to visualize the signal. Photographic films were scanned for quantification of the bands. The pixel intensity of the bands obtained was determined with the ImageJ software from NIH (Maryland, USA).

2.6. Measurement of mitochondrial protein activity

2.6.1. Mitochondrial cytochrome c oxidase (complex IV) enzyme activity assessment

Mitochondial cytocrome C oxidase (complex IV) enzime activity was measured using Complex IV Rodent Enzyme Activity Microplate Assay Kit (ab109911, Abcam, UK) following manufacture's recomendations in cellular extracts from iBAT and epWAT from wild type and aP2HMGA1 transgenic mice.

2.6.2. Citrate synthase activity determination

Tris Buffer (100 mM Tris HCl pH 8, 0,1%(v/v) Triton-x-100. Store at 4ºC); Oxaloacetic acid (10 mg/mL in Tris Buffer. Prepare daily). DTNB (4 mg/mL in Tris Buffer. Prepare daily); AcetylCoA (10 mg/mL in Tris Buffer. Store at -20ºC.) Briefly, warm Tris Buffer at 30oC. Incubate it at 30ºC during the experiment. To a 1 mL cuvette thermostatted at 30ºC add 0,900 mL of buffer, 10 µL of DTNB, 30 µL of Acetyl-CoA and 40 µL of protein/mitochondrial extract. Mix. Start measuring the absorbance at 412 nm. After 2 min add 5 uL oxaloacetate (the rate before addition of oxaloacetate is due to acetyl CoA hydrolyse and this rate should be substracted from de final rate after

addition of oxaloacetate). The increase in absorbance is about 0.025-0.125 A/min-1. The background activity was usually about 10-15% of this rate and was substracted.

2.7. *In vivo* techniques

2.7.1. Food intake determination

Food intake of both STD chow diet and HFD mice was determined in individualized mice. Food intake was obtained from the difference between the amount of food initially added to the cage and the amount of food, which remained on the cage one week later. Results were expressed as grams/day.

2.7.2. Locomotor activity assessment

An indirect open circuit calorimeter (Oxylet; Panlab, Cornella, Spain) was used to monitor oxygen consumption and carbon dioxide production in eight metabolism chambers simultaneously. Mice were acclimatised to the metabolism chambers for 24 h and data were collected for 3 min at 15 min intervals in each cage. Data were taken from the light cycle (basal state) or from a continuous 24 h light–dark cycle (total) and adjusted for body weight. To calculate locomotor the Metabolism software provided by the manufacturer was used.

2.7.3. Energy expenditure

An indirect open circuit calorimeter (Oxylet; Panlab, Cornella, Spain) was used to monitor oxygen consumption and carbon dioxide production in eight metabolism chambers simultaneously. Mice were acclimatised to the metabolism chambers for 24 h and data were collected for 3 min at 15 min intervals in each cage. Data were taken from the light cycle (basal state) or from a continuous 24 h light–dark cycle (total) and adjusted for body weight. To calculate energy expenditure the Metabolism software

provided by the manufacturer was used.

2.7.4. Insulin tolerance test

For insulin tolerance test, insulin (0.75 IU/kg body weight; Humulin regular, Eli Lilly) was injected intraperitoneally into awake, fed control and transgenic mice. Glucose concentration was determined in blood samples obtained from the tail vein at different time points (0, 15, 30, 45 and 60 minutes) after the insulin injection with a Glucometer Elite ® (Bayer, Leverkusen, Germany).

2.7.5. Glucose tolerance test

Overnight fasted (16 h) awake control and transgenic mice with free access to water were given an intraperitoneal injection of glucose (1 g/kg of body weight). Blood samples were obtained from tail vein bleeding before the glucose injection (time 0) and at the indicated time points (15, 30, 45 and 60 minutes) after the glucose load. Glucose concentration was measured with a Glucometer Elite ® (Bayer, Leverkusen, Germany).

2.7.6. Insulin signaling

To study insulin signalling in different tissues, overnight-starved animals were anaesthetized by an intraperitoneal injection of 100-mg/kg body weight of ketamine (Imalgene®, Merial, Lyon, France) and 10-mg/kg body weight of xylazine (Rompun® Bayer, Leverkusen, Germany). Once anaesthetized, quadriceps and gastrocnemius of one leg were excised and frozen into liquid nitrogen. After being clamped, a piece of liver and a piece of epididymal WAT were also excised and frozen. Immediately, mice were injected with an intraperitoneal injection of insulin (dose: 5 U Insulin/g body weight). Fifteen minutes after insulin stimulation, remaining gastrocnemius, quadriceps and a piece of liver and WAT were also excised and frozen. Protein extracts

of different samples were obtained to carry on Western Blot analysis.

2.7.7. Chronic cold exposure

When indicated, wild type and aP2HMGA1 transgenic mice were housed in cambers with environment temperature of 4º C or at 21º C (thermoneutral control) with a 12-hour light and dark cycle for 24 h, 48 h, or 5 days.

Core body temperature was measured in the rectum of wild type and transgenic mice at the indicated time point using a TK-610B digital thermometer (Thermocouple Thermometer, UK)

2.8. Serum parameters determination

For serum sample collection, mice were anaesthetized with isoflourane and euthanized by decapitation. Blood samples were collected during the decapitation of mice. Blood was kept in BD Microtainer® SST™ Tubes and let to coagulate at 4º C for 30 min. Serum fraction was obtained by centrifugation at 12000 g for 5 minutes at 4º C. Serums were separated, aliquoted and kept at -80º C until serum parameters were determined.

2.8.1. Serum metabolites

Blood metabolites such as TG, FFAs, glycerol, cholesterol and BHBA, were determined photometrically using the autoanalyzer PENTRA 400 (Horiba ABX, Montpellier, France) using different and specific kits for each reaction.

2.8.1.1. Glucose

Blood glucose levels are measured with a Glucometer Elite™ (Bayer, Leverkusen, Germany) of blood obtained by cutting off the tip of the animals' tail.

2.8.1.1. Triglycerides (TG)

Serum triglyceride levels were determined spectrophotometrically using the commercial product GPO-PAP (Roche Diagnostics, Basel, Switzerland) and the autoanalyzer PENTRA 400. The method is based on the enzymatic GPO-PAP reaction described by Fossati *et al.,* (Fossati *et al.,* 1982) in which quinoneimina (PAP) chromogen is obtained from p-clorophenol and 4-aminoantipirine reaction catalyzed by glycerol kinase, glycerol-3-phosphate oxidase (GPO) and peroxidase.

2.8.1.2. Free Fatty acids (FFA)

Non-esterified serum free fatty acid levels were determined spectrophotometrically using the commercial product NEFA C (Wako Chemicals, Neuss, Germany) and the autoanalyzer PENTRA 400 (ABX Diagnostics, Montpellier, France). The method is based on the enzymatic reaction of acil-CoA synthetase and acil-Co oxidase.

2.8.1.3. Glycerol

Serum glycerol levels were determined spectrophotometrically using the commercial product provided by Roche Molecular Diagnostics and the autoanalyzer PENTRA 400.

2.8.1.4. Cholesterol

Serum cholesterol levels were determined spectrophotometrically using the commercial product CHOD-PAP and the autoanalyzer PENTRA 400. The method is based on the enzymatic reaction in which quinoneimina chromogen is obtained from p-clorophenol and 4-aminoantipirine reaction catalysed by hydrogen peroxide and peroxidase (Trinder reaction).

2.8.1.5. B-hydroxybutirate

Serum D-3-hydroxybutyric acid concentrations were determined enzymatically (Randox Lab, Crumlin, UK).

2.8.2. Serum hormones

Serum hormones such as insulin, leptin, MCP-1, resistin, PAI-1, TNF-a and IL-6 were measured using the Milliplex Mouse Adipokine Panel (MADPK-71K, Millipore™ Corp., Billerica, MA) and read on a Luminex® 100™ Total System.

2.8.2.1. Insulin

Insulin levels were measured by radioimmunoassay with Sensitive Rouse Insulin RIA Kit (Millipore).

2.8.2.2. Adiponectin

Adiponectin levels were measured by radioimmunoassay with Mouse Adiponectin RIA Kit (Millipore).

2.8.2.3. Ghrelin

Ghrelin levels were measured by radioimmunoassay with Rat/Mouse Ghrelin ELISA Kit (Millipore).

2.9. Whole body fat content determination

2.9.1. Total triglyceride content

The fat content of mouse carcasses was measured as previously described by Salmon & Flatt 1985. Carcasses were digested in alcoholic KOH at 60º C for 48 h. Aliquots of the digestion were adjusted to a final concentration of 0.5 mol/l $MgCl_2$, placed on ice for 10 min, and then centrifuged for 10 min. Triacylglycerol concentrations were measured spectrophotometrically in supernatant fractions using

an enzymatic assay kit (GPO-PAP, Roche Diagnostics, Basel, Switzerland) and the autoanalyzer PENTRA 400.

2.9.2. Specific tissue triglyceride content

To determine the amount of specific tissue triglycerides content, we used the method described by Carr et al. 1993, based on the chloroform:methanol (2:1) extraction described previously by FOLCH et al. 1957). To extract triglycerides, frozen samples of approximately 100 mg were weighted and homogenized in 15 ml chloroform:methanol (2:1). Lipid and aqueous phases were then separated by adding 3 ml of H_2SO_4 0.05% and keeping them overnight at 4º C. Once the phases were separated, the aqueous superior phase was eliminated using a Pasteur pipet and 1 ml of the inferior lipid phase was recuperated in a glass tube. 1 ml of a chloroform and Triton X-100 at 1% solution was added to the glass tube and it was incubated at 90º C in a bath, to evaporate the chloroform. By the use of the chloroform and Triton X-100 mix, any remaining aqueous particle was eliminated from the lipid phase. After the evaporation, chloroform was rinsed to the walls of the tube to concentrate the sample and, it was warmed again at 90º C to evaporate the chloroform. Once the sediment was completely dry and concentrated, it was resuspended by the addition of 500 µl of deionized water at 37º C. The amount of triglycerides was finally determined using the commercial product GPO-PAP (Roche Diagnostics, Basel, Switzerland) and the autoanalyzer PENTRA 400.

2.10. Specific tissue glycogen content

Enzymatic determination of glycogen content was carried out in tissue extracts by the a-amyloglucosidase method as described in Keppler D *et al.* 1981 .

2.11. Flow cytometry and cell sorting

2.11.1. Isolation of the epWAT macrophages

Animals were anesthetized and sacrificed to carry out dissection. Then, epWAT was excised and put in a tube containing 2 ml of a PBS solution with 0.5% BSA at 37º C. The tissue was minced and digested at 37º C for 30 minutes by the addition of 1 mg/ml of Collagenase P (Roche) with mild agitation. Then, supernatant was filtered through a 30-μm pore pre-separation filter (Partec CellTrics®) to obtain a single cell suspension and the filtrate was recollected in a Falcon tubes. After the addition of PBS 0.5% BSA, the filtrate was centrifuged at 1400 rpm for 5 minutes. Supernatant was eliminated and the pellet was resuspended in 500 μl RBC lysis buffer (eBioscience, San Diego, CA, USA) and incubated for 5 minutes to lysate red blood cells. PBS 0.5 % BSA was added again into the Falcon tube and spun at 1200 rpm for 5 minutes. Supernatant was eliminated and the pellet was resuspended in 500 μl PBS 0.5% BSA. Cells were then stained with fluorescently conjugated antibodies specific for the different cell populations described in *Section 1.6* and analysed by flow cytometry as described below.

2.11.2. Antibodies incubation and flow cytometry analysis

Resuspended cells were put in different eppendorf tubes, using 50 μl of cell suspension for each tube, and were incubated for 60 min at 4º C with specific antibodies. Samples were then washed with 100 μl PBS for 10 min at 1800 rpm. Supernatant was eliminated and pellets were resuspended in 200 μl PBS, to perform flow cytometric analysis. The antibodies used are listed in *Section 1.6.* Antibodies were obtained from BD PharMingen or BioLegend. Sorting analysis was performed with a BD FacsAria III cell sorter (BD Biosciences) equipped with four lasers (488 nm, 633 nm, 405

nm and 561 nm). Flow cytometry analysis was performed on a BD LSRFortessa™ cell analyser (BD Biosciences) equipped with four different lasers (488 nm, 50mW output; 640 nm, 40mW output; 355 nm, 20 mW output; 405 nm, 50 mW output). Data were analysed using BD FACSDiva™ v6.2 software.

2.12. Histological analysis

Tissue samples from wild type and transgenic mice were fixed for 12 to 24 h in 10% formalin, embedded in paraffin and sectioned (2-3 mm).

2.12.1. Haematoxylin/eosin staining

Sections were deparaffinised and stained with haematoxylin, rinsed with water and stained again with eosin. Samples were then dehydrated and mounted and viewed with a light microscope (Eclipse iE 900; Nikon, Tokyo, Japan).

2.12.2. Immunohistochemistry

For immunohistochemical detection, sections were deparaffinised and incubated overnight at 4º C with specific antibodies for each protein (see list, *Section 1.6*), washed with PBS three times for 5 minutes each wash and incubated with the corresponding secondary antibodies (see list, *Section 1.6*). Antibodies were revealed with ABC Complex (Vector Laboratories Ltd., UK), which employs 3'3'-diaminobenzidine (DAB) as the substrate chromogen. Sections were counterstained in Mayer's haematoxylin. Images were visualized using a Nikon Eclipse E800 microscope (Nikon, Tokyo, Japan) connected to a videocamera.

2.12.3. Morphometric analysis

For WAT morphometric analysis, 8 hematoxylin/eosin WAT sections from each individual mouse (at least five mice per group) were viewed with a light microscope

(Eclipse iE 900; Nikon, Tokyo, Japan). Images were obtained with a video camera connected to a colour monitor and to an image analyser (analySIS 3.0; Soft Imaging System, Lakewood, CO, USA). Adipocyte's area was determine in images taken at 10X augmentation. The mean surface area and the frequency distribution were calculated from >400 cells for each mouse. Adipocyte size distributions are presented as percentage of total cells.

2.12.4. Skin thickness measurements

Skin from wild type and transgenic mice was fixed in 10% buffered formalin, embedded in paraffin, sectioned and stained with hematoxylin and eosin. Images from transversal slides were taken using light microscope (Eclipse iE 900; Nikon, Tokyo, Japan). Skin thickness was determine measuring its different structural layers from outside to inside (epidermis, dermis and hipodermis). Ten readings were scored from each skin layer of each animal. The epidermal thickness was measured from stratum basale to stratum granulosum (excluding stratum corneum), whereas the dermal thickness was the distance between the epidermis and the hypodermis. Finally, the hypodermal thickness was measured as the distance between the dermis and the panniculus carnosus.

2.13. Statistical analysis

All values are expressed as mean ± SEM. Statistical analysis was carried out using the Student-Newman-Keuls test. Statistical analyses were performed using GraphPad Prism version 5.0a for Mac OS X (GraphPad Software, San Diego, CA, USA). Differences were considered significant at $^{*}P$ <0.05 *vs*. wild type mice fed a STD or $^{\$}P$ <0.05 *vs*. wild type mice fed a HFD.

8. BIBLIOGRAPHY

Ahmadian, M., Wang, Yuhui, Sul, H.S., 2010. Lipolysis in adipocytes. The international journal of biochemistry & cell biology 42, 555–9.

Algire, C., Medrikova, D., Herzig, S., 2012. White and brown adipose stem cells: From signaling to clinical implications. Biochimica et biophysica acta 1–9.

Anand, a, Chada, K., 2000. In vivo modulation of Hmgic reduces obesity. Nature genetics 24, 377–80.

Arlotta, P., Tai, A.K., Manfioletti, G, Clifford, C., Jay, G., Ono, S.J., 2000. Transgenic mice expressing a truncated form of the high mobility group I-C protein develop adiposity and an abnormally high prevalence of lipomas. The Journal of biological chemistry 275, 14394–400.

Armani, A., Mammi, C., Marzolla, V., Calanchini, M., Antelmi, A., Rosano, G.M.C., Fabbri, A., Caprio, M., 2010. Cellular models for understanding adipogenesis, adipose dysfunction, and obesity. Journal of cellular biochemistry 110, 564–72.

Armengol, J., Villena, J.A., Hondares, E., Carmona, María C, Sul, H.S., Iglesias, R., Giralt, M., Villarroya, F., 2012. Pref-1 in brown adipose tissue: specific involvement in brown adipocyte differentiation and regulatory role of C/EBPδ. The Biochemical journal 443, 799–810.

Avram, A.S., Avram, M.M., James, W.D., 2005. Subcutaneous fat in normal and diseased states: 2. Anatomy and physiology of white and brown adipose tissue. Journal of the American Academy of Dermatology 53, 671–83.

Bachman, E.S., Dhillon, H., Zhang, C.-Y., Cinti, Saverio, Bianco, A.C., Kobilka, B.K., Lowell, B.B., 2002. betaAR signaling required for diet-induced thermogenesis and obesity resistance. Science (New York, N.Y.) 297, 843–5.

Baker, D.J., Wijshake, T., Tchkonia, Tamar, LeBrasseur, N.K., Childs, B.G., Van de Sluis, B., Kirkland, J.L., Van Deursen, J.M., 2011. Clearance of p16Ink4a-positive senescent cells delays ageing-associated disorders. Nature 479, 232–6.

Bianchi, M.E., Agresti, A., 2005. HMG proteins: dynamic players in gene regulation and differentiation. Current opinion in genetics & development 15, 496–506.

Billon, N., Dani, C., 2012. Developmental origins of the adipocyte lineage: new insights from genetics and genomics studies. Stem cell reviews 8, 55–66.

Birerdinc, A., Jarrar, M., Stotish, T., Randhawa, M., Baranova, A., 2013. Manipulating molecular switches in brown adipocytes and their precursors: a therapeutic potential. Progress in lipid research 52, 51–61.

Birnboim, H.C., Doly, J., 1979. A rapid alkaline extraction procedure for screening recombinant plasmid DNA. Nucleic acids research 7, 1513–23.

Brocher, J., Vogel, B., Hock, R., 2010. HMGA1 down-regulation is crucial for chromatin composition and a gene expression profile permitting myogenic differentiation. BMC cell biology 11, 64.

Burgess, S.C., He, T., Yan, Z., Lindner, J., Sherry, a D., Malloy, C.R., Browning, J.D., Magnuson, M. a, 2007. Cytosolic phosphoenolpyruvate carboxykinase does not solely control the rate of hepatic gluconeogenesis in the intact mouse liver. Cell metabolism 5, 313–20.

Cannon, B., Nedergaard, J., 2012. Yes, even human brown fat is on fire! The Journal of clinical investigation 122, 486–9.

Cao, Y., 2010. Adipose tissue angiogenesis as a therapeutic target for obesity and metabolic diseases. Nature reviews. Drug discovery 9, 107–15.

Carmona, M Carmen, Hondares, E., Rodríguez de la Concepción, M.L., Rodríguez-Sureda, V., Peinado-Onsurbe, J., Poli, V., Iglesias, R., Villarroya, F., Giralt, M., 2005. Defective thermoregulation, impaired lipid metabolism, but preserved adrenergic induction of gene expression in brown fat of mice lacking C/EBPbeta. The Biochemical journal 389, 47–56.

Carr, T.P., Andresen, C.J., Rudel, L.L., 1993. Enzymatic determination of triglyceride, free cholesterol, and total cholesterol in tissue lipid extracts. Clinical biochemistry 26, 39–42.

Carvajal, I.M., Baron, R.M., Perrella, M. a., 2002. High-mobility group-I/Y proteins: Potential role in the pathophysiology of critical illnesses. Critical care medicine 30, S36–S42.

Cawthorn, W.P., Scheller, E.L., MacDougald, O. a, 2012a. Adipose tissue stem cells meet preadipocyte commitment: going back to the future. Journal of lipid research 53, 227–46.

Cawthorn, W.P., Scheller, E.L., MacDougald, O.A., 2012b. Adipose tissue stem cells: the great WAT hope. Trends in Endocrinology & Metabolism.

Chang, L., Chiang, S.-H., Saltiel, A.R., 2005. Insulin signaling and the regulation of glucose transport. Molecular medicine (Cambridge, Mass.) 10, 65–71.

Charrière, G., Cousin, B., Arnaud, E., André, M., Bacou, F., Penicaud, L., Casteilla, L., 2003. Preadipocyte conversion to macrophage. Evidence of plasticity. The Journal of biological chemistry 278, 9850–5.

Chazenbalk, G., Bertolotto, C., Heneidi, S., Jumabay, M., Trivax, B., Aronowitz, J., Yoshimura, K., Simmons, C.F., Dumesic, D. a, Azziz, R., 2011. Novel pathway of adipogenesis through cross-talk between adipose tissue macrophages, adipose stem cells and adipocytes: evidence of cell plasticity. PloS one 6, e17834.

Chiappetta, G., Avantaggiato, V., Visconti, R., Fedele, M, Battista, S, Trapasso, F., Merciai, B.M., Fidanza, V., Giancotti, V, Santoro, M, Simeone, A., Fusco, A, 1996. High level expression of the HMGI (Y) gene during embryonic development. Oncogene 13, 2439–46.

Chiefari, E., Tanyolaç, S., Iiritano, S., Sciacqua, A., Capula, C., Arcidiacono, B., Nocera, A., Possidente, K., Baudi, F., Ventura, V., Brunetti, G., Brunetti, F.S., Vero, R., Maio, R., Greco, M., Pavia, M., Hodoglugil, U., Durlach, V., Pullinger, C.R., Goldfine, I.D.,

Perticone, F., Foti, D., Brunetti, Antonio, 2013. A polymorphism of HMGA1 is associated with increased risk of metabolic syndrome and related components. Scientific reports 3, 1491.

Chun, T.-H., 2012. Peri-adipocyte ECM remodeling in obesity and adipose tissue fibrosis. Adipocyte 1, 1–7.

Cinti, S, 2005. The adipose organ. Prostaglandins, leukotrienes, and essential fatty acids 73, 9–15.

Cinti, Saverio, 2012. The adipose organ at a glance. Disease models & mechanisms 5, 588–94.

Cinti, Saverio, Mitchell, G., Barbatelli, Giorgio, Murano, Incoronata, Ceresi, E., Faloia, E., Wang, S., Fortier, M., Greenberg, A.S., Obin, M.S., 2005. Adipocyte death defines macrophage localization and function in adipose tissue of obese mice and humans. Journal of lipid research 46, 2347–55.

Cleynen, I., Van de Ven, W.J.M., 2008. The HMGA proteins: a myriad of functions (Review). International journal of oncology 32, 289–305.

Cristancho, A.G., Lazar, M.A., 2011. Forming functional fat: a growing understanding of adipocyte differentiation. Nature reviews. Molecular cell biology 12, 722–34.

Cypess, A.M., Chen, Y.-C., Sze, C., Wang, K., English, J., Chan, O., Holman, A.R., Tal, I., Palmer, M.R., Kolodny, G.M., Kahn, C.R., 2012. Cold but not sympathomimetics activates human brown adipose tissue in vivo. Proceedings of the National Academy of Sciences of the United States of America 109, 10001–5.

De Oliveira Leal, V., Mafra, D., 2013. Adipokines in obesity. Clinica chimica acta; international journal of clinical chemistry 419, 87–94.

De Wet, J.R., Wood, K. V, DeLuca, M., Helinski, D.R., Subramani, S., 1987. Firefly luciferase gene: structure and expression in mammalian cells. Molecular and cellular biology 7, 725–37.

Diabetes, D.O.F., 2013. Diagnosis and classification of diabetes mellitus. Diabetes care 36 Suppl 1, S67–74.

Divoux, A., Clément, K., 2011. Architecture and the extracellular matrix: the still unappreciated components of the adipose tissue. Obesity reviews : an official journal of the International Association for the Study of Obesity 12, e494–503.

Document_not_found, n.d. Document not found (9).

Donath, M.Y., Shoelson, S.E., 2011. Type 2 diabetes as an inflammatory disease. Nature reviews. Immunology 11, 98–107.

Dong, S., Hughes, R.C., 1997. Macrophage surface glycoproteins binding to galectin-3 (Mac-2-antigen). Glycoconjugate journal 14, 267–74.

Dyck, D.J., Heigenhauser, G.J.F., Bruce, C.R., 2006. The role of adipokines as regulators of skeletal muscle fatty acid metabolism and insulin sensitivity. Acta physiologica (Oxford, England) 186, 5–16.

Echtay, K.S., 2007. Mitochondrial uncoupling proteins--what is their physiological role? Free radical biology & medicine 43, 1351–71.

Elias, Ivet, Franckhauser, Sylvie, Ferré, Tura, Vilà, L., Tafuro, S., Muñoz, Sergio, Roca, C., Ramos, D., Pujol, Anna, Riu, E., Ruberte, Jesús, Bosch, Fatima, 2012. Adipose tissue overexpression of vascular endothelial growth factor protects against diet-induced obesity and insulin resistance. Diabetes 61, 1801–13.

Enerbäck, S., Jacobsson, A., Simpson, E.M., Guerra, C., Yamashita, H., Harper, M.E., Kozak, L P, 1997. Mice lacking mitochondrial uncoupling protein are cold-sensitive but not obese. Nature 387, 90–4.

Esposito, F., Pierantoni, Giovanna Maria, Battista, Sabrina, Melillo, Rosa Marina, Scala, Stefania, Chieffi, P., Fedele, Monica, Fusco, Alfredo, 2009. Interaction between HMGA1 and retinoblastoma protein is required for adipocyte differentiation. The Journal of biological chemistry 284, 25993–6004.

Fain, J.N., Bahouth, S.W., Madan, A.K., 2004. TNFalpha release by the nonfat cells of human adipose tissue. International journal of obesity and related metabolic disorders : journal of the International Association for the Study of Obesity 28, 616–22.

Fajas, L., 2003. Adipogenesis: a cross-talk between cell proliferation and cell differentiation. Annals of Medicine 35, 79–85.

Farmer, S.R., 2006. Transcriptional control of adipocyte formation. Cell metabolism 4, 263–73.

Farmer, S.R., 2008. Molecular determinants of brown adipocyte formation and function. Genes & development 22, 1269–75.

Fedele, Monica, Palmieri, D., Fusco, Alfredo, 2010. HMGA2: A pituitary tumour subtype-specific oncogene? Molecular and cellular endocrinology 326, 19–24.

Fedele, Monica, Pentimalli, F., Baldassarre, G., Battista, Sabrina, Klein-Szanto, A.J.P., Kenyon, L., Visone, R., De Martino, I., Ciarmiello, A., Arra, C., Viglietto, Giuseppe, Croce, Carlo M, Fusco, Alfredo, 2005. Transgenic mice overexpressing the wild-type form of the HMGA1 gene develop mixed growth hormone/prolactin cell pituitary adenomas and natural killer cell lymphomas. Oncogene 24, 3427–35.

Fedele, Monica, Visone, R., De Martino, I., Palmieri, D., Valentino, T., Esposito, F., Klein-Szanto, A., Arra, C., Ciarmiello, A., Croce, Carlo M, Fusco, Alfredo, 2011. Expression of a truncated Hmga1b gene induces gigantism, lipomatosis and B-cell lymphomas in mice. European journal of cancer (Oxford, England : 1990) 47, 470–8.

Feldmann, H.M., Golozoubova, V., Cannon, B., Nedergaard, J., 2009. UCP1 ablation induces obesity and abolishes diet-induced thermogenesis in mice exempt from thermal stress by living at thermoneutrality. Cell metabolism 9, 203–9.

FOLCH, J., LEES, M., SLOANE STANLEY, G.H., 1957. A simple method for the isolation and purification of total lipides from animal tissues. The Journal of biological chemistry 226, 497–509.

Foti, D., Chiefari, E., Fedele, Monica, Iuliano, R., Brunetti, L., Paonessa, F., Manfioletti, Guidalberto, Barbetti, F., Brunetti, Arturo, Croce, Carlo M, Fusco, Alfredo, Brunetti, Antonio, 2005. Lack of the architectural factor HMGA1 causes insulin resistance and diabetes in humans and mice. Nature medicine 11, 765–73.

Frontini, A., Cinti, Saverio, 2010. Distribution and development of brown adipocytes in the murine and human adipose organ. Cell metabolism 11, 253–6.

Frühbeck, G., Becerril, S., Sáinz, N., Garrastachu, P., García-Velloso, M.J., 2009. BAT: a new target for human obesity? Trends in pharmacological sciences 30, 387–96.

Frühbeck, G., Salvador, J., 2004. Role of adipocytokines in metabolism and disease. Nutrition Research 24, 803–826.

Galic, S., Oakhill, J.S., Steinberg, G.R., 2010. Adipose tissue as an endocrine organ. Molecular and cellular endocrinology 316, 129–39.

Garg, A., Agarwal, A.K., 2009. Lipodystrophies: disorders of adipose tissue biology. Biochimica et biophysica acta 1791, 507–13.

Gesta, S., Tseng, Y.-H., Kahn, C.R., 2007. Developmental origin of fat: tracking obesity to its source. Cell 131, 242–56.

Girousse, A., Langin, D., 2011. Adipocyte lipases and lipid droplet-associated proteins: insight from transgenic mouse models. International journal of obesity (2005) 36, 581–94.

Gómez-Valadés, A.G., Méndez-Lucas, A., Vidal-Alabró, A., Blasco, F.X., Chillon, M., Bartrons, R., Bermúdez, J., Perales, J.C., 2008. Pck1 gene silencing in the liver improves glycemia control, insulin sensitivity, and dyslipidemia in db/db mice. Diabetes 57, 2199–210.

Graves, R.A., Tontonoz, P, Platt, K.A., Ross, S.R., Spiegelman, B M, 1992. Identification of a fat cell enhancer: analysis of requirements for adipose tissue-specific gene expression. Journal of cellular biochemistry 49, 219–24.

Gregoire, F.M., 2001. Adipocyte differentiation: from fibroblast to endocrine cell. Experimental biology and medicine (Maywood, N.J.) 226, 997–1002.

Guilherme, A., Virbasius, J. V, Puri, V., Czech, M.P., 2008. Adipocyte dysfunctions linking obesity to insulin resistance and type 2 diabetes. Nat Rev Mol Cell Biol 9, 367–377.

Hahn, P., Novak, M., 1975. Development of brown and white adipose tissue. Journal of lipid research 16, 79–91.

Haslam, D.W., James, W.P.T., 2005. Obesity. Lancet 366, 1197–209.

Herrmann, T., Van der Hoeven, F., Grone, H.-J., Stewart, A.F., Langbein, L., Kaiser, I., Liebisch, G., Gosch, I., Buchkremer, F., Drobnik, W., Schmitz, G., Stremmel, W., 2003. Mice with targeted disruption of the fatty acid transport protein 4 (Fatp 4, Slc27a4) gene show features of lethal restrictive dermopathy. The Journal of cell biology 161, 1105–15.

Hock, R., Furusawa, T., Ueda, T., Bustin, M., 2007. HMG chromosomal proteins in development and disease. Trends in cell biology 17, 72–9.

Hoffstedt, J, Arner, E, Wahrenberg, H., Andersson, D.P., Qvisth, V., Löfgren, P., Rydén, M, Thörne, a, Wirén, M., Palmér, M., Thorell, a, Toft, E., Arner, P, 2010. Regional impact of adipose tissue morphology on the metabolic profile in morbid obesity. Diabetologia 53, 2496–503.

Iiritano, S., Chiefari, E., Ventura, V., Arcidiacono, B., Possidente, K., Nocera, A., Nevolo, M.T., Fedele, Monica, Greco, A., Greco, M., Brunetti, G., Fusco, Alfredo, Foti, D., Brunetti, Antonio, 2012. The HMGA1-IGF-I/IGFBP System: A Novel Pathway for Modulating Glucose Uptake. Molecular endocrinology (Baltimore, Md.) 26.

Ishibashi, J., Seale, P., 2010. Medicine. Beige can be slimming. Science (New York, N.Y.) 328, 1113–4.

Ismail, a a, Wagner, S., Murua Escobar, H., Willenbrock, S., Sterenczak, K. a, Samy, M.T., Abd El-Aal, a M., Nolte, I., Wefstaedt, P., 2012. Effects of high-mobility group a protein application on canine adipose-derived mesenchymal stem cells in vitro. Veterinary medicine international 2012, 752083.

Jacene, H.A., Wahl, R.L., 2009. The importance of brown adipose tissue. The New England journal of medicine 361, 417–8; author reply 419–20.

Jastroch, M., Divakaruni, A.S., Mookerjee, S., Treberg, J.R., Brand, M.D., 2010. Mitochondrial proton and electron leaks. Essays in biochemistry 47, 53–67.

Jo, J., Gavrilova, Oksana, Pack, S., Jou, W., Mullen, S., Sumner, A.E., Cushman, S.W., Periwal, V., 2009. Hypertrophy and/or Hyperplasia: Dynamics of Adipose Tissue Growth. PLoS computational biology 5, e1000324.

Jong, M.C., Gijbels, M.J., Dahlmans, V.E., Gorp, P.J., Koopman, S.J., Ponec, M., Hofker, M.H., Havekes, L.M., 1998. Hyperlipidemia and cutaneous abnormalities in transgenic mice overexpressing human apolipoprotein C1. The Journal of clinical investigation 101, 145–52.

Kajimura, S., Seale, P., Spiegelman, Bruce M, 2010. Transcriptional control of brown fat development. Cell metabolism 11, 257–62.

Kajimura, S., Seale, P., Tomaru, T., Erdjument-Bromage, H., Cooper, M.P., Ruas, J.L., Chin, S., Tempst, P., Lazar, M.A., Spiegelman, Bruce M, 2008. Regulation of the brown and white fat gene programs through a PRDM16/CtBP transcriptional complex. Genes & development 22, 1397–409.

Klipper-Aurbach, Y., Wasserman, M., Braunspiegel-Weintrob, N., Borstein, D., Peleg, S., Assa, S., Karp, M., Benjamini, Y., Hochberg, Y., Laron, Z., 1995. Mathematical formulae for the prediction of the residual beta cell function during the first two years of disease in children and adolescents with insulin-dependent diabetes mellitus. Medical hypotheses 45, 486–90.

Kolb, S., Fritsch, R., Saur, D., Reichert, M., Schmid, R.M., Schneider, G., 2007. HMGA1 controls transcription of insulin receptor to regulate cyclin D1 translation in pancreatic cancer cells. Cancer Res 67, 4679–4686.

Koppen, A., Kalkhoven, E., 2010. Brown vs white adipocytes: The PPARgamma coregulator story. FEBS letters.

Kozak, Leslie P, 2013. Genetic variation in brown fat activity and body weight regulation in mice: Lessons for human studies. Biochimica et biophysica acta.

Kozak, Leslie P, Young, M.E., 2012. Heat from calcium cycling melts fat. Nature medicine 18, 1458–9.

Kuilman, T., Michaloglou, C., Mooi, W.J., Peeper, D.S., 2010. The essence of senescence. Genes & development 24, 2463–79.

Laharrague, P., Casteilla, L., 2010. The emergence of adipocytes. Endocrine development 19, 21–30.

Lefterova, M.I., Lazar, M.A., 2009. New developments in adipogenesis. Trends in endocrinology and metabolism: TEM 20, 107–14.

Lepper, C., Fan, C.-M., 2010. Inducible lineage tracing of Pax7-descendant cells reveals embryonic origin of adult satellite cells. Genesis (New York, N.Y. : 2000) 48, 424–36.

Li, P., Lu, M., Nguyen, M.T.A., Bae, E.J., Chapman, J., Feng, D., Hawkins, M., Pessin, J.E., Sears, D.D., Nguyen, A.-K., Amidi, A., Watkins, S.M., Nguyen, U., Olefsky, J.M., 2010. Functional heterogeneity of CD11c-positive adipose tissue macrophages in diet-induced obese mice. The Journal of biological chemistry 285, 15333–45.

Longo, K. a, Wright, W.S., Kang, S., Gerin, I., Chiang, S.-H., Lucas, P.C., Opp, M.R., MacDougald, O. a, 2004. Wnt10b inhibits development of white and brown adipose tissues. The Journal of biological chemistry 279, 35503–9.

Lowell, B.B., Bachman, E.S., 2003. Beta-Adrenergic receptors, diet-induced thermogenesis, and obesity. The Journal of biological chemistry 278, 29385–8.

Makowski, L., Brittingham, K.C., Reynolds, J.M., Suttles, J., Hotamisligil, G.S., 2005. The fatty acid-binding protein, aP2, coordinates macrophage cholesterol trafficking and inflammatory activity. Macrophage expression of aP2 impacts peroxisome proliferator-activated receptor gamma and IkappaB kinase activities. The Journal of biological chemistry 280, 12888–95.

Mariman, E.C.M., Wang, P., 2010. Adipocyte extracellular matrix composition, dynamics and role in obesity. Cellular and molecular life sciences : CMLS 67, 1277–92.

Martinez Hoyos, J., Fedele, Monica, Battista, Sabrina, Pentimalli, F., Kruhoffer, M., Arra, C., Orntoft, T.F., Croce, Carlo Maria, Fusco, Alfredo, 2004. Identification of the genes up- and down-regulated by the high mobility group A1 (HMGA1) proteins: tissue specificity of the HMGA1-dependent gene regulation. Cancer research 64, 5728–35.

Melillo, R M, Pierantoni, G M, Scala, S, Battista, S, Fedele, M, Stella, A., De Biasio, M.C., Chiappetta, G., Fidanza, V., Condorelli, G., Santoro, M, Croce, C M, Viglietto, G, Fusco, A, 2001. Critical role of the HMGI(Y) proteins in adipocytic cell growth and differentiation. Molecular and cellular biology 21, 2485–95.

Minamino, T., Orimo, M., Shimizu, I., Kunieda, T., Yokoyama, M., Ito, T., Nojima, A., Nabetani, A., Oike, Y., Matsubara, H., Ishikawa, F., Komuro, I., 2009. A crucial role for adipose tissue p53 in the regulation of insulin resistance. Nature medicine 15, 1082–7.

Moitra, J., Mason, M.M., Olive, M., Krylov, D., Gavrilova, O., Marcus-Samuels, B., Feigenbaum, L., Lee, E., Aoyama, T., Eckhaus, M., Reitman, M.L., Vinson, C., 1998. Life without white fat: a transgenic mouse. Genes & Development 12, 3168–3181.

Muñoz, S, Franckhauser, S, Elias, I, Ferré, T, Hidalgo, A., Monteys, A.M., Molas, M., Cerdán, S., Pujol, A, Ruberte, J, Bosch, F, 2010. Chronically increased glucose uptake by adipose tissue leads to lactate production and improved insulin sensitivity rather than obesity in the mouse. Diabetologia.

Murano, I, Barbatelli, G, Giordano, A., Cinti, S, 2009. Noradrenergic parenchymal nerve fiber branching after cold acclimatisation correlates with brown adipocyte density in mouse adipose organ. Journal of anatomy 214, 171–8.

Musri, M.M., Gomis, R., Párrizas, M., 2010. A chromatin perspective of adipogenesis. Organogenesis 6, 15–23.

Narita, M, 2007. Cellular senescence and chromatin organisation. British journal of cancer 96, 686–91.

Narita, Masashi, Narita, Masako, Krizhanovsky, V., Nuñez, S., Chicas, A., Hearn, S. a, Myers, M.P., Lowe, S.W., 2006. A novel role for high-mobility group a proteins in cellular senescence and heterochromatin formation. Cell 126, 503–14.

Nyman, L.R., Tian, L., Hamm, D. a, Schoeb, T.R., Gower, B. a, Nagy, T.R., Wood, P. a, 2011. Long term effects of high fat or high carbohydrate diets on glucose tolerance in mice with heterozygous carnitine palmitoyltransferase-1a (CPT-1a) deficiency: Diet influences on CPT1a deficient mice. Nutrition & diabetes 1, e14.

Olds, T., Maher, C., Zumin, S., Péneau, S., Lioret, S., Castetbon, K., Bellisle, De Wilde, J., Hohepa, M., Maddison, R., Lissner, L., Sjöberg, A., Zimmermann, M., Aeberli, I., Ogden, C., Flegal, K., Summerbell, C., 2011. Evidence that the prevalence of childhood overweight is plateauing: data from nine countries. International journal of pediatric obesity : IJPO : an official journal of the International Association for the Study of Obesity 6, 342–60.

Olefsky, J.M., Glass, C.K., 2010. Macrophages, inflammation, and insulin resistance. Annual review of physiology 72, 219–46.

Ouchi, N., Parker, J.L., Lugus, J.J., Walsh, K., 2011. Adipokines in inflammation and metabolic disease. Nature reviews. Immunology 11, 85–97.

Pierantoni, Giovanna Maria, Battista, Sabrina, Pentimalli, F., Fedele, Monica, Visone, R., Federico, A., Santoro, Massimo, Viglietto, Giuseppe, Fusco, Alfredo, 2003. A truncated

HMGA1 gene induces proliferation of the 3T3-L1 pre-adipocytic cells: a model of human lipomas. Carcinogenesis 24, 1861–9.

Prieur, X., Mok, C.Y.L., Velagapudi, V.R., Núñez, V., Fuentes, L., Montaner, D., Ishikawa, K., Camacho, A., Barbarroja, N., O'Rahilly, S., Sethi, J.K., Dopazo, J., Orešič, M., Ricote, M., Vidal-Puig, A., 2011. Differential lipid partitioning between adipocytes and tissue macrophages modulates macrophage lipotoxicity and M2/M1 polarization in obese mice. Diabetes 60, 797–809.

Reeves, R, 2001a. Molecular biology of HMGA proteins: hubs of nuclear function. Gene 277, 63–81.

Reeves, R, 2001b. HMGI/Y proteins: flexible regulators of transcription and chromatin structure. Biochimica et Biophysica Acta (BBA) - Gene Structure and Expression 1519, 13–29.

Reeves, Raymond, 2010. Nuclear functions of the HMG proteins. Biochimica et biophysica acta 1799, 3–14.

Resar, L.M.S., 2010. The high mobility group A1 gene: transforming inflammatory signals into cancer? Cancer research 70, 436–9.

Reshef, L., Olswang, Y., Cassuto, H., Blum, B., Croniger, C.M., Kalhan, S.C., Tilghman, S.M., Hanson, R.W., 2003. Glyceroneogenesis and the triglyceride/fatty acid cycle. The Journal of biological chemistry 278, 30413–6.

Richard, D., Carpentier, a C., Doré, G., Ouellet, V., Picard, F., 2010. Determinants of brown adipocyte development and thermogenesis. International journal of obesity (2005) 34 Suppl 2, S59–66.

Rodeheffer, M.S., Birsoy, K., Friedman, J.M., 2008. Identification of white adipocyte progenitor cells in vivo. Cell 135, 240–9.

Rosen, E.D., Spiegelman, Bruce M, 2000. Molecular regulation of adipogenesis. Annual review of cell and developmental biology 16, 145–71.

Rosenbaum, M., Leibel, R.L., 2010. Adaptive thermogenesis in humans. International journal of obesity (2005) 34 Suppl 1, S47–55.

Sackmann-Sala, L., Berryman, D.E., Munn, R.D., Lubbers, E.R., Kopchick, J.J., 2012. Heterogeneity among white adipose tissue depots in male C57BL/6J mice. Obesity (Silver Spring, Md.) 20, 101–11.

Sahoo, S.K., Shaikh, S. a, Sopariwala, D.H., Bal, N.C., Periasamy, M., 2013. Sarcolipin protein interaction with sarco(endo)plasmic reticulum Ca2+ ATPase (SERCA) is distinct from phospholamban protein, and only sarcolipin can promote uncoupling of the SERCA pump. The Journal of biological chemistry 288, 6881–9.

Salmon, D.M., Flatt, J.P., 1985. Effect of dietary fat content on the incidence of obesity among ad libitum fed mice. International journal of obesity 9, 443–9.

Saltiel, A.R., 2012. Insulin resistance in the defense against obesity. Cell metabolism 15, 798–804.

Savage, D.B., 2009. Mouse models of inherited lipodystrophy. Disease models & mechanisms 2, 554–62.

Schenk, S., Saberi, M., Olefsky, J.M., 2008. Insulin sensitivity: modulation by nutrients and inflammation. The Journal of clinical investigation 118, 2992–3002.

Schipper, H.S., Prakken, B., Kalkhoven, E., Boes, M., 2012. Adipose tissue-resident immune cells: key players in immunometabolism. Trends in endocrinology and metabolism: TEM 23, 407–15.

Seale, P., Bjork, B., Yang, W., Kajimura, S., Chin, S., Kuang, S., Scimè, A., Devarakonda, S., Conroe, H.M., Erdjument-Bromage, H., Tempst, P., Rudnicki, M.A., Beier, D.R., Spiegelman, Bruce M, 2008. PRDM16 controls a brown fat/skeletal muscle switch. Nature 454, 961–7.

Semple, R.K., 2009. From bending DNA to diabetes: the curious case of HMGA1. Journal of biology 8, 64.

Sgarra, R., Rustighi, A., Tessari, M. a, Di Bernardo, J., Altamura, S., Fusco, Alfredo, Manfioletti, Guidalberto, Giancotti, Vincenzo, 2004. Nuclear phosphoproteins HMGA and their relationship with chromatin structure and cancer. FEBS letters 574, 1–8.

Shah, S.N., Kerr, C., Cope, L., Zambidis, E., Liu, C., Hillion, J., Belton, A., Huso, D.L., Resar, L.M.S., 2012. HMGA1 Reprograms Somatic Cells into Pluripotent Stem Cells by Inducing Stem Cell Transcriptional Networks. PloS one 7, e48533.

Shoelson, S.E., Herrero, L., Naaz, A., 2007. Obesity, inflammation, and insulin resistance. Gastroenterology 132, 2169–80.

Smeitink, J., Van den Heuvel, L., DiMauro, S., 2001. The genetics and pathology of oxidative phosphorylation. Nature reviews. Genetics 2, 342–52.

Smorlesi, a, Frontini, a, Giordano, a, Cinti, S, 2012. The adipose organ: white-brown adipocyte plasticity and metabolic inflammation. Obesity reviews : an official journal of the International Association for the Study of Obesity 13 Suppl 2, 83–96.

Solinas, G., Vilcu, C., Neels, J.G., Bandyopadhyay, G.K., Luo, J.-L., Naugler, W., Grivennikov, S., Wynshaw-Boris, A., Scadeng, M., Olefsky, J.M., Karin, M., 2007. JNK1 in hematopoietically derived cells contributes to diet-induced inflammation and insulin resistance without affecting obesity. Cell metabolism 6, 386–97.

Song, Y., Altarejos, J., Goodarzi, M.O., Inoue, H., Guo, X., Berdeaux, R., Kim, J.-H., Goode, J., Igata, M., Paz, J.C., Hogan, M.F., Singh, P.K., Goebel, N., Vera, L., Miller, N., Cui, J., Jones, M.R., Chen, Y.-D.I., Taylor, K.D., Hsueh, W. a, Rotter, J.I., Montminy, M., 2010. CRTC3 links catecholamine signalling to energy balance. Nature 468, 933–9.

Spalding, K.L., Arner, Erik, Westermark, P.O., Bernard, S., Buchholz, B. a, Bergmann, O., Blomqvist, L., Hoffstedt, Johan, Näslund, E., Britton, T., Concha, H., Hassan, M., Rydén, Mikael, Frisén, J., Arner, Peter, 2008. Dynamics of fat cell turnover in humans. Nature 453, 783–7.

Speakman, J.R., 2013. Measuring energy metabolism in the mouse - theoretical, practical, and analytical considerations. Frontiers in physiology 4, 34.

Speakman, J.R., O'Rahilly, S., 2012. Fat: an evolving issue. Disease models & mechanisms 5, 569–73.

Stefan, N., Pfannenberg, C., Häring, H.-U., 2009. The importance of brown adipose tissue. The New England journal of medicine 361, 416–7; author reply 418–21.

Stommel, M., Schoenborn, C.A., 2010. Variations in BMI and prevalence of health risks in diverse racial and ethnic populations. Obesity (Silver Spring, Md.) 18, 1821–6.

Sun, K., Kusminski, C.M., Scherer, P.E., 2011a. Adipose tissue remodeling and obesity. The Journal of clinical investigation 121, 2094–101.

Sun, K., Kusminski, C.M., Scherer, P.E., 2011b. Adipose tissue remodeling and obesity. The Journal of clinical investigation 121, 2094–101.

Sun, Z., Lazar, M. a, 2013. Dissociating fatty liver and diabetes. Trends in endocrinology and metabolism: TEM 24, 4–12.

Sun, Z., Miller, R. a, Patel, R.T., Chen, J., Dhir, R., Wang, H., Zhang, D., Graham, M.J., Unterman, T.G., Shulman, G.I., Sztalryd, C., Bennett, M.J., Ahima, R.S., Birnbaum, M.J., Lazar, M. a, 2012. Hepatic Hdac3 promotes gluconeogenesis by repressing lipid synthesis and sequestration. Nature medicine 18, 934–42.

Symonds, M.E., 2012. Adipose Tissue Biology. Springer New York, New York, NY.

Tang, Q.Q., Lane, M.D., 2012. Adipogenesis: From Stem Cell to Adipocyte. Annual review of biochemistry.

Tchernof, A., Després, J.-P., 2013. Pathophysiology of human visceral obesity: an update. Physiological reviews 93, 359–404.

Tchkonia, Tamara, Thomou, T., Zhu, Y., Karagiannides, I., Pothoulakis, C., Jensen, M.D., Kirkland, J.L., 2013. Mechanisms and Metabolic Implications of Regional Differences among Fat Depots. Cell metabolism 1–13.

Tilg, H., Moschen, A.R., 2008. Insulin resistance, inflammation, and non-alcoholic fatty liver disease. Trends in endocrinology and metabolism: TEM 19, 371–9.

Tontonoz, Peter, Spiegelman, Bruce M, 2008. Fat and beyond: the diverse biology of PPARgamma. Annual review of biochemistry 77, 289–312.

Trayhurn, P., Drevon, C.A., Eckel, J., 2011. Secreted proteins from adipose tissue and skeletal muscle - adipokines, myokines and adipose/muscle cross-talk. Archives of physiology and biochemistry 117, 47–56.

Tseng, Y.-H., Kokkotou, E., Schulz, T.J., Huang, T.L., Winnay, J.N., Taniguchi, C.M., Tran, T.T., Suzuki, R., Espinoza, D.O., Yamamoto, Y., Ahrens, M.J., Dudley, A.T., Norris, A.W., Kulkarni, R.N., Kahn, C.R., 2008. New role of bone morphogenetic protein 7 in brown adipogenesis and energy expenditure. Nature 454, 1000–4.

Ueda, Y., Watanabe, S., Tei, S., Saitoh, N., Kuratsu, J.-I., Nakao, M., 2007. High mobility group protein HMGA1 inhibits retinoblastoma protein-mediated cellular G0 arrest. Cancer science 98, 1893–901.

Urs, S., Harrington, A., Liaw, L., Small, D., 2006. Selective expression of an aP2/Fatty Acid Binding Protein 4-Cre transgene in non-adipogenic tissues during embryonic development. Transgenic research 15, 647–53.

Van Marken Lichtenbelt, W.D., Vanhommerig, J.W., Smulders, N.M., Drossaerts, J.M. a F.L., Kemerink, G.J., Bouvy, N.D., Schrauwen, P., Teule, G.J.J., 2009. Cold-activated brown adipose tissue in healthy men. The New England journal of medicine 360, 1500–8.

Van Tienen, F.H.J., Van der Kallen, C.J.H., Lindsey, P.J., Wanders, R.J., Van Greevenbroek, M.M., Smeets, H.J.M., 2011. Preadipocytes of type 2 diabetes subjects display an intrinsic gene expression profile of decreased differentiation capacity. International journal of obesity (2005) 35, 1154–64.

Villarroya, J., Dorado, B., Vilà, M.R., Garcia-Arumí, E., Domingo, P., Giralt, M., Hirano, M., Villarroya, F., 2011. Thymidine kinase 2 deficiency-induced mitochondrial DNA

depletion causes abnormal development of adipose tissues and adipokine levels in mice. PloS one 6, e29691.

Vitali, a, Murano, I, Zingaretti, M.C., Frontini, a, Ricquier, D., Cinti, S, 2012. The adipose organ of obesity-prone C57BL/6J mice is composed of mixed white and brown adipocytes. Journal of lipid research 53, 619–29.

Waki, H., Tontonoz, Peter, 2007. Endocrine functions of adipose tissue. Annual review of pathology 2, 31–56.

Wang, Yuhui, Sul, H.S., 2009. Pref-1 regulates mesenchymal cell commitment and differentiation through Sox9. Cell metabolism 9, 287–302.

Wells, J.C.K., 2012. The evolution of human adiposity and obesity: where did it all go wrong? Disease models & mechanisms 5, 595–607.

Whittle, A., Vidal-Puig, A., 2013. When BAT is lacking, WAT steps up. Cell research.

Williams, M.J., Almén, M.S., Fredriksson, R., Schiöth, H.B., 2012. What model organisms and interactomics can reveal about the genetics of human obesity. Cellular and molecular life sciences : CMLS 69, 3819–34.

Wu, J., Cohen, P., Spiegelman, Bruce M, 2013. Adaptive thermogenesis in adipocytes: Is beige the new brown? Genes & development 27, 234–50.

Yao, X., Shan, S., Zhang, Ying, Ying, H., 2011. Recent progress in the study of brown adipose tissue. Cell & bioscience 1, 35.

Yin, H., Pasut, A., Soleimani, V.D., Bentzinger, C.F., Antoun, G., Thorn, S., Seale, P., Fernando, P., Van Ijcken, W., Grosveld, F., Dekemp, R. a, Boushel, R., Harper, M.-E., Rudnicki, M. a, 2013. MicroRNA-133 Controls Brown Adipose Determination in Skeletal Muscle Satellite Cells by Targeting Prdm16. Cell metabolism 17, 210–24.

Zhang, Q., Wang, Yinsheng, 2010. HMG modifications and nuclear function. Biochimica et biophysica acta 1799, 28–36.

Zhang, Yong, Zeng, X., Jin, S., 2012. Autophagy in adipose tissue biology. Pharmacological research : the official journal of the Italian Pharmacological Society 66, 505–12.